

AN OIL-SOURCE ROCK CORRELATION EXAMINING THE POTENTIAL OF THE
CHATTANOOGA SHALE AS A SOURCE ROCK FOR OIL WITHIN THE SPIVEY-GRABS-
BASIL FIELD, KINGMAN AND HARPER COUNTIES, KANSAS

by

MEAGAN WALL

B.S., UNIVERSITY OF PITTSBURGH

A THESIS

submitted in partial fulfillment of the requirements for the degree

MASTER OF SCIENCE

Department of Geology
College of Arts and Science

KANSAS STATE UNIVERSITY
Manhattan, Kansas

2015

Approved by:

Major Professor
Dr. Matthew Totten

Copyright

MEAGAN WALL

2015

Abstract

Oil production in Kansas has a long history with plays being found on all sides of the state. The source of Kansas's hydrocarbons has been traditionally thought to be outside the state due to low thermal maturity and the shallow burial of potential source rocks within Kansas. This research addresses the question regarding the source of the oil in Kansas, at least within a small geographic area of roughly $146mi^2$. The Spivey-Grabs-Basil Field has been one of the more successful fields within the state of Kansas since the 1960's.

This field is compartmentalized and offers a natural laboratory in which to conduct the field's first formal oil-source rock correlation since oils are locked into place. While the main focus of this research relies heavily on pyrolysis and GCMS for biomarker analysis, it also investigates the possibility of using rare earth element (REE) concentrations as a possible fingerprint of organic matter within a source bed.

TOC values of the Chattanooga shale samples from the Spivey-Grabs-Basil field range from 0.75 and 3.95 wt. %, well within productive capacity. Pyrograms show both the potential for additional production, and the likely previous expulsion of hydrocarbons. Biomarker concentration percentages between C_{27} , C_{28} , and C_{29} steranes, as well as pentacyclic terpane ratios compared between crude oil from the Spivey-Grabs-Basil and the Chattanooga shale show a definite genetic relationship. REE values of the organic fraction of the Chattanooga inversely correlate with those of the crude oils, suggesting fractionation during oil generation.

After comparison of results with the Woodford shale in Oklahoma, the conclusion of this study is that the Chattanooga shale which underlies the Spivey-Grabs-Basil oil field of southern Kansas is the probable source rock which generated the oil now being produced.

Table of Contents

| | |
|--|----|
| List of Figures | vi |
| List of Tables | ix |
| Acknowledgements..... | x |
| Dedication..... | xi |
| Chapter 1 - Introduction..... | 1 |
| 1.1 – Spivey-Grabs-Basil Field History..... | 2 |
| 1.2 – Previous Research..... | 3 |
| 1.2.1 – Recent Oil-Source Rock Correlations in Publications..... | 4 |
| 1.2.2 – TOC/Pyrolysis Conducted in Western Kansas in Examination of Potential Source Rocks..... | 4 |
| 1.2.3 – Investigation of Biomarkers in Oils Produced in Kansas | 6 |
| 1.2.4 – Rare Earth Elements and Their Use in Fingerprinting Source Rocks..... | 8 |
| 1.2.5 – Concurrent Research Using REE’s in Crude Oil | 8 |
| Chapter 2 – Stratigraphy and Depositional Environment..... | 9 |
| 2.1 – Stratigraphy..... | 9 |
| 2.2 – Depositional Environment | 11 |
| Chapter 3 – Materials and Methods..... | 13 |
| 3.1 – Sample Selection and Extraction | 13 |
| 3.2 –Sample Preparation | 16 |
| Chapter 4 – Results | 20 |
| 4.1 – Pyrolysis Results..... | 20 |
| 4.2 – Gas Chromotography and Mass Spectrometry Results | 27 |
| 4.3 – Inductively Coupled Plasma - Mass Spectrometry and Inductively Coupled - Atomic Emission Spectrometry Results | 31 |
| Chapter 5 – Discussion | 33 |
| 5.1 – Total Organic Carbon | 33 |
| 5.2 – Biomarkers..... | 37 |
| 5.3 – Rare Earth Elements | 44 |
| 5.3.1 – REE Organic Fraction..... | 44 |

| | |
|--|----|
| 5.3.2 – REE Correlation between Source Rock and Crude Oils..... | 46 |
| 5.3.3 – Comparison of Chattanooga and Woodford Organic Fraction..... | 47 |
| 5.3.4 – REE’s of the Silicate-Carbonate Fraction..... | 48 |
| Chapter 6 – Conclusions..... | 51 |
| 6.1 – Recommended Future Research..... | 52 |
| References..... | 53 |
| Appendix A – GeoMark Methodology..... | 56 |
| Appendix B – Additional Figures..... | 60 |
| Appendix C – Information on Biomarkers and Rare Earth Elements..... | 62 |

List of Figures

| | |
|---|----|
| Figure 1 – Map showing potential oil migration from the Anadarko basin (modified from Gerhard, 2004) | 1 |
| Figure 2 – Map of Kansas’ major geologic formations with the counties from Hill (2009) study areas highlighted in red. The Spivey-Grabs-Basil is circled in red (Modified from Merriam, 1963) | 5 |
| Figure 3 – Top: Location of Spivey-Grabs-Basil oil field in relation to other regional structures; Bottom: Location of Spivey-Grabs-Basil oil field in relation to other oil fields (Watney et al., 2001). | 7 |
| Figure 4 – Stratigraphic column depicting southern Kansas and northern Oklahoma geological units (Mazzullo et al., 2009) | 10 |
| Figure 5 – Image of North America during the late Devonian. Courtesy Ron Blakely, Professor Emeritus, North Arizona University, Dept. of Geology, 2011 | 11 |
| Figure 6 – Geophysical log for the Phoenix #1 Orme well, located in Kingman Country, south-central Kansas (Sec. 4, T. 28, R. 6W) (Lambert et al., 1994) | 12 |
| Figure 7a – Modified field map from Kansas Geological Survey website. Red wells indicate potential source rock cutting sample locations. Gray wells indicate well sampled for oil analysis (biomarkers and lanthanides by Evans, 2011 and Kwasny, 2015 respectively) | 14 |
| Figure 7b – Closer view of 7a: Modified field map from Kansas Geological Survey website. Red wells indicate potential source rock cutting sample locations. Gray wells indicate well sampled for oil analysis (biomarkers and lanthanides by Evans, 2011 and Kwasny, 2015 respectively) | 14 |
| Figure 8 – Flow chart outlining ICP-MS/ICP-AES preparation process in steps. A table with measurements from this particular preparation can be found in Appendix B | 19 |
| Figure 9 – Two pyrograms showing average results (three gave results indicating previous production mimicking the left image, while two had higher future production potential much like the right image) | 20 |
| Figure 10a – Depth vs. Organic Carbon (wt.% HC) and their evaluated values as potential source rocks (1-3 of 5)..... | 21 |

| | |
|---|----|
| Figure 10b – Depth vs. Organic Carbon (wt.% HC) and their evaluated values as potential source rocks (4-5 of 5)..... | 22 |
| Figure 11 – S2 values vs. depth and their evaluated potential as source rocks | 23 |
| Figure 12 – HI values (S2/TOC) vs. depth and their evaluated source rock type | 24 |
| Figure 13 – Oxygen Index vs. Hydrogen Index and predicted kerogen type | 25 |
| Figure 14 – TOC vs. S2 (remaining hydrocarbon potential) and their generative capacity type . | 26 |
| Figure 15 – Gas chromatography peaks for terpanes and steranes with important ratios outlined to the right | 27 |
| Figure 16 – Gas chromatography peaks for aromatics and isoprenoids with key ratios in the top right section..... | 28 |
| Figure 17 – Compositional breakdown of biomarkers found in the Chattanooga shale: Tricyclic terpanes and pentacyclic terpanes | 29 |
| Figure 18 – Compositional breakdown of biomarkers found in the Chattanooga Shale: steranes and key ratios | 30 |
| Figure 19 – TOC Evaluation. McCarthy, et al., 2011 | 34 |
| Figure 20 – Hydrogen Index (mg HC/gTOC) vs Tmax showing kerogen type of all 5 wells and oil generative capacity based on Ro values | 35 |
| Figure 21 – Chattanooga wt. % TOC with lines representing minimum acceptable TOC values for production and average TOC wt. % for the Woodford shale and samples across the state of Kansas..... | 36 |
| Figure 22 – Well locations and lineaments (maps modified by Kansas Geological Society from Frensley and Darmstetter, 1965)..... | 37 |
| Figure 23 – Biomarker maturation index from Evans (2011) | 38 |
| Figure 24 – Comparison of biomarkers (steranes) from crude oils against the Chattanooga shale | 39 |
| Figure 25 – Comparison of biomarkers (pentacyclic terpanes) from crude oil against the Chattanooga shale | 39 |
| Figure 26 – Predicted oil source rock values are circled in red. Chattanooga terpane vs. hopane ratios represented by the red star..... | 40 |
| Figure 27 – Predicted oil source rock type values derived from tricyclic terpanes are circled in red while the red star represents the Chattanooga shale | 41 |

| | |
|--|----|
| Figure 28 – Crude oil source rock prediction type circled in red, and source rock tricyclic terpane ratio vs. hopanese represented by the red star..... | 42 |
| Figure 29 – Ternary diagram of C_{27} , C_{28} , and C_{29} steranes for Woodford shale samples, with Spivey-Grabs-Basil field data added (Modified from Moldowan, et al., 1985; Woodford data added by Philp and Romero, 2012)..... | 42 |
| Figure 30 – Average oil and Chattanooga shale pristane/phytane ratios..... | 43 |
| Figure 31 – Organic fraction of the Chattanooga shale corrected for dilution and plotted relatively against the rare earth element constituents | 44 |
| Figure 32 – Organic fraction of the Chattanooga shale corrected for dilution and plotted relatively against the rare earth element constituents (minus outliers) | 45 |
| Figure 33 – Crude oil concentrations corrected for dilution and plotted relatively against the rare earth element constituents..... | 46 |
| Figure 34 – Grey trend lines represent the Chattanooga shale in Harper and Kingman Co. Blue is the average of two wells in Garfield county. Red is the data from a well located closer to Kansas in Grant Co., OK | 47 |
| Figure 35 – Inorganic fraction of the Chattanooga shale corrected for dilutions and plotted relatively against the rare earth elements..... | 49 |
| Figure 36 – Inorganic fraction of the Chattanooga shale plotted with the Woodford Shale inorganic fraction. The bottom two trend lines represent the Woodford..... | 49 |
| Figure 37 – Inorganic fraction of the Woodford shale | 50 |
| Figure 38 – TOC Evaluation. Modified from Peters (2006)..... | 60 |
| Figure 39 –Additional pyrograms provided by GeoMark | 60 |
| Figure 40 – Sterane compound structure (Waples et al., 1990)..... | 63 |
| Figure 41 – Triterpane compound structure (Waples et al., 1990)..... | 64 |
| Figure 42 – Periodic table of elements with the lanthanide group, or rare earth elements highlighted in dark pink | 66 |
| Figure 43 – REE distribution pattern normalized to PAAS for the organic portion of the Woodford Shale taken from Ramirez-Caro (2013)..... | 68 |

List of Tables

| | |
|---|----|
| Table 1 – Sample cutting information including API#, well location and production history | 15 |
| Table 2 – Detailing the type of experiments applied to each sample taken from KGS Library in Wichita. | 17 |
| Table 3 – GeoMark LECO TOC and other pyrolysis results. Table with additional information (sample depth, type, etc.) can be found in Appendix B. | 20 |
| Table 4 – Organic fraction results from ICP-MS/AES experiment run by the University of Strasbourg, corrected for dilutions. | 31 |
| Table 5 – Inorganic fraction results from ICP-MS/AES experiment run by the University of Strasbourg, corrected for dilutions. | 32 |
| Table 6 – LECO TOC values from Ramirez-Caro (2013). Lab testing conducted by Weatherford Laboratories | 35 |
| Table 7 – Tyler Hill’s unified TOC data. | 59 |
| Table 8 – GeoMark LECO TOC (FULL) and other pyrolysis results. | 60 |

Acknowledgements

I'd firstly like to thank my Major Professor, Matthew Totten for consistently and patiently answering questions and pushing me to be in the lead throughout this project. I have a firmer grasp of the scientific method, and a better appreciation for what shall be expected of me in the future.

Dr. Sambhudas Chaudhuri is a master in the lab, and without him, my methods might have been less pristine. His guidance, along with Dr. Totten's, provided me with paths for study and research that proved insightful and without their help this research would be poorly understood.

Thank you, also, to Dr. Matthew Kirk for sitting on my board and holding a calm demeanor as well as ripping my research to pieces in an effort to make it better—I think it worked!

My family has borne the brunt of my work, cooking and caring for themselves and enduring my absence at many points in my research. Their endurance has been appreciated. Brian: you are the best sounding board a woman could ask for, and Kevin and Jennifer: I'm proud of you for growing up so strong and able to take the knocks life gives us all. I have no doubts of your future success in this world.

Drew Evans has been a wonderful contact during this research, even mailing off two very expensive books for biomarker interpretation. Without his previous research and recent assistance, the conclusions of this research might be a good deal less firm.

To my compatriots in the department, Tyler Willey, Austin McColloch, Helder Alvarez, Brianna Kwasny, Jasper Hobbs, Anna Downey, and Jennifer Roozeboom: I have never suffered alongside a better group of people. You will always have a friend in me.

Dedication

For Walter David Heinlen, Jr. Esteemed petroleum geologist, mentor, and father. You are missed.

For Daniel 'Keith' Heinlen, petroleum geologist, best friend, and brother. You are a brat.

Chapter 1 – Introduction

The Spivey-Grabs-Basil oil field in Harper and Kingman Counties is one of the largest fields in Kansas. Production is from Mississippian-aged rocks, and the field has produced over 74 million barrels since it was first discovered in 1949. The source of this oil remains unknown, as an oil to source rock correlation has not been attempted for this part of Kansas. The organic source is a major element of the petroleum system and responsible for the creation of the oil that has been produced in south-central Kansas. A primary question that this research is formatted to investigate is: does the oil in this field originate from a local source, or has the oil in this field migrated from a more distant source (e.g. the Woodford shale in the Anadarko Basin to the south – Figure 1)?

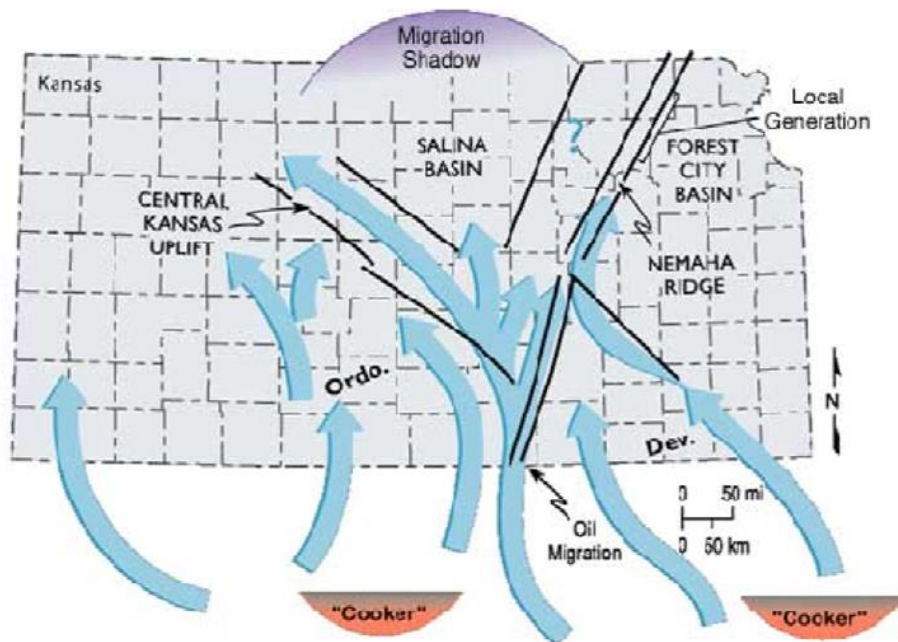


Figure 1 – Map showing potential oil migration from the Anadarko basin. (Modified from Gerhard, 2004)

The Mississippian reservoir of the Spivey-Grabs-Basil appears to be compartmentalized, sometimes complicating production. This offers a natural laboratory for examining biomarkers and their variation within this particular petroleum system, as investigated by Evans (2011). Previous examination of organic biomarkers in crude oil, found using gas chromatography and mass spectrometry (GCMS), has established that there are at least two different oil maturities within the Spivey-Grabs-Basil field. These data provide an opportunity to use new experiments to perform an oil-source rock correlation by comparatively examining the pre-existing biomarker results.

Organic and inorganic fingerprinting of the source rock have been examined to reveal the source of oil generation for this particular field, and offer insight into the system in the interest of future production. GCMS, which is traditionally used in oil-source rock correlations, is the main experimental process used for analysis. Pyrolysis was run first to examine total organic carbon (TOC) of this field before conducting further, more extensive experiments. Using inductively coupled plasma – mass spectrometry (ICP-MS) to examine rare earth elements (REE's) offers an opportunity to investigate an additional method for correlation. ICP-MS has been administered to fractionated portions (separated into organics, carbonates, and silicates) of the potential source rock and analyzed for relationships to possibly extend methodology and perhaps validate GCMS findings.

1.1 – Spivey-Grabs-Basil Field History

The Spivey-Grabs-Basil is known to have widely varied porosity that precludes lateral migration and oil mixing within small areas. This varied porosity acts as a stratigraphic trap with up-dip pinch outs or truncations, and down-dip the field is less oil rich and holds more water.

The field is also widely believed to be heavily compartmentalized, which also adds to its variability so far as porosity and permeability are concerned (Frensley, 1965).

The field's production started up in the 1950's after its discovery. It has experienced a slow decline since its initial production in 1966 with nearly 3 million barrels per year to around 360,000 barrels per year in 2014. Gas production started two years later in 1968 and started out with well over 227 million mcf and then declining to 5 million mcf in 2014 (Kansas Geological Survey Historical Report).

1.2 – Previous Research

The “biomarker revolution” began in 1964 when it was found that biological markers or ‘geochemical fossils’ could be studied within sediment and crude oil compounds. They are used to understand petroleum occurrence and origin, as well as perform correlations between oils, and oil and possible source rocks (Hunt et al., 2002).

An oil-source rock correlation is loosely defined as biomarker fingerprinting, or the comparison of biomarkers, analyzed using GC or GCMS, in both a produced oil and a potential source rock. A relationship cannot be ascertained with one similar biomarker, but 30 to 40 similar biomarkers are considered enough to make a “confident” positive correlation (Hunt et al., 2002), the unstated assumption being that more is always preferable. Based on research by Peters (2006), biomarker group concentrations can also be used for substantial and accurate correlation.

1.2.1 – Recent Oil-Source Rock Correlations

Oil-source rock correlation studies are a common practice. Though none were found to have been completed in south-central Kansas for comparison, several studies throughout the world have been successfully conducted recently. An oil-source correlation study in the Sinop Basin in Turkey was conducted by Korkmaz et al. (2013) and proved that oil from a seep had

been locally produced using TOC and GCMS experimentation. Another study performed by Gratzer et al. (2011) was extended to include oil to oil, as well as oil to source rock correlation in the Alpine Foreland Basin of Austria using biomarker and stable carbon isotope analyses. Gratzer's study was able to identify a relationship between oils and several source rocks, indicative of oil mixing through migration and diagenesis. Since correlation is still approached through biomarkers and little to no variation has been introduced to the approach as shown in these two studies, this study also focuses on traditional methodology.

1.2.2 – TOC/Pyrolysis Conducted in Western Kansas in Examination of Potential Source Rocks

Hill (2011) examined possible source rocks and their potential productivity and oil-generative properties in various regions of western Kansas. His use of pyrolysis, and his investigation of TOC and vitrinite reflectance, provides excellent comparative data to this study. His raw data from Weatherford Labs have been manually reorganized into a single spreadsheet for comparative analysis to this study (Table 7 - Appendix B). His dataset revealed exceptional TOC numbers ranging up to 13.33%, and immature T_{max} values of 428°C average. His vitrinite reflectance values proved thermally immature in most samples, which are in keeping with traditional thought on Kansas' source potential, but two samples fell over 0.6% value which categorically defines them as ideally mature, or within the oil generative window.

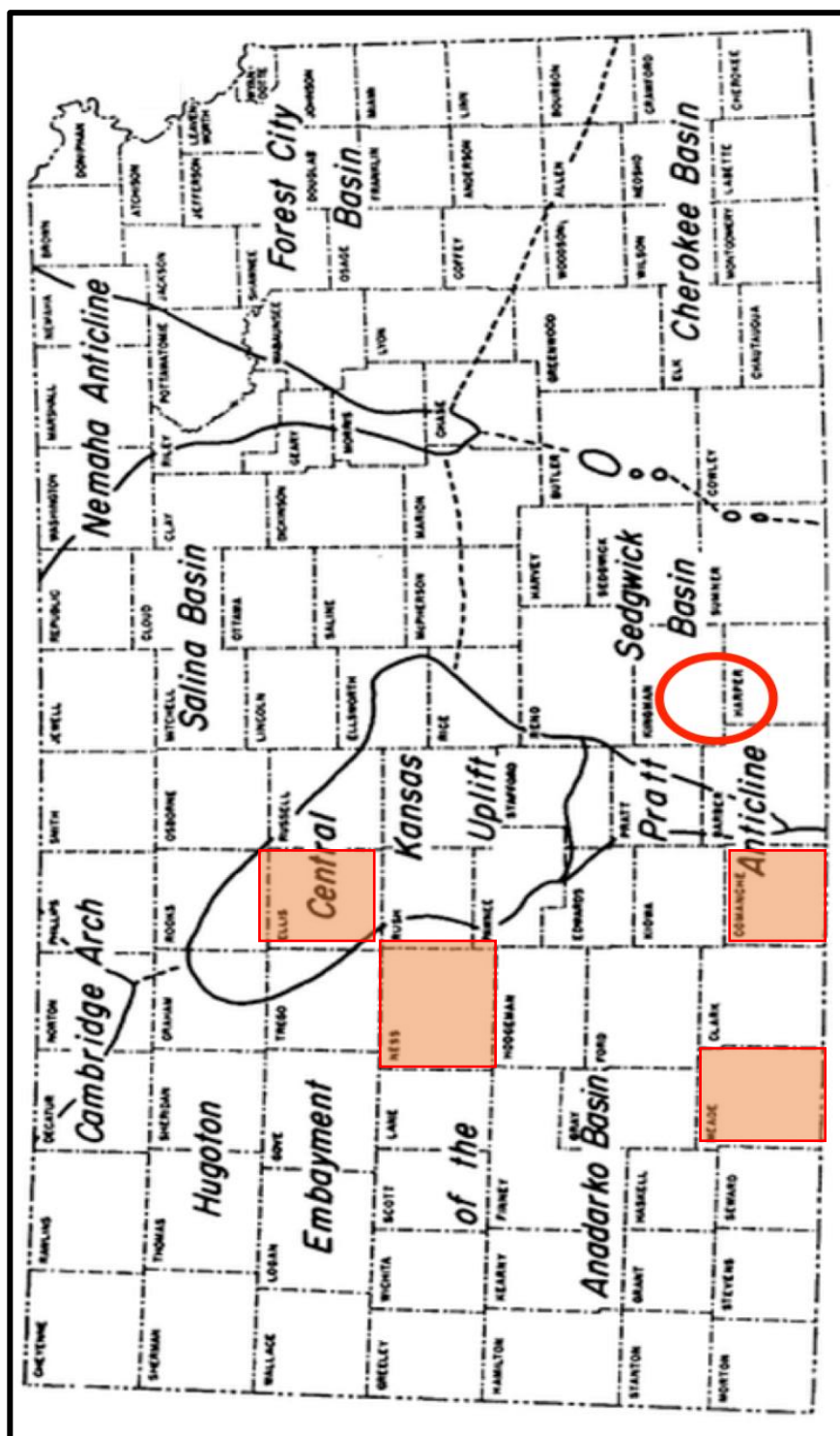


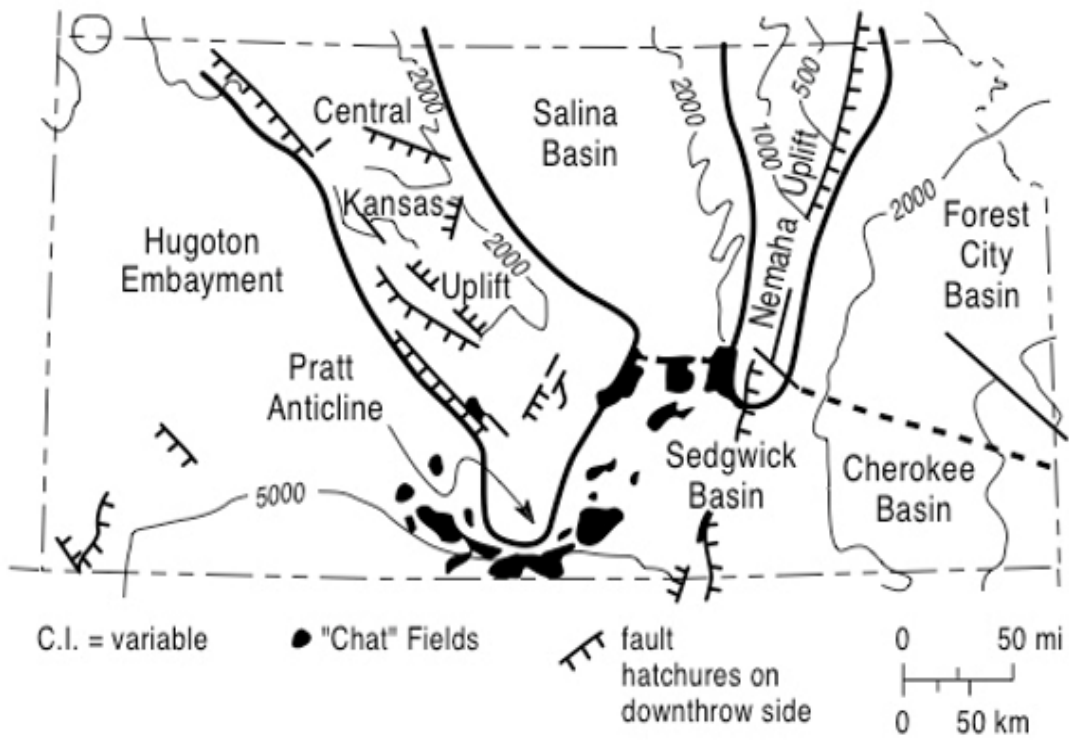
Figure 2 - Map of Kansas' major geologic formations with the counties from Hill (2009) study areas highlighted in red. The Spivey-Grabs-Basil oil field location is circled in red. (Modified from Merriam, 1963).

Hill's evaluation of shale units to the west of the Central Kansas Uplift (Figure 3) concluded that many of the potential rocks in southern Kansas are thermally mature enough to produce hydrocarbons, though his Cherokee and Morrow units proved to have higher TOC and maturity values than the other units he investigated. He suggested testing biomarkers within overlying oil to see if production from those units could be verified. Unfortunately, he did not have Chattanooga samples for comparison, as it was not penetrated in the wells included in his study.

Ramirez-Caro (2013) obtained TOC values for the stratigraphically equivalent Woodford shale in north-central Oklahoma, which is a known oil source rock. His LECO (machine-type) TOC ranged up to 11.5 wt. %. He also analyzed the organic fraction of his rocks for REE and other trace elements, which can be compared to the Chattanooga shale in this study.

1.2.3 – Investigation of Biomarkers in Oils Produced in Kansas

Evans (2011) conducted a biomarker analysis of the oils in the Spivey-Grabs-Basil in Kingman County in 2011. His analysis of the oil led to several conclusions, including: the indication of compartmentalization in the area, in agreement with Frensley and Darmstetter (1965); the presence of two distinctly different oil maturities. He also postulated that the oil's source rock would likely be carbonate due to the prevalence of C₂₉ and C₂₇ steranes within the oils. He additionally found that the oils in the Spivey-Grabs-Basil have experienced little-to-no biodegradation, which would imply a local source. Evans' study suggested that the oils within the Spivey-Grabs share a common source, but their thermal maturities are varied, likely due to the compartmentalization keeping the oils from mixing during generative pulses.



C.I. = variable ● "Chat" Fields fault hatchures on downthrow side 0 50 mi
 0 50 km

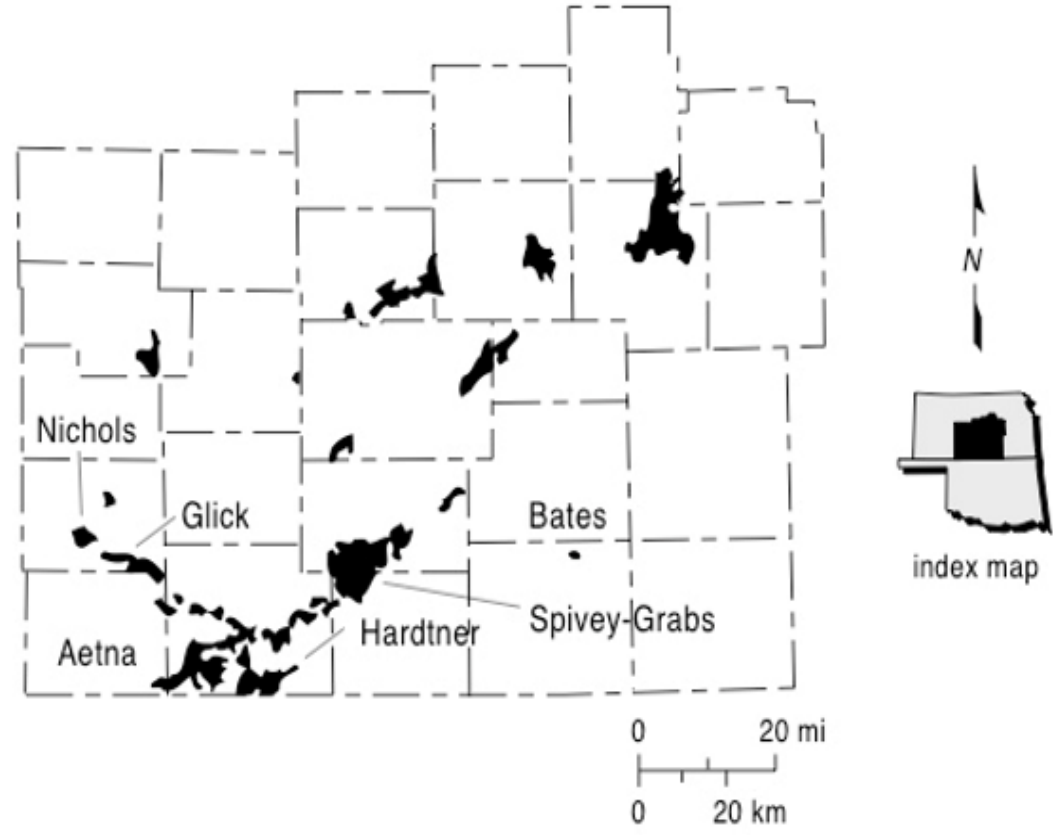


Figure 3 - Above: Location of Spivey-Grabs-Basil oil field in relation to other regional structures. Bottom: Location of Spivey-Grabs-Basil oil field in relation to other local fields (Watney et al., 2001).

1.2.4 – Rare Earth Elements and Their Use in Fingerprinting Source Rocks

The use of the lanthanide series elements in petroleum systems analysis is a relatively new experimental approach. Two studies of note have been completed by previous graduates of Kansas State. Some of their methodology and conclusions will be used in a comparative context. Ramirez-Caro (2013) examined REE's as possible clues to 'reconstruct hydrocarbon generation history' of the Woodford shale in parts of Oklahoma (his solid rock coming from the north-central section of the state to the west of the Nemaha uplift, and his oil samples being taken from Payne county to the east of the Nemaha). McIntire (2014) looked at the Lansing Kansas City group, specifically, and focused on oil without a potential source rock for comparison. His data led him to conclude that the oils in northern Kansas very likely did not come from the Anadarko Basin, and instead are a mix with several different possible (local) sources.

1.2.5 – Concurrent Research Using REE's in Crude Oil

A current project in the Spivey-Grabs-Basil is being conducted by Brianna Kwasny to investigate the produced crude oils. While Evans approached his analysis solely through biomarkers, Kwasny is investigating the same section of the field by looking at REE's. Their results will be included herein for comparison, looking for possible trends suggestive of a correlation between the Chattanooga shale and the Mississippian oils.

Chapter 2 - Stratigraphy and Depositional Environment

The Chattanooga shale was deposited during the late Devonian. The Chattanooga shale is silty, rich in pyrite, and partially dolomitic in some locations (KGS – “Undifferentiated Upper Devonian and Lower Mississippian”). It should be noted that there are terminology discrepancies between geologists in Kansas where the Chattanooga shale is considered to be both stratigraphically related to the Woodford shale in Oklahoma, but also Kinderhookian in age. This research is adopting the approach of Lambert et al. (1994) that the Chattanooga and Woodford shales are stratigraphically equivalent and Devonian in age.

2.1 – Stratigraphy

The Chattanooga lies unconformably atop the Misener sandstone and extends across most of eastern and central Kansas (Figure 4). It is absent north of the Nemaha Uplift and grades from darker shale to a light, less organic-rich shale as it extends northward. Its thickness varies from 0 to 250 feet. Below the Chattanooga shale is the Misener sandstone—a unit that is considered a marker for the start of the Woodford Shale in north and central Oklahoma. Above the Chattanooga shale lays Mississippian Limestone (reservoir rock) which is sealed by Pennsylvanian system units (Jewett et al.1968).

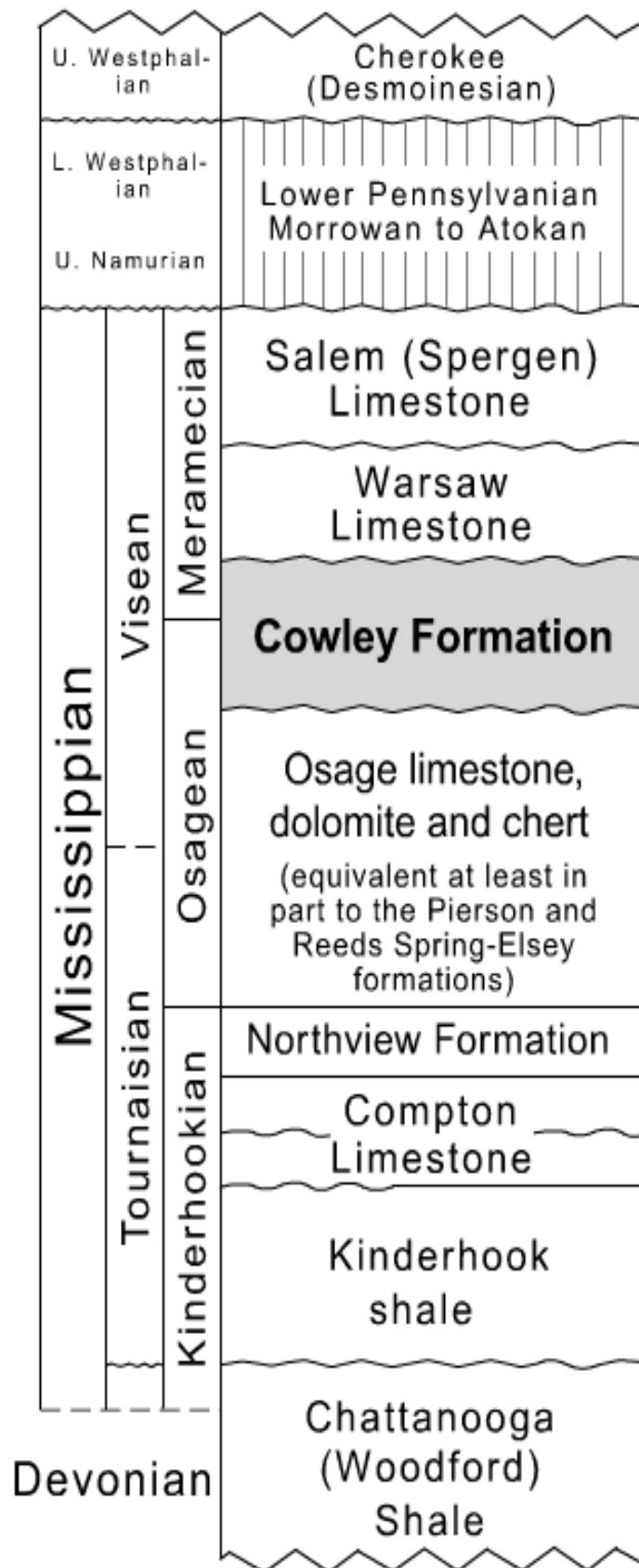


Figure 4 – Stratigraphic column depicting southern Kansas and northern Oklahoma geological units (Mazzullo et al., 2009).

2.2 – Depositional Environment

In Kansas, the late Devonian period during which the Chattanooga shale was deposited, was marked by anoxic, epicontinental seas. Deposition increased due to the continuation of the Acadian orogeny (Figure 5). During this time, the stratigraphically equivalent Woodford Shale to the south in Oklahoma was deposited from the Anadarko Shelf into the Anadarko Basin. Because of their synformation (Lambert et al., 1994), the Woodford shale and Chattanooga shale share a nearly identical gamma ray wire-line profile (Figure 6).

During the following Mississippian period, limestone reservoir rock was deposited and eventually became the host rock for petroleum, and one of the largest oil plays the state of Kansas. Following this time period, additional shales and further infill from the Acadian orogeny buried the Chattanooga deeply before the seas receded. To date, uplift and erosion are the active geologic influences in this section of Kansas.

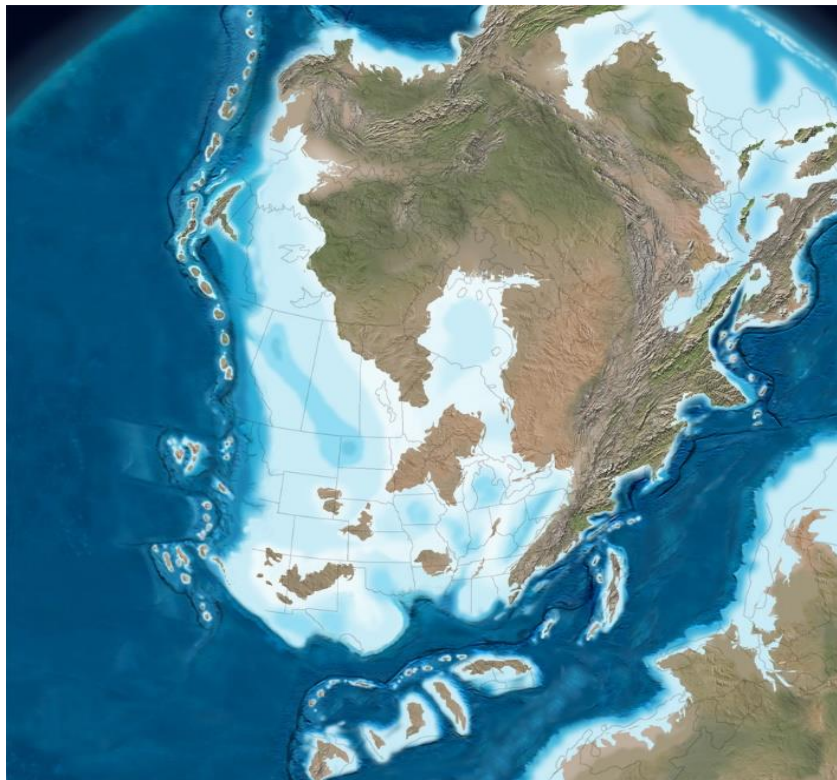


Figure 5 – Image of North America during the late Devonian. Courtesy Ron Blakely, Professor Emeritus, North Arizona University, Dept. of Geology, 2011.

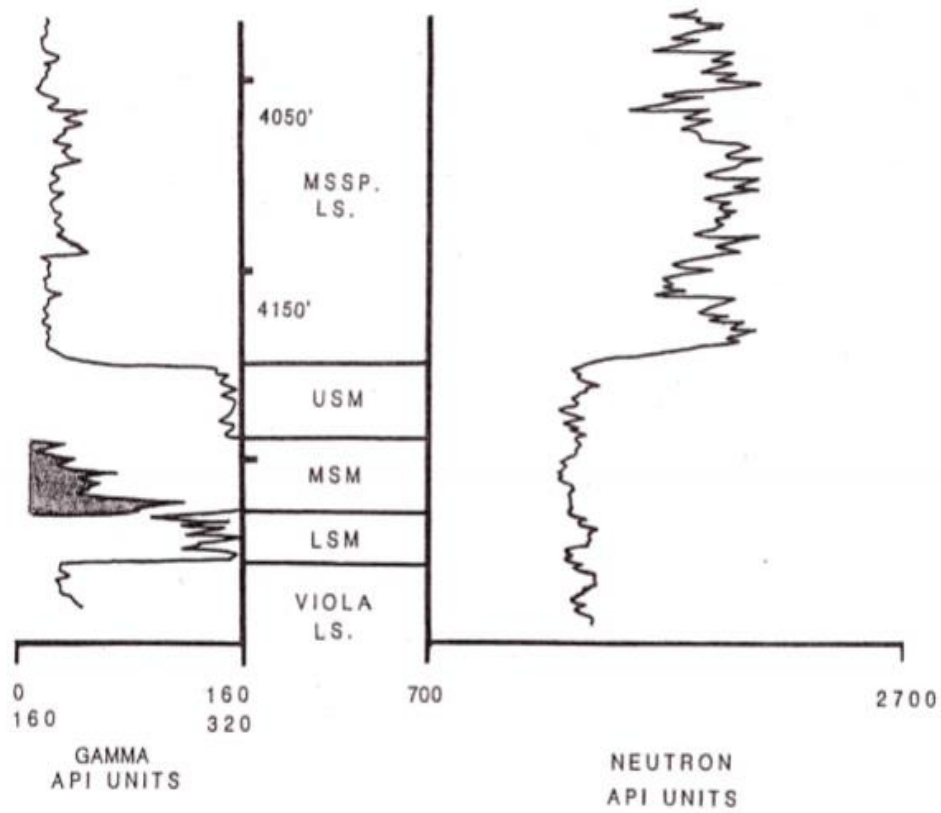


Figure 6 - Geophysical log for the Phoenix #1 Orme well, located in Kingman County, south-central Kansas (Sec. 4, T. 28, R. 6W). Depth below surface (feet) is shown in the central column. All three shale members of the Chattanooga Shale are present. LSM = lower shale member, MSM = middle shale member, and USM = upper shale member (Lambert et al., 1994).

Chapter 3 – Materials and Methods

3.1 – Sample Selection and Extraction

Oil samples from Kingman Co. were studied by Evans (2011) and as a result, the study area for the source rock was restricted to Kingman and nearby Harper Co.'s for the oil source rock correlation (Figure 2). The crude oil samples being used for comparison to the source rock data are located towards the north-eastern corner of the field (Figures 7a and 7b). The Mississippian play is the most prolific oil producer in the area. Since drilling stops at production depth, the number of wells penetrating the Chattanooga shale is limited in this field.

As previously stated, the Chattanooga shale shares a very similar gamma-ray profile to the Woodford Shale, a known source rock in the Anadarko Basin, across the border into Oklahoma. The Chattanooga shale was located in wells that were drilled deeply enough to penetrate it using tops reported by KGS. Wireline logs of these wells verified that the Chattanooga in each sample did indeed resemble the Woodford. The corresponding cuttings across the Chattanooga interval were checked out from the Kansas Geological Survey Library in Wichita, KS.

The cuttings from the sections with the highest gamma-ray spike (most organic-rich) were hand-picked under a binocular microscope. Additional feet above and below had to be used in two instances as the amount of cuttings were far too small to analyze. Samples from seven wells were used in the study (Table 1). Other wells were considered, but either did not have enough sample for use, or the cuttings from and around the increments shown on wireline did not appear to be shale, but instead were limestone.

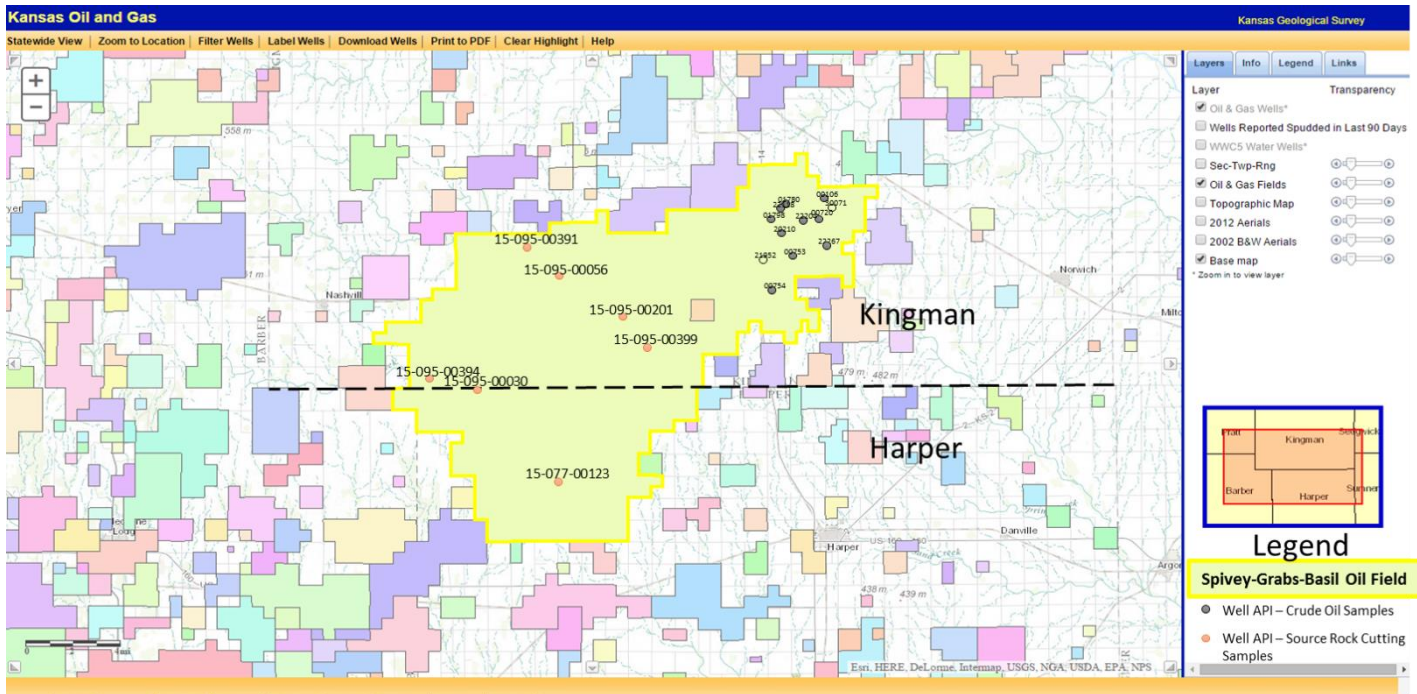


Figure 7a – Modified field map from Kansas Geological Survey website. Red dots indicate wells with potential source rock cutting samples. Gray dots indicate wells sampled for oil analysis (GCMS and REE, by Evans,2011 and Kwasny, 2015 respectively).

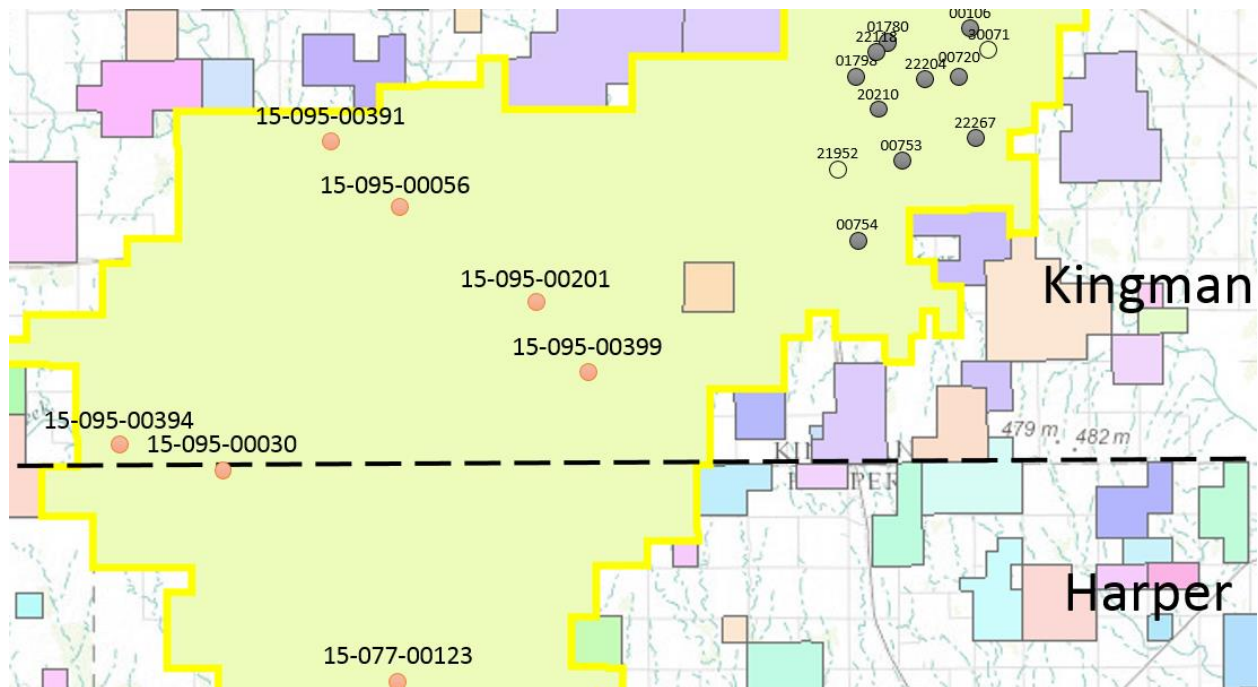


Figure 7b. – Closer view of Figure 7a. Modified field map from Kansas Geological Survey website. Red dots indicate potential source rock cutting sample locations. Gray dots indicate wells sampled for oil analysis (GCMS and REE, by Evans,2011 and Kwasny, 2015 respectively).

| Well Name | API# | KGS# | Surface Location | Production History |
|---------------|--------------|-------|------------------|--|
| Morris & Wolf | 15-095-00030 | 43501 | 35-30S-9W | Gas - Producing |
| Antrim 1 | 15-077-00123 | 42574 | 25-31S-9W | Oil - Converted to Salt Water Deposit Well |
| Boyle 'A' | 15-095-00399 | 29889 | 27-30S-8W | O&G - Inactive |
| Boyle 'A' | 15-095-00201 | 37600 | 23-30S-8W | O&G - Inactive |
| Hartshorn | 15-095-00391 | 39457 | 36-29S-9W | O&G - Producing |
| Folkes | 15-095-00394 | 52936 | 32-30S-9W | Gas - Plugged and Abandoned |
| Nirschl | 15-095-00056 | 39170 | 6-30S-8W | Gas - Plugged and Abandoned |

Table 1 – Sample cutting information including API#, well location and production history.

3.2 –Sample Preparation

Approximately 2.0 grams of sample are required to obtain TOC and basic source rock data. This amount was extracted and weighed before being packaged and sent to GeoMark Laboratories in Houston, Texas. Of the seven samples, five appeared to be darker, or more organic rich, and the two that were less organic-rich were excluded. Once the data were returned with TOC, the most promising samples were sent for additional analyses (Table 2).

Carbonates were extracted from the source rock by treatment with hydrochloric acid. The Chattanooga and the Woodford shales are both highly carbonate-rich (Goebel, 1963), hence a large amount of sample was treated in order to have enough sample left to extract the organic fraction. After the carbonate fraction was dissolved, the sample was rinsed with deionized water, centrifuged and dried. 10.0 grams of carbonate residue from each sample were weighed for silicate extraction. There were ~24.0 grams of total carbonate residue left, which was combined, packaged and sent to GeoMark for GCMS analyses. A workflow of sample preparation is shown in Figure 8.

What is not included in the workflow are some of the materials description. Because dissolution of the silicate fraction of the samples required treatment using HF, Teflon crucibles were used. For consistency in weighing and measuring, the same crucibles were used throughout and cleaned in a nitric acid bath and deionized water rinse in between uses. For the heating phase of the organic fraction, Vycor crucibles were used.

After preparation, silicate, carbonate and organic fraction samples were placed into new 30 ml Nalgene bottles that had also been cleaned in a nitric acid bath and rinsed before use. Twenty-one total samples were taken to the University of Strasbourg for ICP-MS: seven carbonate fraction, seven silicate fraction, and seven organic fraction.

| Well Name | API# | Sample Depth Location | Pyrolysis | ICP-MS | GC-MS |
|---------------|--------------|-----------------------|--|--------|----------------|
| Morris & Wolf | 15-095-00030 | 4645'-55' | X | X | X |
| Antrim 1 | 15-077-00123 | 4695'-00' | X | X | X |
| Boyle 'A' | 15-095-00399 | 4570'-80' | X | X | No sample left |
| Boyle 'A' | 15-095-00201 | 4485'-90' | X | X | X |
| Hartshorn | 15-095-00391 | 4460'-75' | Less organic material than other samples | X | No sample left |
| Folkes | 15-095-00394 | 4575'-90' | X | X | X |
| Nirschl | 15-095-00056 | 4475'-90' | Less organic material than other samples | X | X |

Table 2 – Detailing type of experiments applied to each sample taken from the KGS Library in Wichita.

*Samples were tested based on amount available vs. amount needed and funding.

**Pyrolysis testing was limited by funding to samples with more organic material (darker shale/limestone)

Although the carbonate and silicate fractions of each sample were prepared and analyzed separately, for the purposes of this study the data are combined into a single component representing the inorganic component of each sample from the Chattanooga. This is for a simpler approach to REE data, as well as a necessity based upon the strength of the acid used to separate the carbonate fraction (12N HCl) which is strong enough to have broken silicate bonds and cause anomalous numbers in the silicate fraction, which taken separately would appear to be far too low. The fractionation of the source rock for ICP-MS was based on the techniques used by Ramirez-Caro (2013) and with the guidance of Dr. Chaudhuri.

The process by which GeoMark laboratories extracted the TOC and GCMS data can be found in Appendix A.

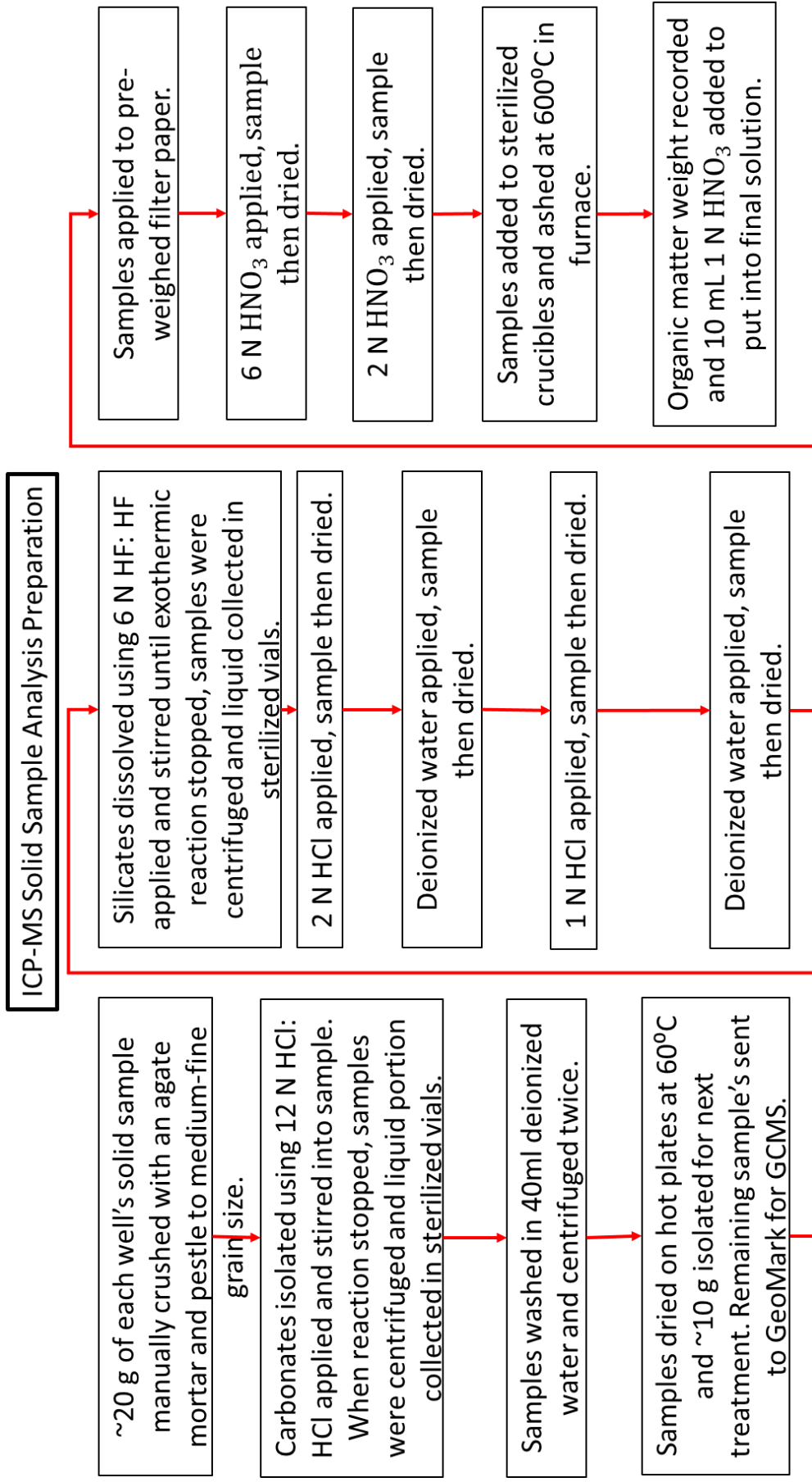


Figure 8– Flow chart outlining ICP-MS/ICP-AES preparation process in steps. A table with actual measurements of each step can be found in Appendix B.

Chapter 4 – Results

4.1 – Pyrolysis Results

The following results are unaltered numbers and images supplied by GeoMark Laboratories. Methodology for data extraction can be found in Appendix B. Samples sent to GeoMark for initial evaluation were unaltered (had yet to be fractionated). Table 3 is the combined data from GeoMark Leco TOC Rock-Eval and the parameters applied to gauge maturity and source rock quality are investigated using Figure 19 (p. #) and Figure 38 (p. #).

| API Number | Percent Carbonate (wt%) | Leco TOC (wt%) | Rock-Eval-2 S1 (mg HC/g) | Rock-Eval-2 S2 (mg HC/g) | Rock-Eval-2 S3 (mg CO2/g) | Rock-Eval-2 Tmax (°C) | Calculated % Ro (RE TMAX) | Hydrogen Index (S2x100/TOC) | Oxygen Index (S3x100/TOC) | S2/S3 Conc. (mg HC/mg CO2) | S1/TOC Norm. Oil Content | Production Index (S1/(S1+S2)) |
|--------------|-------------------------|----------------|--------------------------|--------------------------|---------------------------|-----------------------|---------------------------|-----------------------------|---------------------------|----------------------------|--------------------------|-------------------------------|
| 15-095-00030 | 11.57 | 0.72 | 0.32 | 0.98 | 0.39 | 430 | 0.58 | 136 | 54 | 3 | 44 | 0.25 |
| 15-077-00123 | 4.64 | 3.55 | 1.33 | 14.32 | 0.39 | 436 | 0.69 | 403 | 11 | 37 | 37 | 0.08 |
| 15-095-00201 | 22.75 | 0.88 | 0.22 | 1.25 | 0.34 | 440 | 0.76 | 142 | 39 | 4 | 25 | 0.15 |
| 15-095-00394 | 15.73 | 0.80 | 0.20 | 0.42 | 0.52 | 428 | 0.54 | 53 | 65 | 1 | 25 | 0.32 |
| 15-095-00399 | 10.22 | 3.95 | 1.22 | 15.69 | 0.47 | 439 | 0.74 | 397 | 12 | 33 | 31 | 0.07 |

Table 3 – GeoMark LECO TOC and other pyrolysis results. Table with additional information (sample depth, type, etc.) can be found in Appendix B.

The pyrograms created by GeoMark fall into two categories: the first with a low intensity S2 curve, implying a history of hydrocarbon generation, and the second with high intensity S2 values (Figure 9) implying high potential for hydrocarbon production (McCarthy et al., 2011). The T_{max} for all of the samples lies between 428 and 440°C. These data are also assessed using the parameters laid out by McCarthy et al. (2011) (Figure 19) and Peters (2006) (Figure 38).

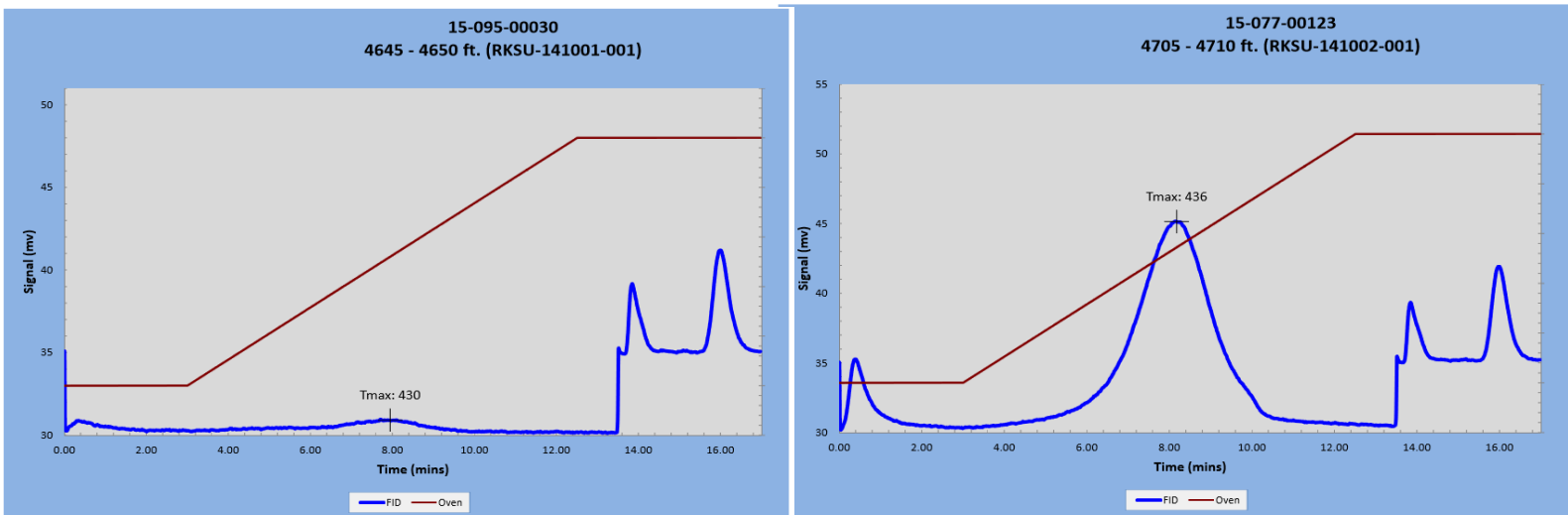


Figure 9 - Two pyrograms showing average results. Three gave results similar to the left image (15-097-00394 and 15-095-00201) while the one other gave results similar to the right image (15-095-00399). All images can be found in Appendix B, p.60.)

Figures 10a and 10b are graphs modified from GeoMark and representation of the percent carbonate rock fraction's TOC value as well as the overall TOC. These values are classified by weight percent organic carbon and show values within the oil generative range (adopted by GeoMark) that allowed for the continuation of the correlation using the Chattanooga shale.

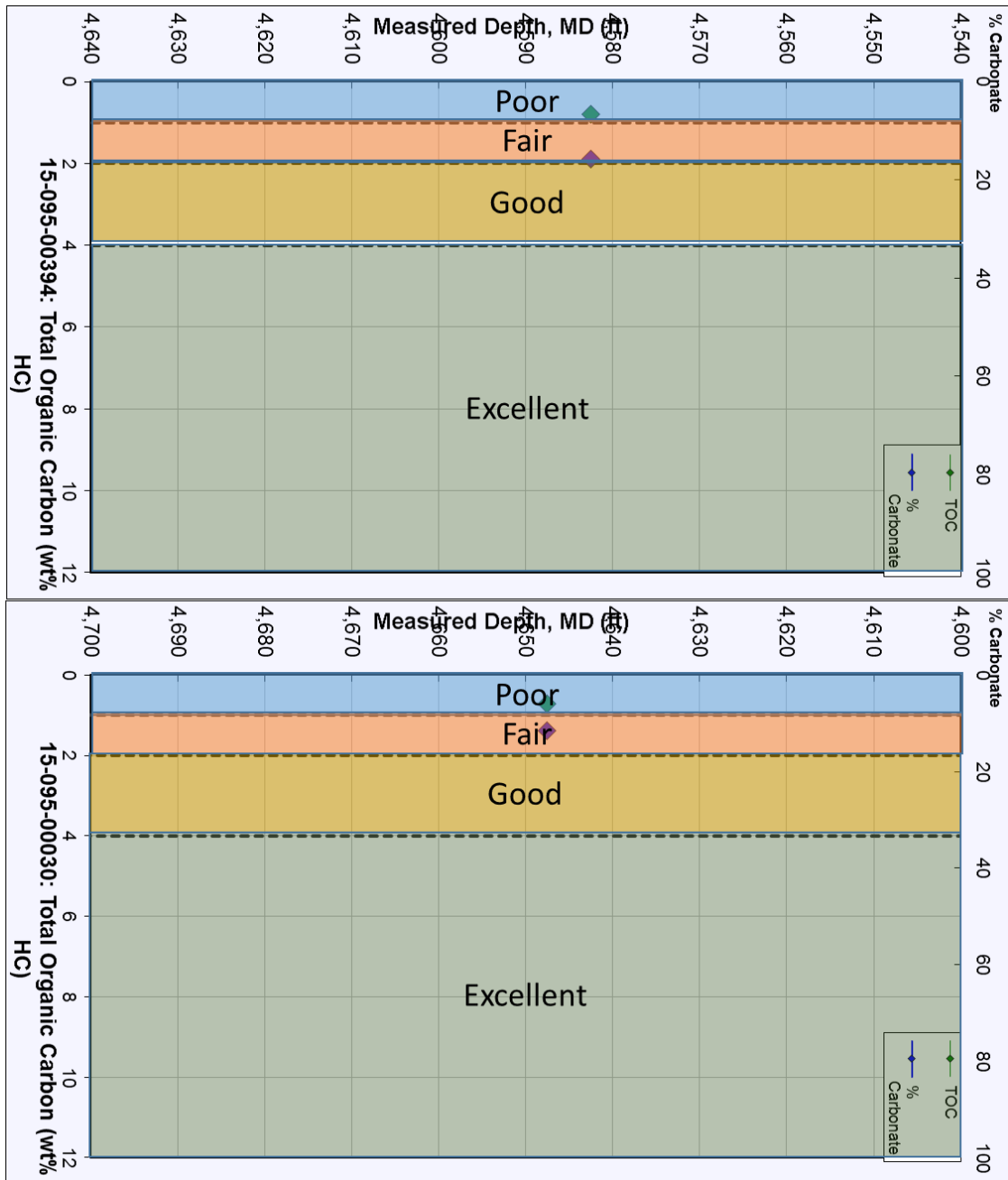


Figure 10a - Depth vs. Organic Carbon (wt.% HC) and their evaluated values as potential source rocks (1-2 of 5).

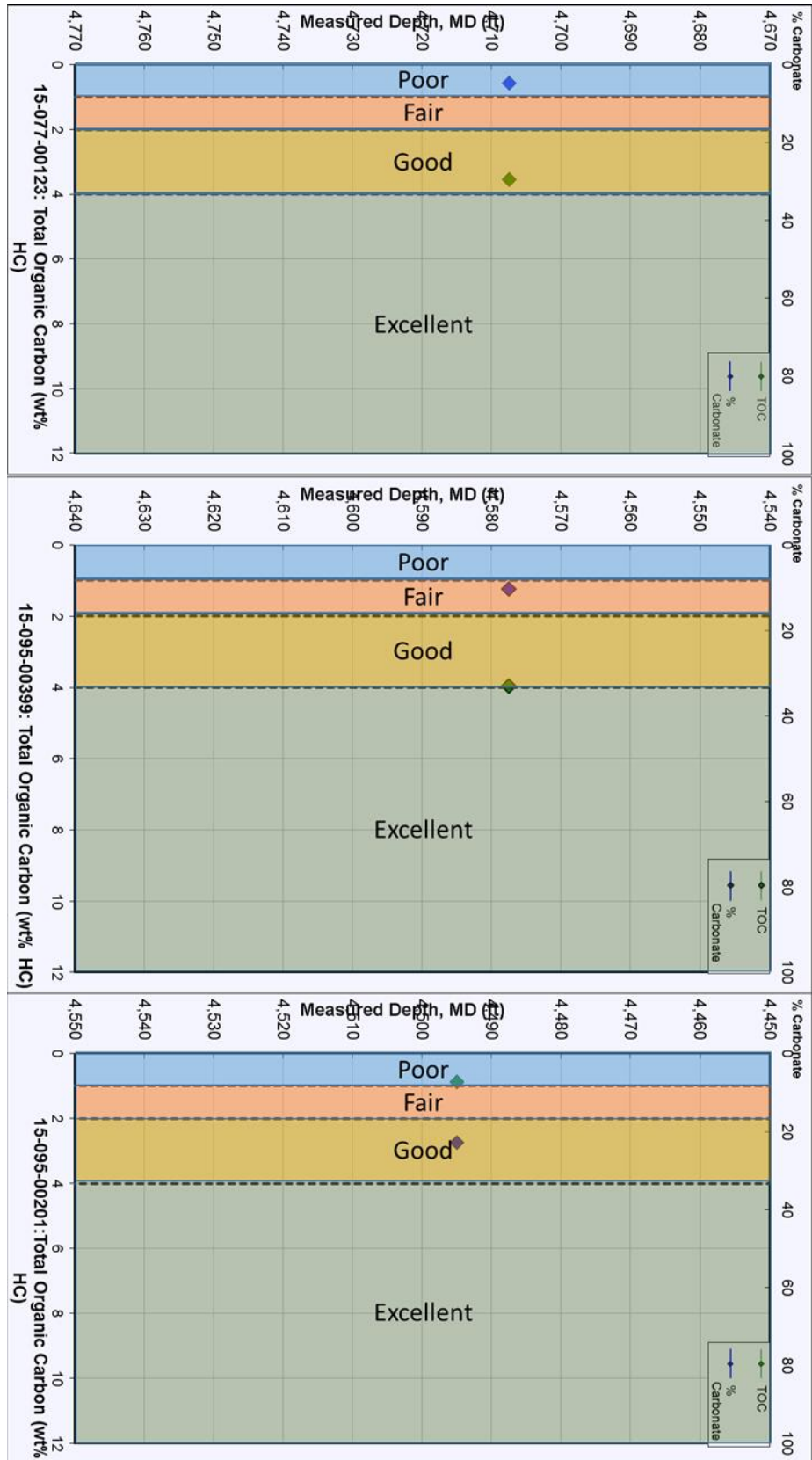


Figure 10a - Depth vs. Organic Carbon (wt.% HC) and their evaluated values as potential source rocks (1-3 of 5).

Figure 11 is a modified graph from GeoMark where all the samples have been plotted onto the same graph for comparison with one another. Again, it is obvious that three of the samples were picked from the upper, less organic rich portion of the Chattanooga. This does not preclude oil generation due to the T_{max} , TOC and vitrinite reflectance values.

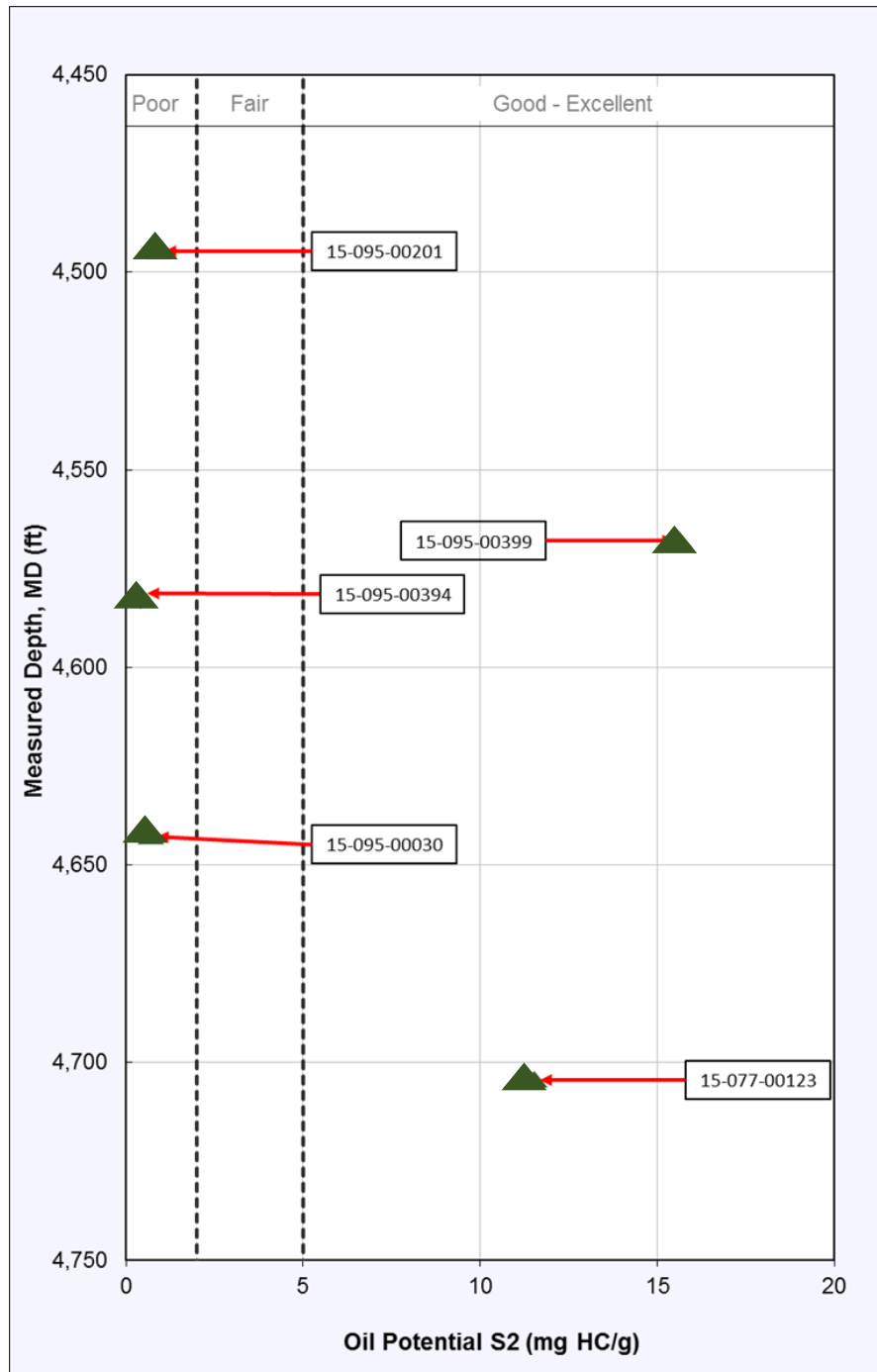


Figure 11 - S2 values vs. depth and their evaluated potential as source rocks.

Figure 12 is another modified graph from GeoMark with all samples plotted on the same graph for comparative purposes. The S2 curve intensity is low enough for three of the samples to decrease their oil generative type to gas, while the two from the more organic rich portion of the Chattanooga are Type II kerogen which is ideal for oil production. Since all five are hydrocarbon capable, the entirety of the Chattanooga shows value for industry.

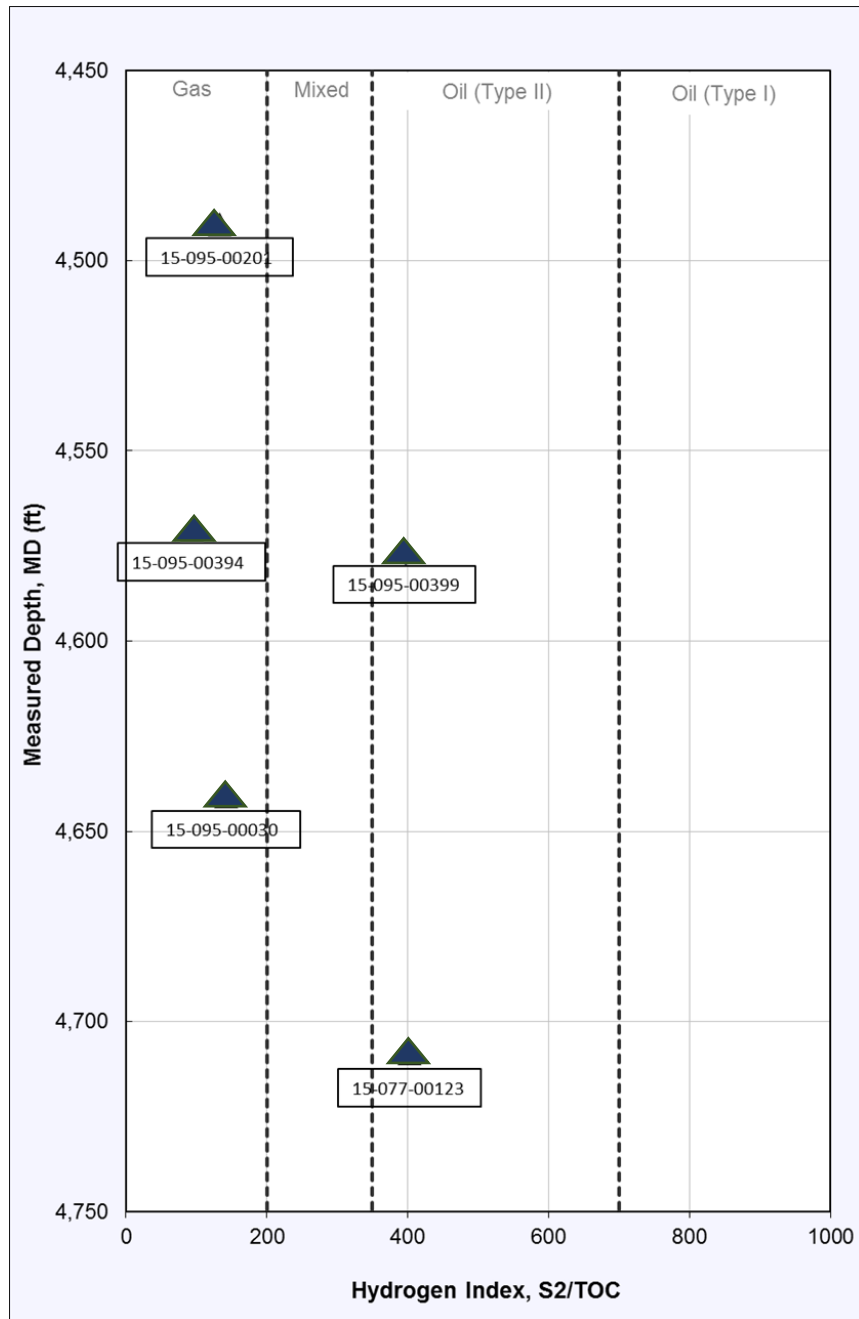


Figure 12 - HI values (S2/TOC) vs. depth and their evaluated source rock type.

Figure 13 shows the samples plotted using both the oxygen index (y-axis) and the hydrogen index (x-axis) over TOC. This is another general indicator for kerogen type and again shows the same three samples within the Type III kerogen parameters for gas production and the others as Type I and II (oil generative) kerogen type.

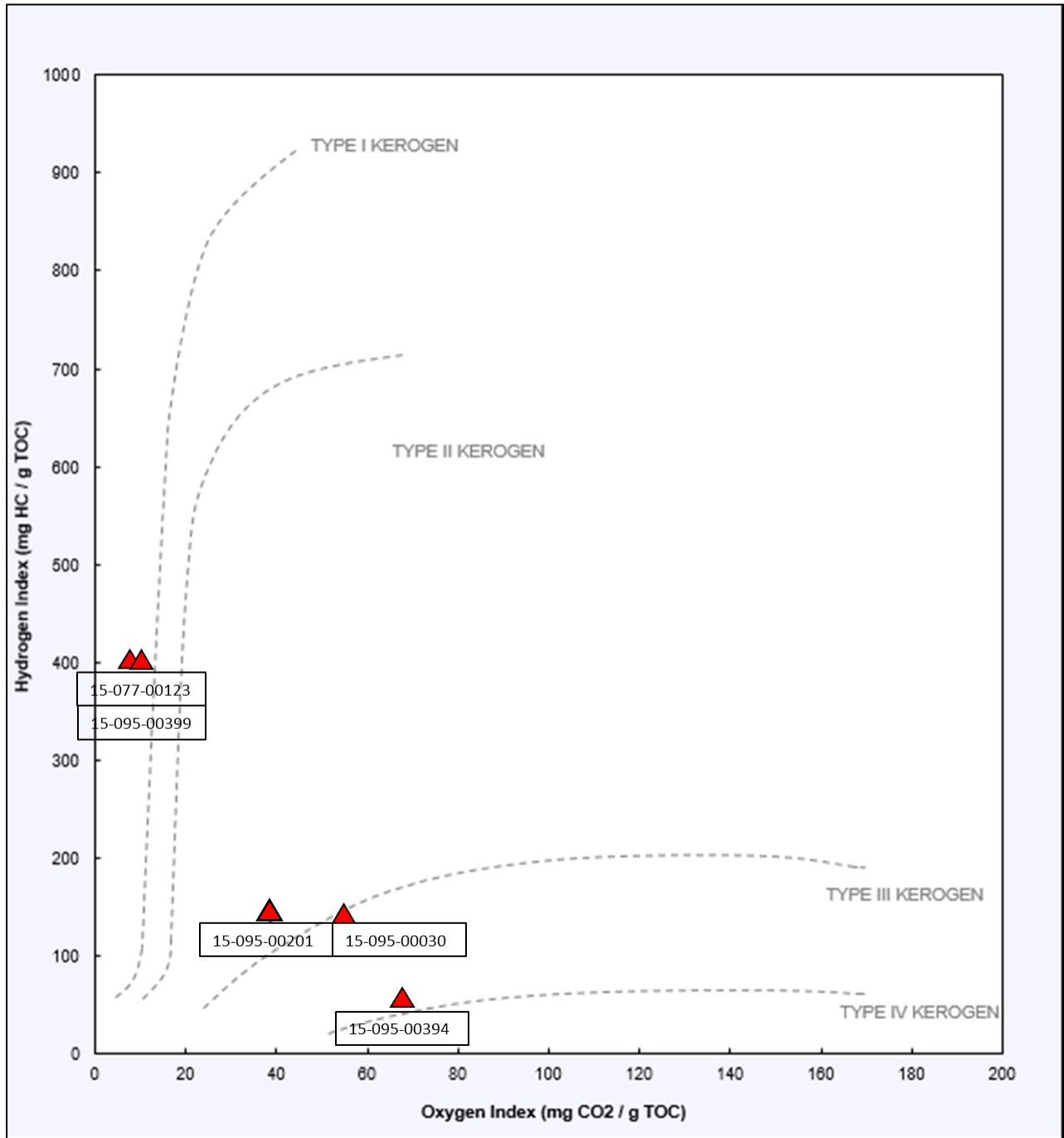


Figure 13 - Oxygen Index vs. Hydrogen Index and predicted kerogen type.

Figure 14 displays the samples in their kerogen type regimes once more, this time using TOC and S2 data.

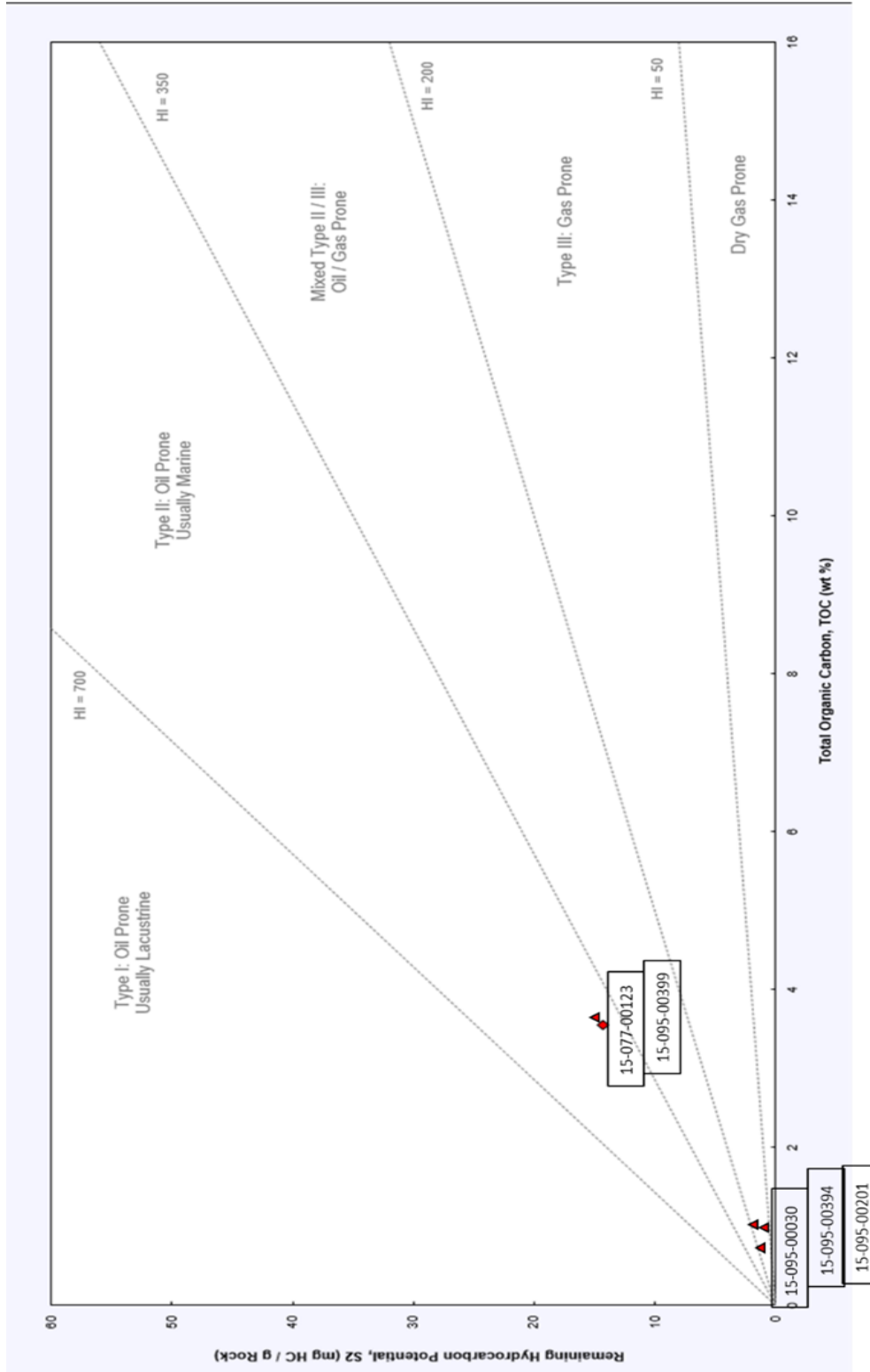


Figure 14 - TOC vs. S2 (remaining hydrocarbon potential) and their generative capacity

4.2 – Gas Chromatography and Mass Spectrometry Results

The gas chromatography diagrams supplied by GeoMark came with the peaks and important ratios already provided as shown in Figures 15 and 16.

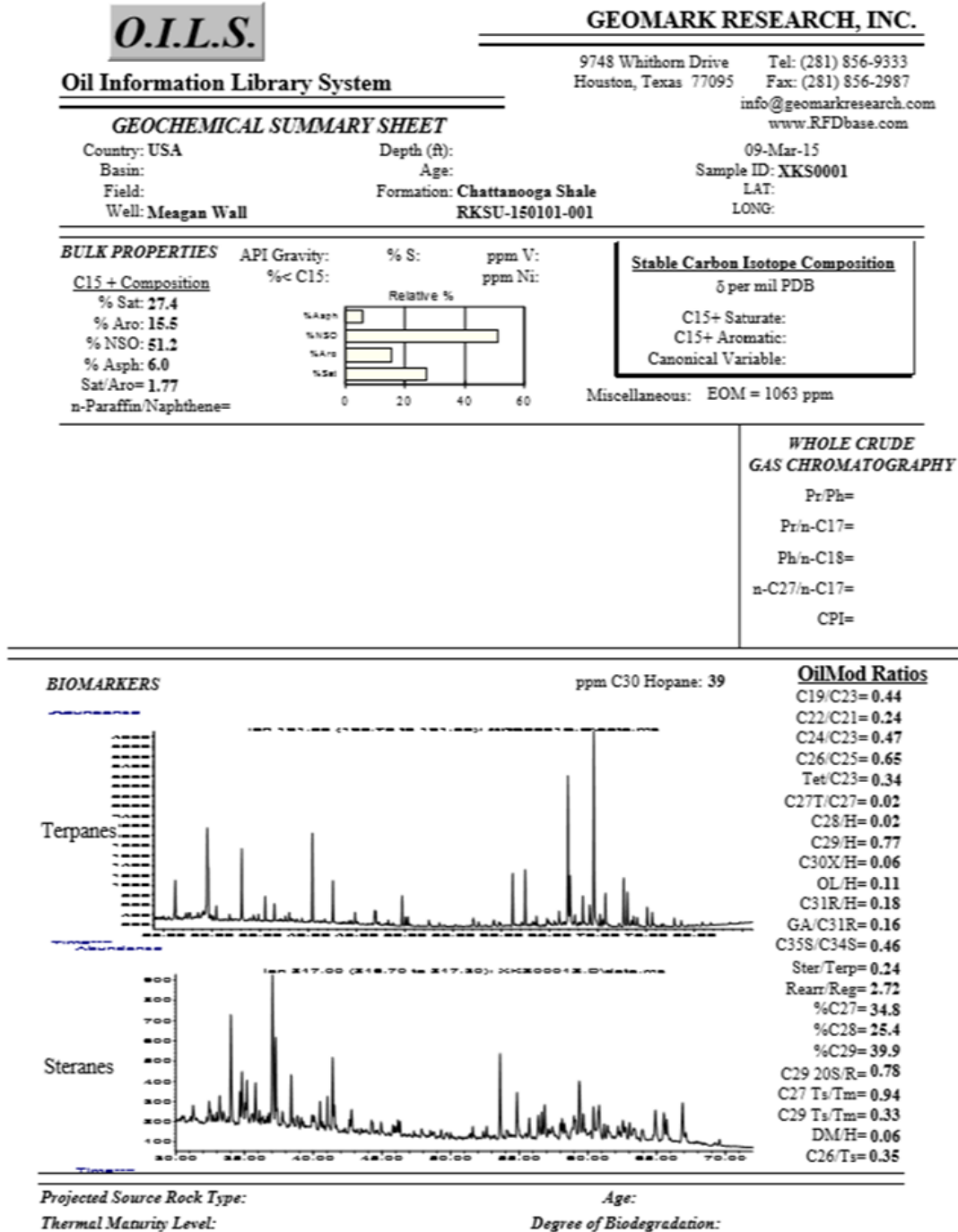


Figure 15 - Gas chromatography peaks for terpanes and steranes with important ratios outlined to the right.

The basic report from GeoMark is shown in Figures 17 and 18. The values were used to compare to the crude oils in Evans (2011). The biomarkers used were restricted to the information provided by the previous study, and most of the shorter chain hydrocarbons (less than C19) are not shown.

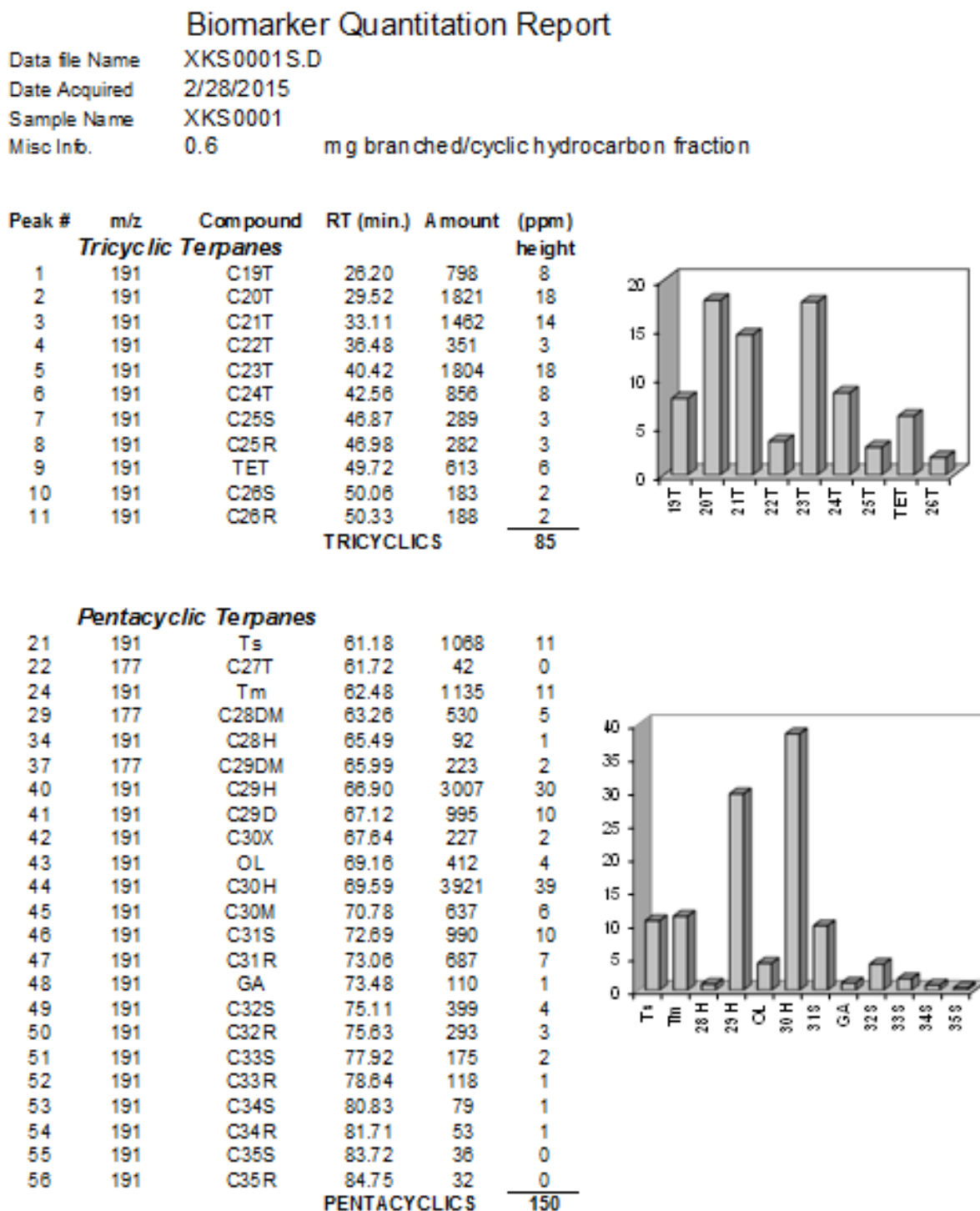
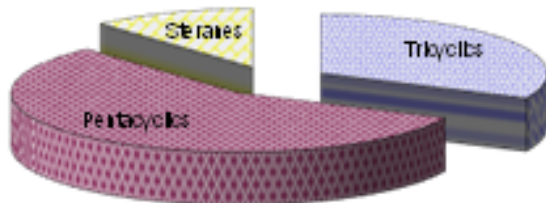
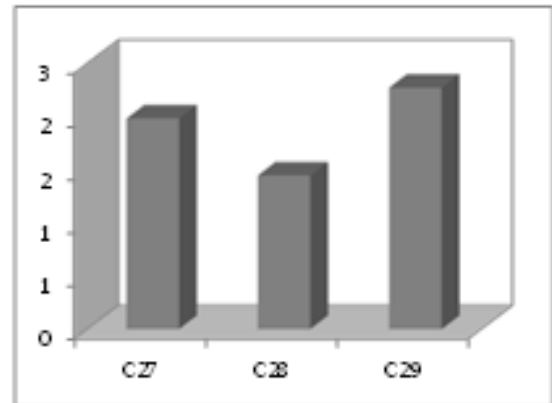


Figure 17 - Compositional breakdown of biomarkers found in the Chattanooga Shale: Tricyclic Terpanes and Pentacyclic Terpanes.

Biomarker Quantitation Report (Cont.)
XKS0001

| Peak # | m/z | Compound | RT (min.) | Amount | (ppm) |
|-----------------|-----|----------|-----------|--------|-----------|
| Steranes | | | | | |
| 12 | 217 | S1 | 53.81 | 424 | 6 |
| 13 | 217 | S2 | 54.85 | 224 | 3 |
| 14 | 217 | S3 | 58.99 | 66 | 1 |
| 15 | 217 | S4 | 59.38 | 280 | 4 |
| 16 | 218 | S4B | 59.38 | 214 | 3 |
| 17 | 217 | S5 | 59.85 | 98 | 1 |
| 18 | 218 | S5B | 59.85 | 144 | 2 |
| 19 | 217 | S6 | 60.40 | 156 | 2 |
| 20 | 217 | S7 | 60.81 | 168 | 2 |
| 23 | 217 | S8 | 62.19 | 60 | 1 |
| 25 | 217 | S9 | 62.72 | 58 | 1 |
| 26 | 218 | S9B | 62.75 | 82 | 1 |
| 27 | 217 | S10 | 63.03 | 80 | 1 |
| 28 | 218 | S10B | 63.03 | 105 | 1 |
| 30 | 217 | S11 | 63.98 | 59 | 1 |
| 31 | 217 | S12 | 64.92 | 154 | 2 |
| 32 | 217 | S13 | 65.52 | 140 | 2 |
| 33 | 218 | S13B | 65.52 | 184 | 3 |
| 35 | 217 | S14 | 65.73 | 108 | 1 |
| 36 | 218 | S14B | 65.74 | 165 | 2 |
| 38 | 221 | ISTD | 66.78 | 6048 | 83 |
| 39 | 217 | S15 | 66.90 | 197 | 3 |
| STERANES | | | | | 31 |



| Key Ratios | | | |
|-------------------|--------|---------|--------|
| | Height | | Height |
| C19/C23 | 0.44 | Ts/Tm | 0.94 |
| C21/C23 | 0.81 | 29D/29 | 0.33 |
| C22/C23 | 0.19 | C27T/27 | 0.02 |
| C24/C23 | 0.47 | DM/H | 0.06 |
| C26/C25 | 0.63 | C27/H | 0.56 |
| Tet/C23 | 0.34 | C28/H | 0.02 |
| | | X/H | 0.06 |
| S1/S6 | 2.72 | C29/H | 0.77 |
| %C27 | 35 | M/H | 0.16 |
| %C28 | 25 | OL/H | 0.11 |
| %C29 | 40 | GA/H | 0.03 |
| 20S/20R | 0.78 | C31/H | 0.18 |
| S/T | 0.24 | C35/C34 | 0.46 |
| | | C23/H | 0.46 |

Figure 18 - Compositional breakdown of biomarkers found in the Chattanooga shale: Steranes and key ratios.

4.3 - Inductively Coupled Plasma-Mass Spectrometry and Inductively Coupled Plasma-Atomic Emission Spectrometry Results

Tables 4 and 5 are the raw data supplied by the University of Strausburg in France and have been corrected for this study's dilution preparation. Charts created for this study and shown in the discussion precluded the major elements (ICP-AES data).

| Element-> | La | Ce | Pr | Nd | Sm | Eu | Gd | Tb | Dy | Ho | Er | Tm | Yb | Lu |
|-------------|--------|--------|-------|--------|-------|------|-------|------|-------|------|------|------|------|------|
| Sample ID | | | | | | | | | | | | | | |
| MW-OM-00030 | 34.60 | 77.70 | 9.97 | 38.80 | 5.05 | 1.10 | 4.40 | 0.88 | 6.15 | 1.40 | 4.75 | 0.73 | 5.25 | 0.88 |
| MW-OM-00056 | 187.00 | 375.00 | 47.30 | 186.00 | 30.40 | 4.72 | 27.70 | 2.43 | 14.40 | 2.83 | 9.20 | 1.16 | 7.88 | 1.16 |
| MW-OM-00123 | 61.20 | 130.00 | 16.10 | 61.40 | 7.51 | 1.65 | 7.10 | 1.23 | 9.09 | 2.06 | 7.00 | 1.05 | 7.59 | 1.20 |
| MW-OM-00201 | 60.10 | 121.00 | 15.10 | 55.10 | 6.51 | 1.45 | 5.50 | 0.73 | 4.48 | 0.89 | 2.86 | 0.36 | 2.46 | 0.35 |
| MW-OM-00391 | 82.20 | 167.00 | 19.10 | 70.80 | 8.26 | 1.73 | 7.30 | 1.24 | 8.80 | 1.96 | 6.77 | 1.01 | 7.36 | 1.13 |
| MW-OM-00394 | 68.00 | 139.00 | 16.20 | 59.70 | 6.90 | 1.47 | 5.80 | 1.03 | 7.59 | 1.70 | 5.85 | 0.87 | 6.17 | 0.97 |
| MW-OM-00399 | 105.00 | 204.00 | 23.50 | 84.00 | 9.35 | 1.95 | 8.00 | 1.33 | 9.67 | 2.11 | 7.14 | 1.03 | 7.33 | 1.11 |

ICP-MS Organic Fraction: Lanthanide concentrations

| Element-> | Rb | Y | Zr | Cd | Sn | Sb | Cs | Pb | Th | U |
|-------------|-------|-------|--------|------|------|------|-------|-------|-------|-------|
| Sample ID | | | | | | | | | | |
| MW-OM-00030 | 65.10 | 47.60 | 172.00 | 0.78 | 0.09 | 0.09 | 8.63 | 6.40 | 3.05 | 10.60 |
| MW-OM-00056 | 19.80 | 76.10 | 74.60 | 0.35 | 0.02 | 0.02 | 6.22 | 34.40 | 31.20 | 10.90 |
| MW-OM-00123 | 81.80 | 56.10 | 131.00 | 4.15 | 0.03 | 0.14 | 15.80 | 29.80 | 15.10 | 37.60 |
| MW-OM-00201 | 30.10 | 20.40 | 7.85 | 0.16 | 0.02 | 0.05 | 16.30 | 8.97 | 12.70 | 4.68 |
| MW-OM-00391 | 11.60 | 51.70 | 138.00 | 4.10 | 0.01 | 0.02 | 9.45 | 17.80 | 36.70 | 17.90 |
| MW-OM-00394 | 79.40 | 43.00 | 120.00 | 5.94 | 0.04 | 0.05 | 10.40 | 46.80 | 16.90 | 17.60 |
| MW-OM-00399 | 22.00 | 52.30 | 79.50 | 1.00 | 0.03 | 0.05 | 21.20 | 25.80 | 34.00 | 20.50 |

ICP-MS Organic Fraction: Element concentrations

| Num Lab | Si | Al | Mg | Ca | Fe | Mn | Ti | Na | K | P | Sr | Ba | V | Ni | Co | Cr | Zn | Cu |
|-------------|------|-------|-------|-------|-------|------|------|-------|-------|------|--------|-------|-------|-------|-------|------|---------|-------|
| MW-OM-00030 | 1.89 | 7.33 | 16.20 | 15.50 | 1.95 | 0.13 | 0.05 | 7.66 | 49.32 | 0.03 | 217.00 | 35.52 | 14.30 | 34.80 | 15.10 | 0.50 | 177.20 | 54.50 |
| MW-OM-00056 | 1.52 | 6.11 | 13.20 | 15.50 | 8.23 | 0.12 | 0.02 | 4.17 | 25.54 | 0.26 | 296.00 | 75.84 | 11.80 | 17.30 | 9.60 | 3.90 | 48.00 | 21.10 |
| MW-OM-00123 | 1.86 | 7.96 | 26.00 | 24.90 | 3.39 | 0.28 | 0.05 | 6.91 | 67.83 | 0.13 | 388.00 | 35.54 | 20.70 | 63.20 | 27.00 | 1.40 | 266.40 | 55.60 |
| MW-OM-00201 | 1.55 | 10.10 | 1.86 | 20.20 | 1.62 | 0.05 | 0.03 | 5.86 | 32.81 | 0.16 | 415.00 | 60.89 | 18.00 | 1.40 | 1.10 | 1.40 | 8.30 | 4.50 |
| MW-OM-00391 | 2.42 | 7.39 | 4.27 | 25.30 | 0.41 | 0.18 | 0.07 | 17.50 | 21.25 | 0.09 | 497.00 | 57.80 | 14.60 | 4.40 | 6.40 | 0.40 | 855.90 | 18.10 |
| MW-OM-00394 | 1.17 | 6.23 | 19.10 | 17.10 | 15.30 | 0.32 | 0.03 | 8.37 | 56.64 | 0.10 | 316.00 | 96.93 | 11.40 | 79.20 | 27.00 | 2.40 | 1080.00 | 73.50 |
| MW-OM-00399 | 1.56 | 9.05 | 3.19 | 34.60 | 0.41 | 0.13 | 0.05 | 10.80 | 37.37 | 0.16 | 841.00 | 39.46 | 23.90 | 3.90 | 3.40 | 0.50 | 73.50 | 6.80 |

ICP-AES Organic Fraction: Element concentrations

Table 4 - Organic fraction results from ICP-MS/ICP-AES experiment run by the University of Strasbourg, corrected for dilutions.

| élément | La | Ce | Pr | Nd | Sm | Eu | Gd | Tb | Dy | Ho | Er | Tm | Yb | Lu |
|-------------|--------|--------|-------|--------|-------|------|-------|------|-------|------|-------|------|------|------|
| MW-IN-00030 | 108.33 | 246.95 | 36.42 | 168.51 | 28.79 | 6.95 | 24.43 | 3.72 | 20.03 | 3.51 | 9.17 | 1.00 | 6.17 | 0.84 |
| MW-IN-00056 | 150.13 | 275.31 | 41.56 | 191.18 | 34.09 | 8.15 | 31.27 | 4.82 | 26.56 | 4.67 | 12.34 | 1.34 | 8.12 | 1.13 |
| MW-IN-00123 | 90.72 | 179.19 | 26.05 | 87.52 | 19.02 | 4.54 | 17.24 | 2.76 | 14.78 | 2.69 | 7.23 | 0.81 | 4.96 | 0.70 |
| MW-IN-00201 | 101.35 | 224.00 | 32.03 | 147.59 | 25.72 | 5.90 | 21.61 | 3.30 | 17.86 | 3.15 | 8.47 | 0.95 | 5.96 | 0.83 |
| MW-IN-00391 | 87.24 | 189.94 | 25.42 | 112.53 | 19.10 | 4.39 | 16.68 | 2.47 | 13.55 | 2.38 | 6.40 | 0.71 | 4.41 | 0.62 |
| MW-IN-00394 | 95.04 | 185.30 | 24.66 | 76.47 | 15.82 | 3.72 | 13.09 | 2.11 | 11.24 | 2.00 | 5.44 | 0.61 | 3.77 | 0.53 |
| MW-IN-00399 | 93.51 | 209.87 | 29.52 | 128.53 | 21.52 | 5.02 | 16.91 | 2.64 | 14.49 | 2.50 | 6.66 | 0.73 | 4.55 | 0.61 |

ICP-MS Inorganic Fraction: Lanthanide concentrations

| élément | Rb | Y | Zr | Cd | Sn | Sb | Cs | Pb | Th | U |
|-------------|-------|--------|--------|------|-------|------|------|--------|-------|-------|
| MW-IN-00030 | 26.26 | 150.08 | 124.11 | 1.51 | 7.49 | 3.16 | 2.12 | 184.90 | 51.51 | 9.28 |
| MW-IN-00056 | 17.23 | 212.09 | 89.39 | 3.11 | 6.99 | 5.19 | 1.60 | 99.64 | 55.29 | 16.85 |
| MW-IN-00123 | 18.36 | 123.26 | 97.48 | 2.12 | 7.19 | 8.51 | 1.57 | 205.69 | 23.79 | 14.51 |
| MW-IN-00201 | 12.60 | 143.17 | 96.24 | 1.96 | 15.54 | 5.63 | 0.93 | 434.93 | 46.51 | 12.78 |
| MW-IN-00391 | 14.94 | 91.61 | 123.19 | 1.87 | 8.03 | 5.39 | 1.53 | 107.10 | 31.71 | 9.54 |
| MW-IN-00394 | 14.16 | 74.80 | 104.25 | 1.06 | 6.67 | 1.98 | 1.09 | 52.28 | 23.01 | 8.59 |
| MW-IN-00399 | 19.53 | 81.08 | 127.20 | 2.15 | 8.38 | 3.50 | 1.88 | 75.83 | 48.27 | 11.65 |

ICP-MS Inorganic Fraction: Element concentrations

| Num Lab | Si | Al | Mg | Ca | Fe | Mn | Ti | Na | K | P | Sr | Ba | V | Ni | Co | Cr | Zn | Cu |
|-------------|------|-------|--------|------|--------|------|------|-------|-------|-------|---------|--------|--------|--------|-------|--------|--------|--------|
| MW-IN-00030 | 0.25 | 14.71 | 91.87 | 2.24 | 73.90 | 2.86 | 2.39 | 13.88 | 10.95 | 11.39 | 1072.49 | 142.71 | 219.60 | 295.30 | 72.10 | 269.20 | 609.10 | 61.80 |
| MW-IN-00056 | 0.07 | 17.02 | 95.74 | 0.60 | 73.80 | 4.18 | 1.93 | 17.94 | 12.88 | 6.27 | 874.44 | 57.60 | 180.40 | 232.70 | 72.10 | 256.90 | 306.80 | 31.50 |
| MW-IN-00123 | 0.18 | 14.55 | 65.57 | 2.32 | 59.50 | 3.07 | 2.06 | 7.80 | 10.25 | 5.01 | 956.31 | 88.04 | 267.60 | 204.80 | 57.20 | 243.50 | 557.30 | 42.50 |
| MW-IN-00201 | 0.21 | 16.09 | 103.04 | 0.43 | 140.20 | 5.03 | 2.15 | 16.33 | 11.55 | 4.98 | 723.94 | 82.39 | 189.60 | 264.50 | 77.10 | 313.30 | 485.00 | 129.70 |
| MW-IN-00391 | 0.05 | 13.81 | 88.11 | 1.87 | 73.60 | 2.58 | 2.31 | 7.25 | 9.85 | 4.26 | 929.30 | 151.14 | 218.30 | 250.40 | 69.10 | 297.20 | 521.20 | 54.20 |
| MW-IN-00394 | 0.05 | 15.73 | 59.49 | 0.79 | 47.40 | 2.15 | 2.11 | 8.52 | 10.02 | 3.42 | 17.56 | 119.94 | 168.80 | 152.30 | 48.20 | 202.70 | 276.00 | 29.90 |
| MW-IN-00399 | 0.96 | 15.63 | 70.53 | 3.75 | 80.10 | 2.10 | 2.29 | 14.46 | 10.94 | 6.77 | 1383.00 | 172.41 | 265.80 | 190.40 | 64.60 | 362.90 | 446.50 | 51.40 |

ICP-AES Inorganic Fraction: Element concentrations

Table 5 - Inorganic fraction (combined carbonate-silicate) results from ICP-MS/ICP-AES experiment run by the University of Strasbourg, corrected for dilutions.

Chapter 5 – Discussion

5.1 – Total Organic Carbon

The total organic carbon is a measure of the organic richness of a shale. All of the samples in this study have TOC values that fall within the parameters for oil generation as set forth by McCarthy (2011) (Figure 19). The TOC weight percent totals for all five of the samples run are considered to have a fair or higher value (Table 3). Three of the samples were not picked at the richest part of the Chattanooga shale, and that is reflected in the TOC values. Both of the samples that represent the highest organic content of the Chattanooga (and are likely the best picked), are within the appropriate TOC window. They are also classified as the optimal Type II (algal/marine type) for oil generation (Figure 20). They have peak R_0 (percent of reflected light immersed in oil) values, and early-mature T_{max} values. Conversely, both also have an immature production index ($S1/(S1+S2)$) by comparison to the other picks (Table 3). Given the high likelihood that this shale has produced hydrocarbons, an oil-source rock correlation using the Chattanooga shale unit against the overlying oils in the Spivey-Grabs-Basil was a warranted experiment to run in order to assess economic value. The likelihood of presence of a viable source-rock beneath a producible field that is not genetically related to the oil seems improbable.

The pyrolysis results here have been compared to the average wt. % TOC of the samples collected and analyzed by Hill (2011). His data suggests that there are several units in the state of Kansas that are generating, or have generated, producible hydrocarbons. The results from the Chattanooga shale endorse that perspective.

The R_0 values in the Spivey-Grabs-Basil are higher than those in Hill (2011) (Figure 20), especially given the small number of data points used in this analysis. Given the location of the Spivey-Grabs-Basil, closer to the Anadarko Basin than the localities studied by Hill (2011), these

initial results are within reason for appropriate thermal maturity values (Figure 38). Both his results and the results from the Chattanooga shale in the Spivey-Grabs-Basil show a very high likelihood for oil generation within the state of Kansas, sans migration from the Anadarko Basin.

These TOC data were compared to two sets of data. First the LECO TOC results from producing wells in the Woodford shale (Ramirez-Caro, 2013) a known commercially producing unit in Oklahoma shows a range of 0.36 to 11.5 wt. % (Table 6). The results outlined by Hill (2011) show a range of 1.8 to 13.3 wt.% for multiple shales in Kansas which, when compared to the Woodford are reasonable values for oil generation. The Chattanooga shale TOC values have a range between 0.72 and 3.95 wt.% and fits into the range of values from the Woodford well enough to conclude that the Chattanooga shale is a viable source rock (Figure 21). While the TOC results above may not be strong enough to conclude that the Chattanooga shale is commercially productive, it is in keeping with results in other parts of Kansas and Oklahoma that show values that could be linked to generative capability.

| Source rock quality | TOC, % | Pyrolysis S2, mg hydrocarbons/g rock | EOM weight, % | Hydrocarbons, ppm |
|---------------------|----------|--------------------------------------|---------------|-------------------|
| None | < 0.5 | < 2 | < 0.05 | < 200 |
| Poor | 0.5 to 1 | 2 to 3 | 0.05 to 0.1 | 200 to 500 |
| Fair | 1 to 2 | 3 to 5 | 0.1 to 0.2 | 500 to 800 |
| Good | 2 to 5 | 5 to 10 | > 0.2 | > 1,200 |
| Very good | > 5 | > 10 | | |

| Product type | Hydrogen index |
|--------------|----------------|
| Gas | 50 to 200 |
| Gas and oil | 200 to 300 |
| Oil | > 300 |

| Stage | T_{max} |
|------------------|-----------|
| Onset of oil | |
| Type I kerogen | -445°C |
| Type II kerogen | -435°C |
| Type III kerogen | -440°C |
| Onset of gas | -460°C |

Figure 19 – TOC Evaluation. McCarthy et al., 2011

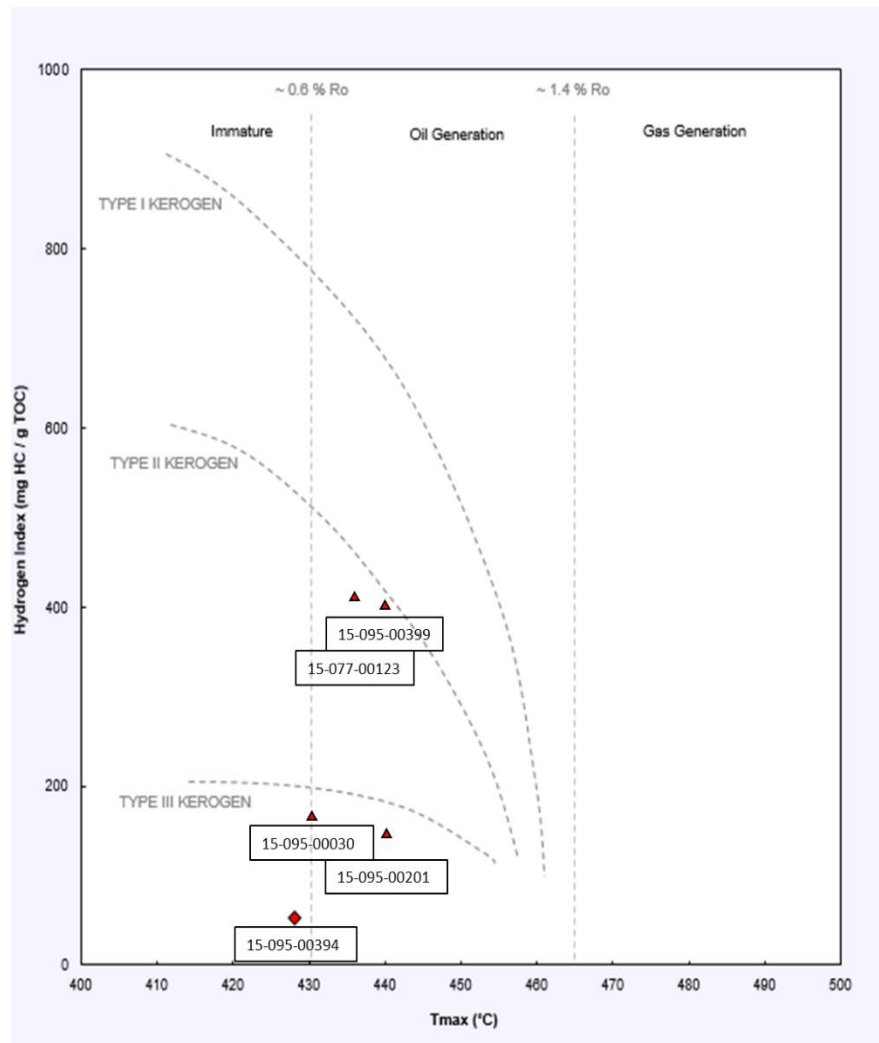


Figure 20 – Hydrogen Index (mg HC/gTOC) vs. T_{max} ($^{\circ}$ C), showing Kerogen type of all 5 wells and oil generative capacity based on R_0 values.

| WELL NAME | LECO |
|--------------------------|-------|
| | TOC |
| Shell McCalla Ranch WF#1 | 1.74 |
| Mobil Sara Kirk WF#2 | 1.09 |
| Mobil Rahm Lela WF#3 | 4.62 |
| Shell Guthrie WF#4 | 6.51 |
| Mobil Dwyer Mt WF#5 | 6.05 |
| Mobil Cement Ord WF#6 | 6.54 |
| Amerada Chenoweth WF#7 | 3.19 |
| Apexco Curtis WF #8 | 11.50 |
| Jones and Pellow WF#9 | 6.05 |
| Lonestar Hannah WF#10 | 0.36 |

Table 6 – LECO TOC values from Ramirez-Caro, 2013. Lab testing conducted by Weatherford Laboratories.

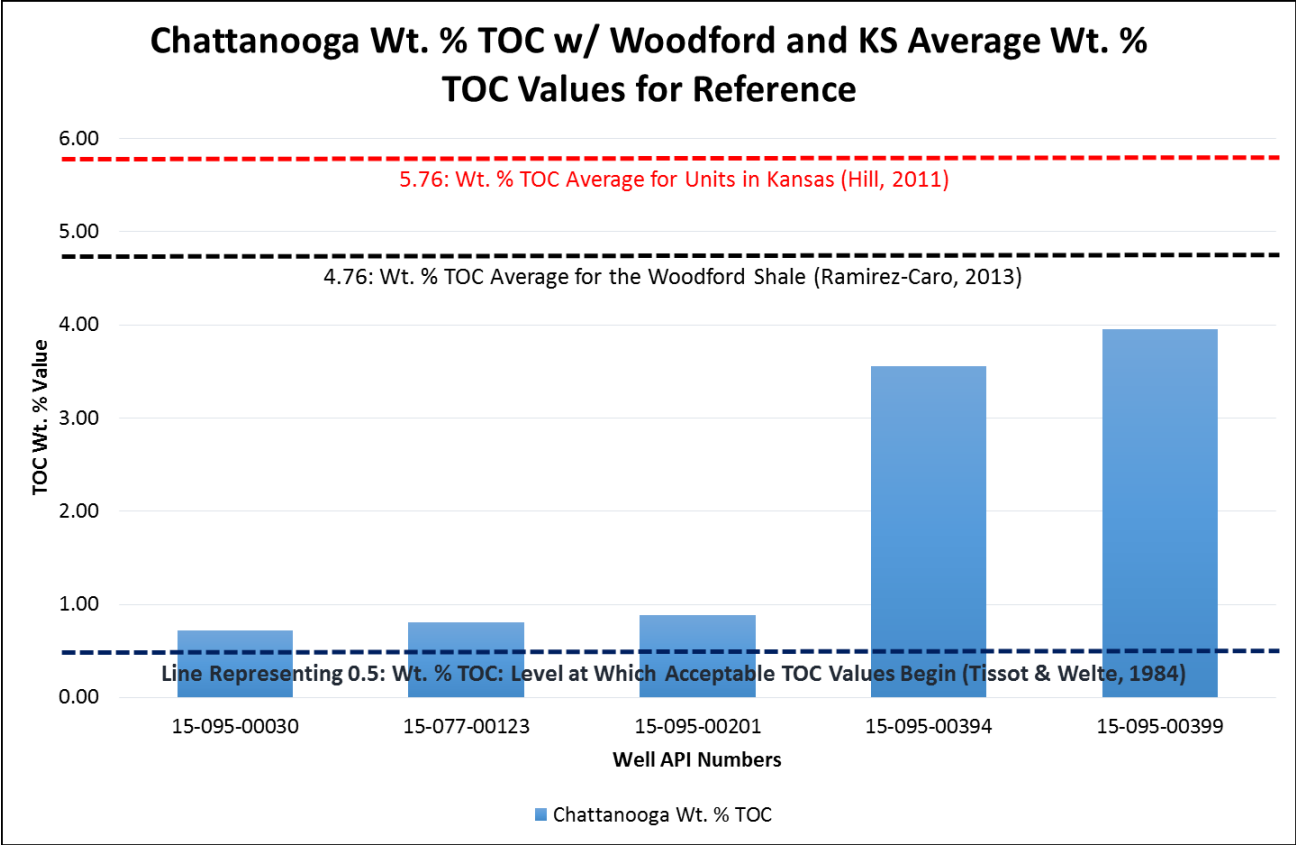


Figure 21 – Chattanooga Wt. % TOC with lines representing minimum acceptable TOC values for production and average TOC wt. % for the Woodford shale and samples across the state of Kansas

5.2 – Biomarkers

The Chattanooga shale is organically rich enough to be a source rock. Did the Chattanooga shale produce the oil which overlies it in the Spivey-Grabs-Basil field? The biomarker results can tell us detailed story about both potential source rocks and crude oils such as “source, maturity, age, migration, depositional environment and extent of biodegradation” (Philp, 2004). The purpose of this research, however, is to relate the potential source rock to the overlying crude oils. Oils produced during pyrolysis of Chattanooga shale are compared to actual oils as described in Evans (2011). In particular, the sterane percentages are evaluated, and the pentacyclic terpanes are also compared.

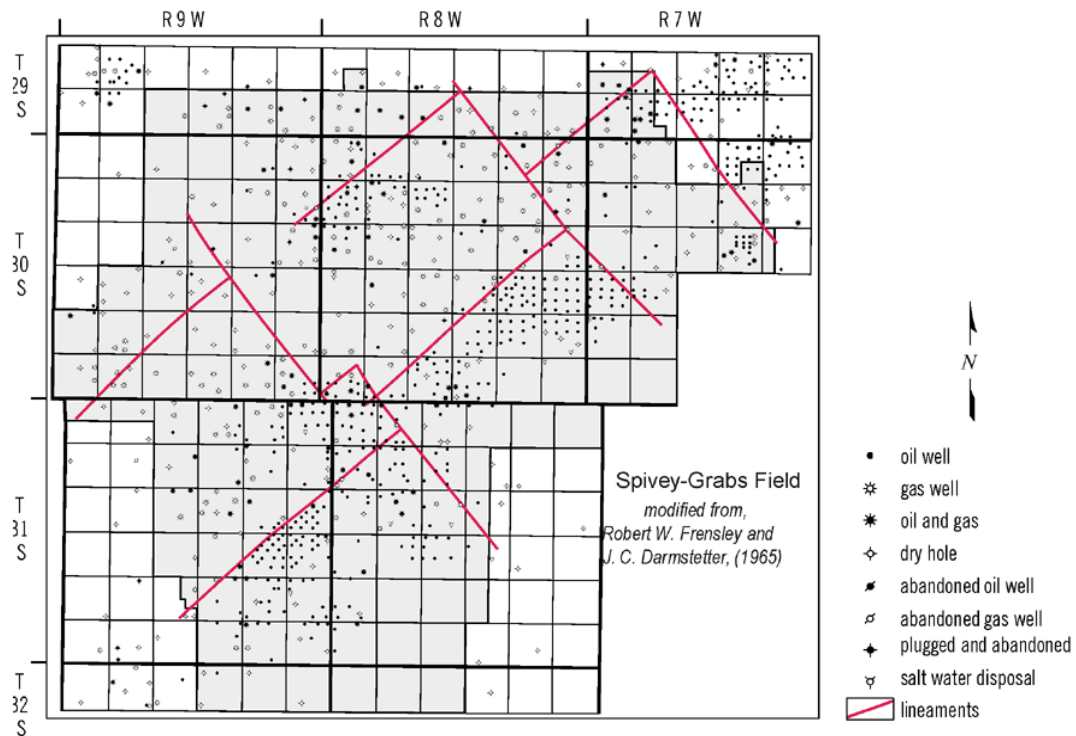


Figure 22 - Well locations and lineaments (maps modified by Kansas Geological Survey from Frensley and Darmstetter, 1965).

Evans' thesis was designed to explore and verify the hypothesis that the Spivey-Grabs-Basil is compartmentalized, as outlined by Frenley and Darmstetter (1965) (Figure 22). His results show a carbonate shale source rock with two different maturities on a biomarker maturation index. He concluded that no mixing has taken place between the two oils, and that there have been at least two charge events leading to different maturities from a single source (Figure 23).

Considering the findings that the crude oils in the Spivey-Grabs-Basil is single-sourced (Evans, 2011), similarities in percent composition and pentacyclic terpanes are very indicative of source. Additional comparison to the source rock depositional environment and source type will be used to substantiate the initial comparative results.

By comparing biomarker ratios, notably the sterane percentages (Figure 24) and the pentacyclic terpanes (Figure 25), a consistent similarity in composition between the crude oil and the source rock is seen, which is indicative of a positive oil-source rock correlation.

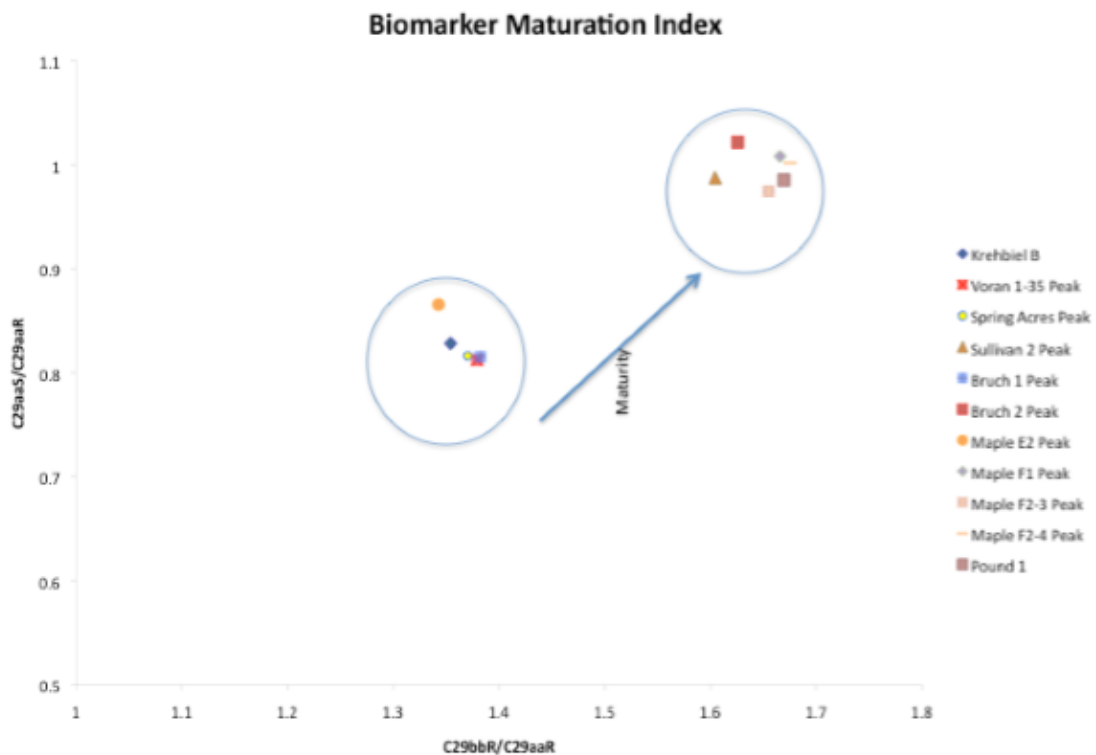


Figure 23 – Biomarker maturation index from Evans,

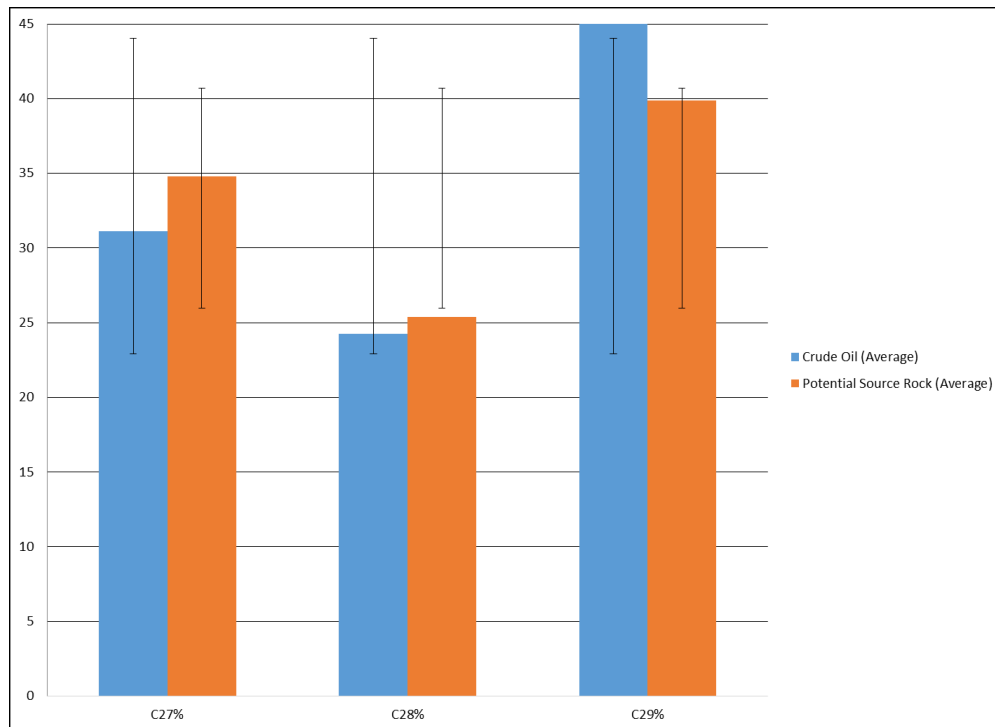


Figure 24 - Comparison of biomarkers (steranes) from crude oil (Evans, 2011) against the Chattanooga shale with standard deviation.

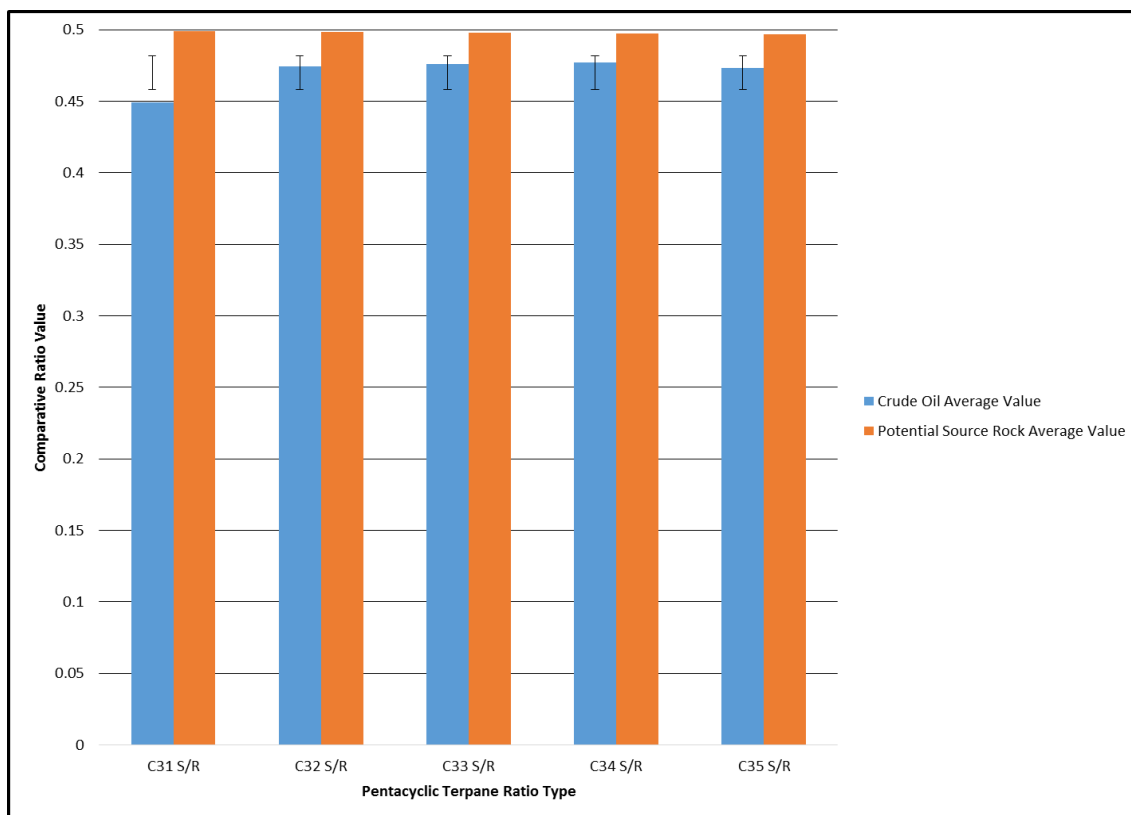


Figure 25 - Comparison of biomarkers (pentacyclic terpanes) from crude oil (Evans, 2011) against the Chattanooga shale with standard deviation error bars.

Additional comparisons to be considered are the predicted source rock's depositional environment, as well as the predicted source type from the biomarkers in the crude oil. Both figures below are from Evans (2011) with the red star on each plot representing the values for the combined source rock sterane and terpane ratios from this study. In Figure 26 and Figure 27, while the source rock values occur outside of the specific scatter area indicated by the original data, the numbers indicate a rock type and source type that lies within the same parameters of the crude oils predictions.

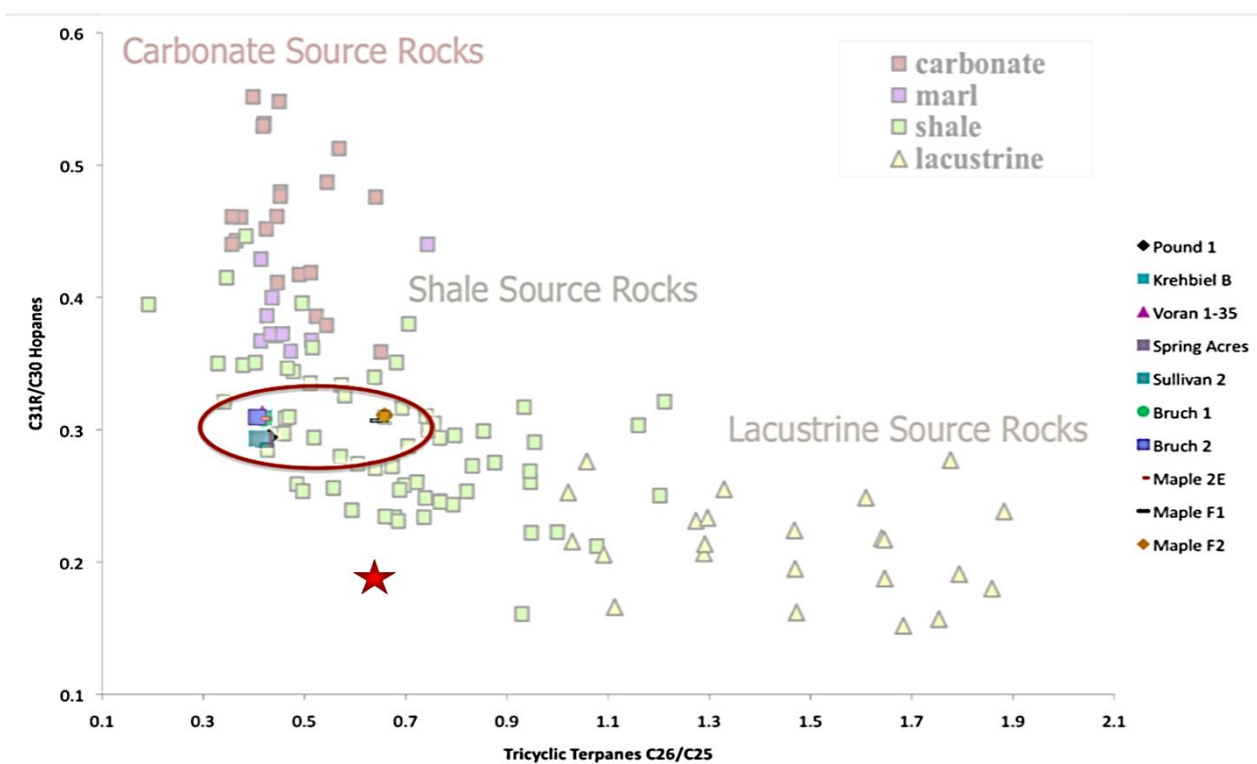


Figure 26 - Predicted oil source rock values are circled in red. Chattanooga terpane vs. hopane ratios represented by the red star (Ferworn et al., 2003)

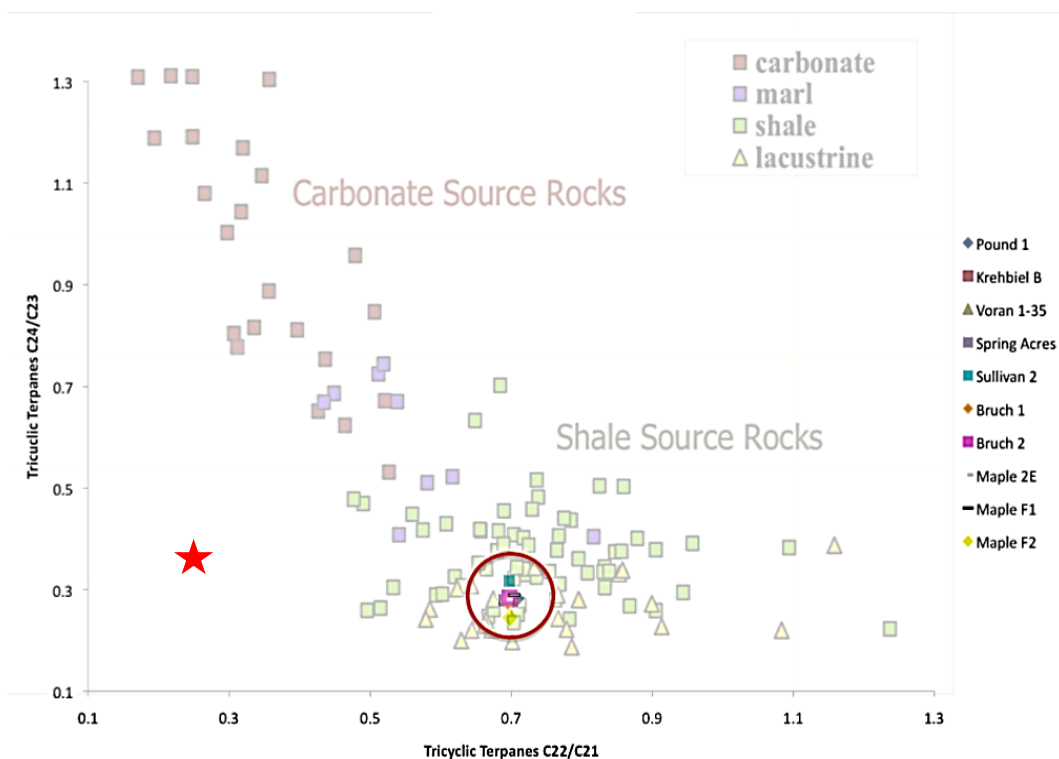


Figure 27 - Predicted oil source rock type values derived from tricyclic terpanes are circled in red while the red star represents the source as a shale type. (Ferworn et al., 2003)

The crude oil tricyclic terpanes predict the rock type and most closely match the source rock numbers (Figure 28). This very close match is strong evidence that the underlying Chattanooga was the source of the oils in the field. This source only requires upward migration on the order of a few hundred feet which, while difficult, is much more likely than the long distance migration of previous models given the resolving correlation.

Consideration must also be given for the Woodford as a possible source rock, considering the relationship between the Chattanooga and the Woodford being formed at the same time. With the use of a ternary diagram, it is possible to see that, while the Woodford resembles the Chattanooga in depositional environment, its sterane concentrations are not as close a match to the Spivey-Grabs-Basil crude oil (Figure 29).

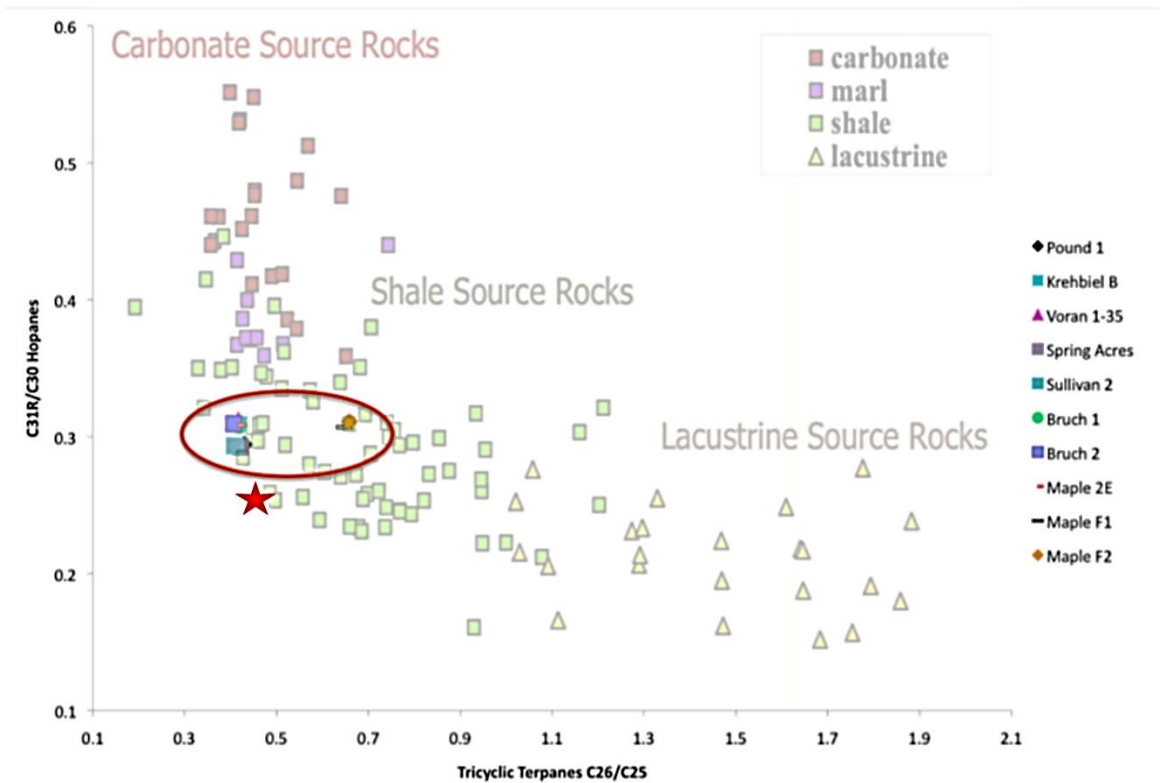


Figure 28 - Crude oil source rock prediction type circled in red and source rock tricyclic terpane ratios vs. hopanes represented by the red star (Ferworn et al., 2003)

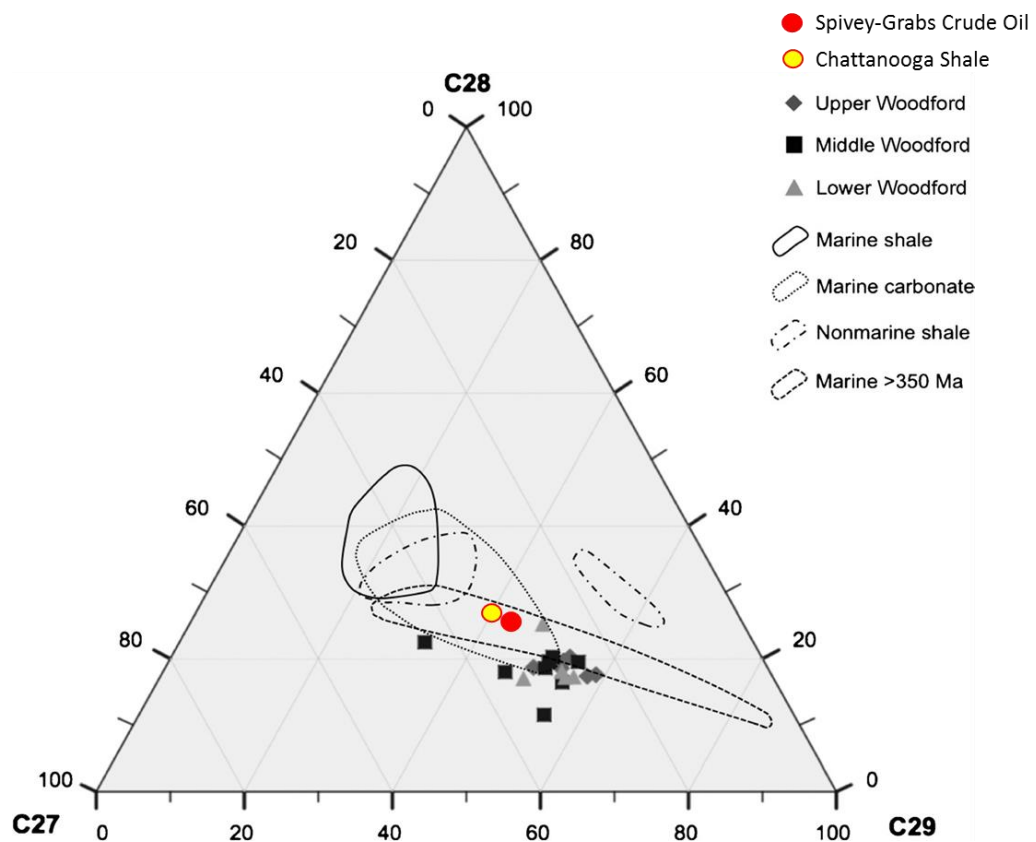


Figure 29 - Ternary diagram of C₂₇, C₂₈, and C₂₉ steranes Woodford Shale samples, with Spivey-Grabs-Basil field data added (Modified from: Woodford values by Philp, 2012, and plot template from Moldowan et al., 1985).

The biomarker analysis of the crude oils encompass pristane (C19) and phytane (C20) ratios. The Pr/Ph ratio in a crude oil can be used to predict source rock type (marine or terrigenous). That being said, the crude oil Pr/Ph and Pr/Pr+Ph was plotted against the same values for the Chattanooga (Figure 30). While the ratios here appear to deviate from the positive oil-source rock correlation that has been proven, Peters et al. (2005) warns against basing the entirety, or even partiality of the correlation on these ratios since “the origins of [pristane] and [phytane] are more complex than simply the reduction or oxidation of the phytol side chain in chlorophylls”. He continues to state that while some pristane might evolve from reduction and oxidation, “most of the pristane in crude oils originates by thermal cleavage of isoprenoid moieties bound by non-hydrolyzable C-C and/or C-O bonds within the kerogen matrix” (Peters et al., 2005). This shows that over time, the crude oil pristane levels should grow while the source rock will maintain original pristane levels, making sense of the inverse Pr/Ph relationship.

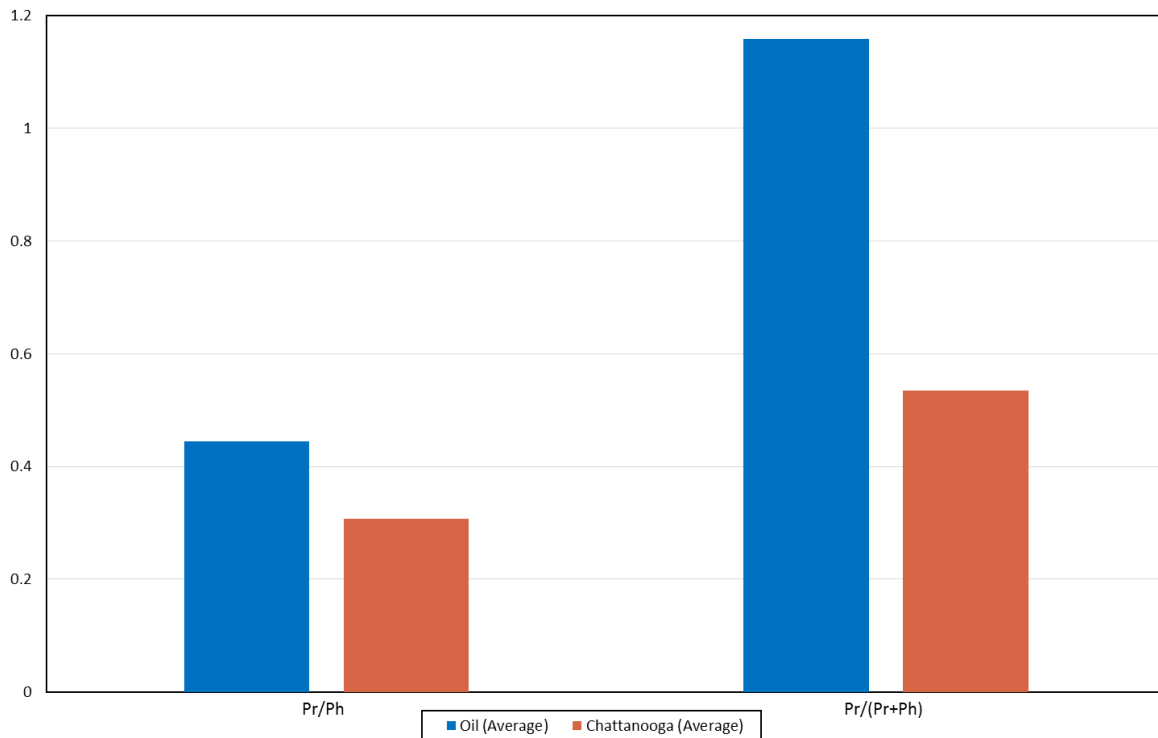


Figure 30 – Average oil and Chattanooga shale Pristane/Phytane ratio concentrations.

5.3 – Rare Earth Element Chemistry of the Chattanooga Shale

5.3.1 – REE's of the Organic Fraction

Here the REE concentrations have been normalized to PAAS (Post Archean Australian Shale). The REE patterns of the Chattanooga shale within the Spivey Grabs are very consistent with the exception of one sample. The patterns show an enrichment of the light rare earth elements (LREE) and heavy rare earth elements (HREE), with a middle rare earth element (MREE's) depletion (Figure 31). The one outlier (MW-OM-00056) has a similar HREE pattern, but is enriched in both LREE and MREE over the other samples.

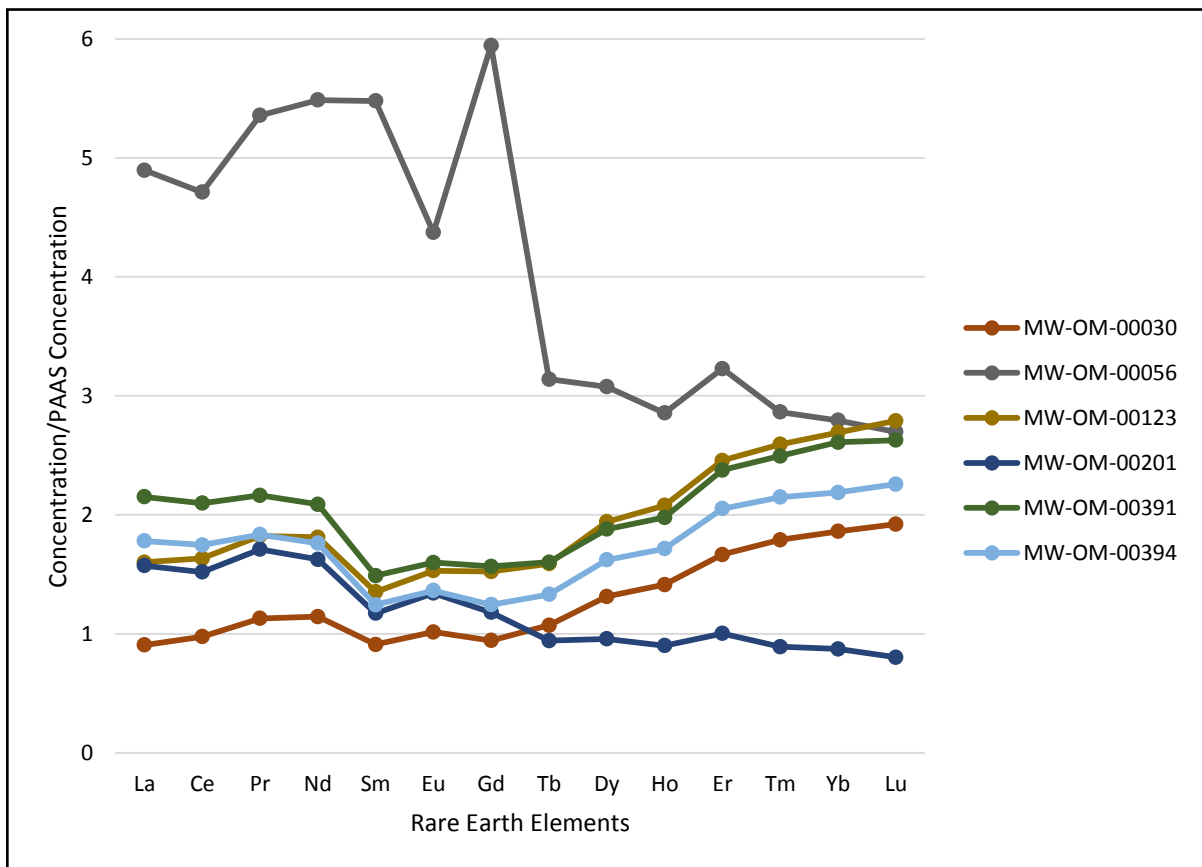


Figure 31 - Organic fraction of the Chattanooga shale normalized to PAAS, corrected for dissolved organic matter dilution and plotted relatively against the rare earth element constituents.

When the outlier is excluded, depletion versus enrichment patterns of the typical samples are more easily compared (Figure 32). The depletion in the MREE's is much more obvious, with a positive europium anomaly. They all show a gradual enrichment in the HREE's and a general enrichment in the LREE's, with a small negative cerium anomaly.

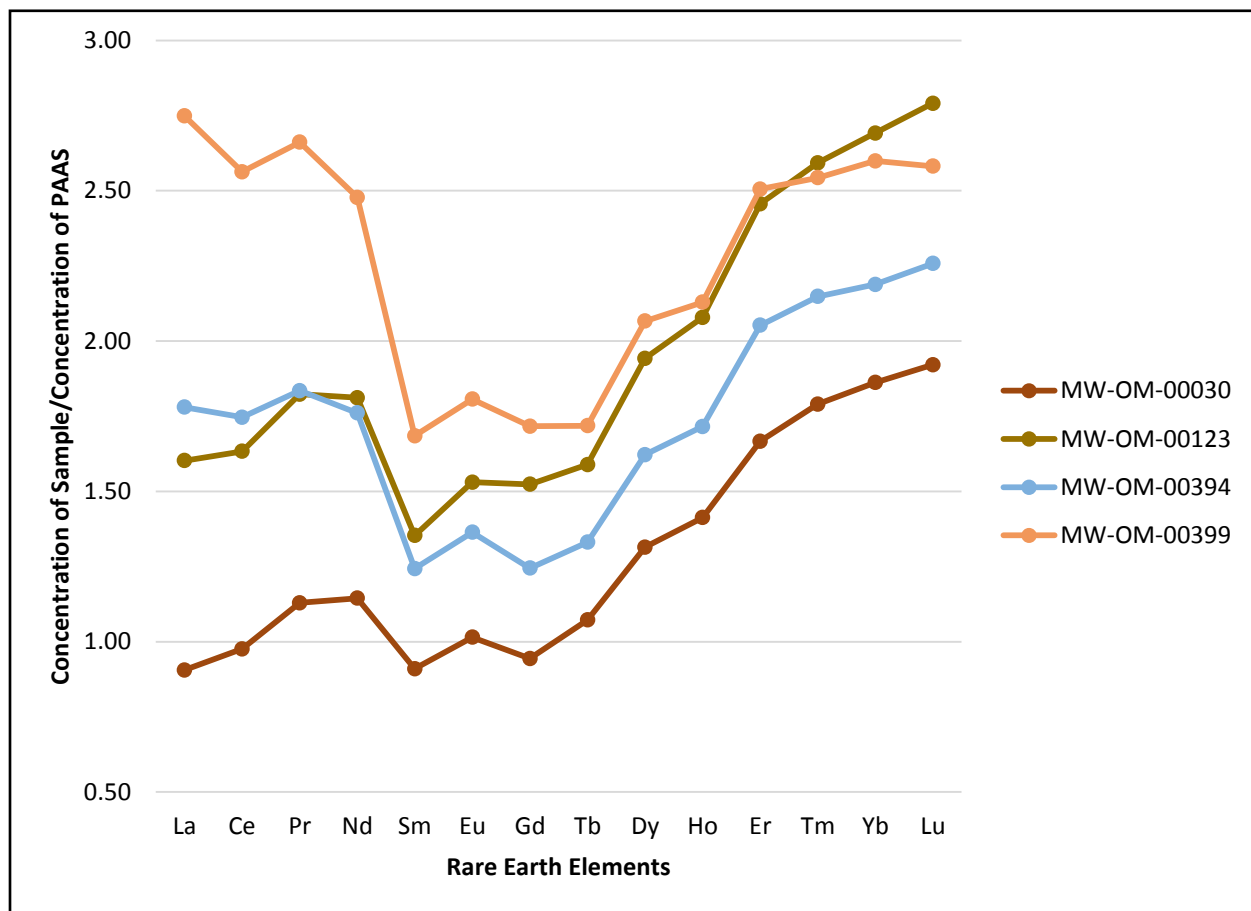


Figure 32 - Organic fraction of the Chattanooga shale normalized to PAAS, corrected for dilution and plotted relatively against the rare earth element

5.3.2 – REE Correlation between Source and Crude Oils

Brianna Kwasny's concurrent research is investigating the utility of rare earth elements within the crude oil, in relation to Drew Evans' biomarker research, to learn what components might be useful fingerprints. Since her research to date is still underway, only her REE results are shown to compare with the Chattanooga patterns (Figure 33).

The most obvious trends in the crude oil REE data are an enrichment of cerium, which inversely reflects the depletion seen in the source rock. Also, the negative europium anomalies in the crude oil contrast to the slight positive anomalies in the source rock. This suggests a connection where cerium is preferred in the crude, leaving a corresponding depletion in the parent organic matter. The inverse relation is seen in europium, where this element is preferred in the source material, hence is depleted in the crude. In both cases, the overall patterns in the crude oil are an inverse of the potential source rock: overall depleted in LREE's, enriched in MREE's and again, depleted in HREE's (Figure 33).

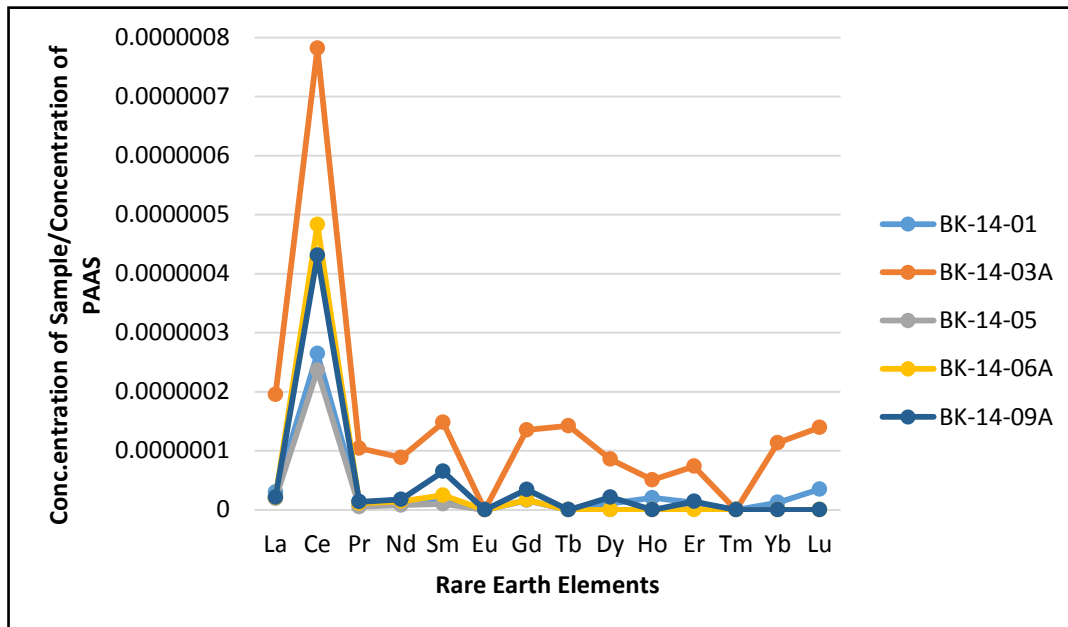


Figure 33 – Crude oil concentrations corrected for dilution and plotted relatively against the rare earth element constituents.

5.3.3 – Comparison of Chattanooga and Woodford Organic Fraction

Ramirez-Caro (2013) examined REE's in both source rock and crude oils from the Woodford shale in Oklahoma, and his combined organic fraction trace element data can be found in Appendix C. The organic fraction of the Woodford shale samples closer to the Kansas border (also analyzed by ICP-MS through the University of Strasbourg) have been added to REE patterns from this study (Figure 34).

The REE patterns in the Woodford are variable, but follow the same general pattern as the Chattanooga samples. The most northward Woodford sample (Grant County, Oklahoma) is in very good agreement. Since the Woodford shale and the Chattanooga are stratigraphically equivalent, the matching pattern was expected. It is not known what the variation in Woodford over such a short distance means.

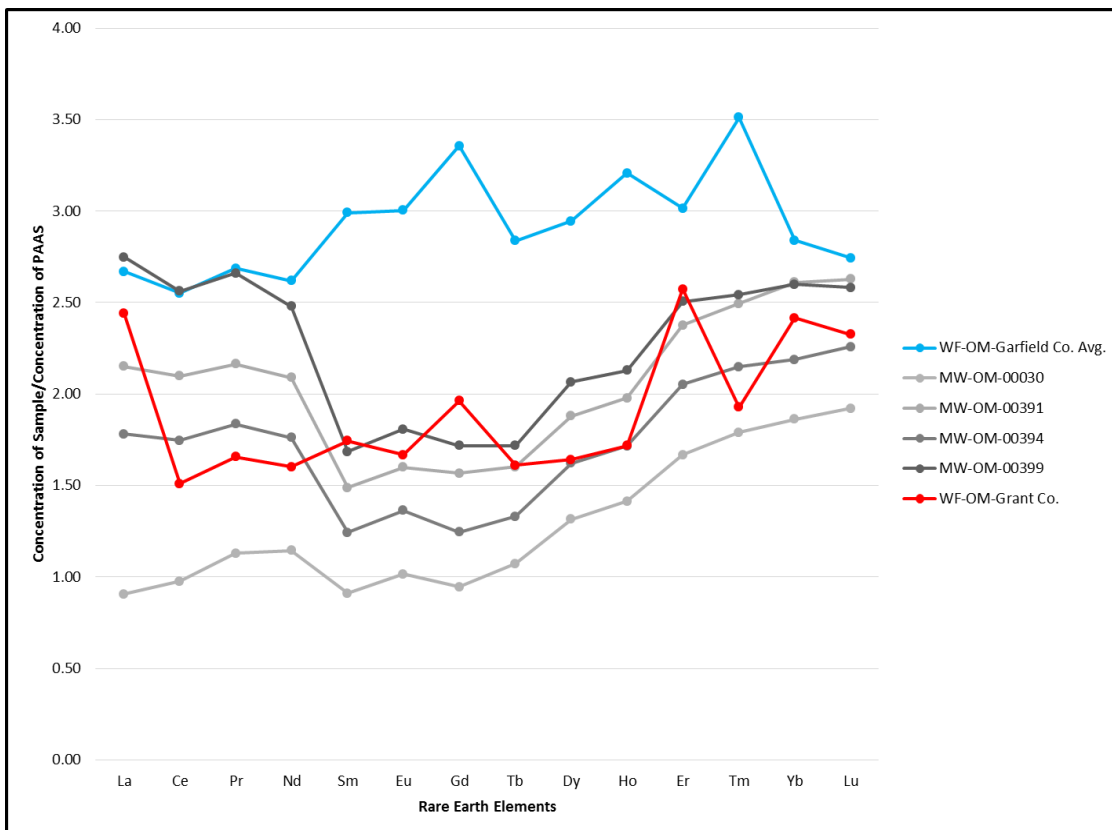


Figure 34 – REE patterns for Chattanooga shale in Harper and Kingman counties (this study) shown in gray. Data from Ramirez-Caro (2013) shown in blue and for a well in Grant County, OK, shown in red.

5.3.4 – REE's of the Silicate-Carbonate Fraction

The patterns shown here show a high enrichment in europium and the other MREE's and depletion throughout the LREE and HREE's by comparison (Figure 35). Several phosphate phases (such as biogenic phosphate, apatite and monazite) are known to be rich in the MREE's (Nagasawa, 1970; Gromet et al., 1983; Grandjean et al., 1989; Demartin et al., 1991).

All of the sampled wells from the Spivey-Grabs-Basil field in Kansas show patterns similar to one another. The concentrations from the Woodford shale are less varied in their concentration by comparison and plotted against the Chattanooga are undistinguishable lines, as shown in Figure 36. A closer look (Figure 37) reveals another striking difference in these two REE compositions, as well as a possible evolving trend in the Woodford towards Kansas. While the negative cerium anomaly can be seen once again, the HREE's reflect depletion in Grant County, which is closer to the Kansas state line than the wells in Garfield County.

The carbonate-silicate REE's offer some insight, however they do not as clearly illustrate relationships as the organic fraction. For the purposes of this oil to source rock correlation, the findings concerning the REE's from the carbonate-silicate fraction are very interesting. The findings imply an intriguing new approach to understanding compositional changes in shales. But, effectiveness of the carbonate-silicate fraction REE's in showing much more than a shift in trend with location is minimal for the purposes of this experiment.

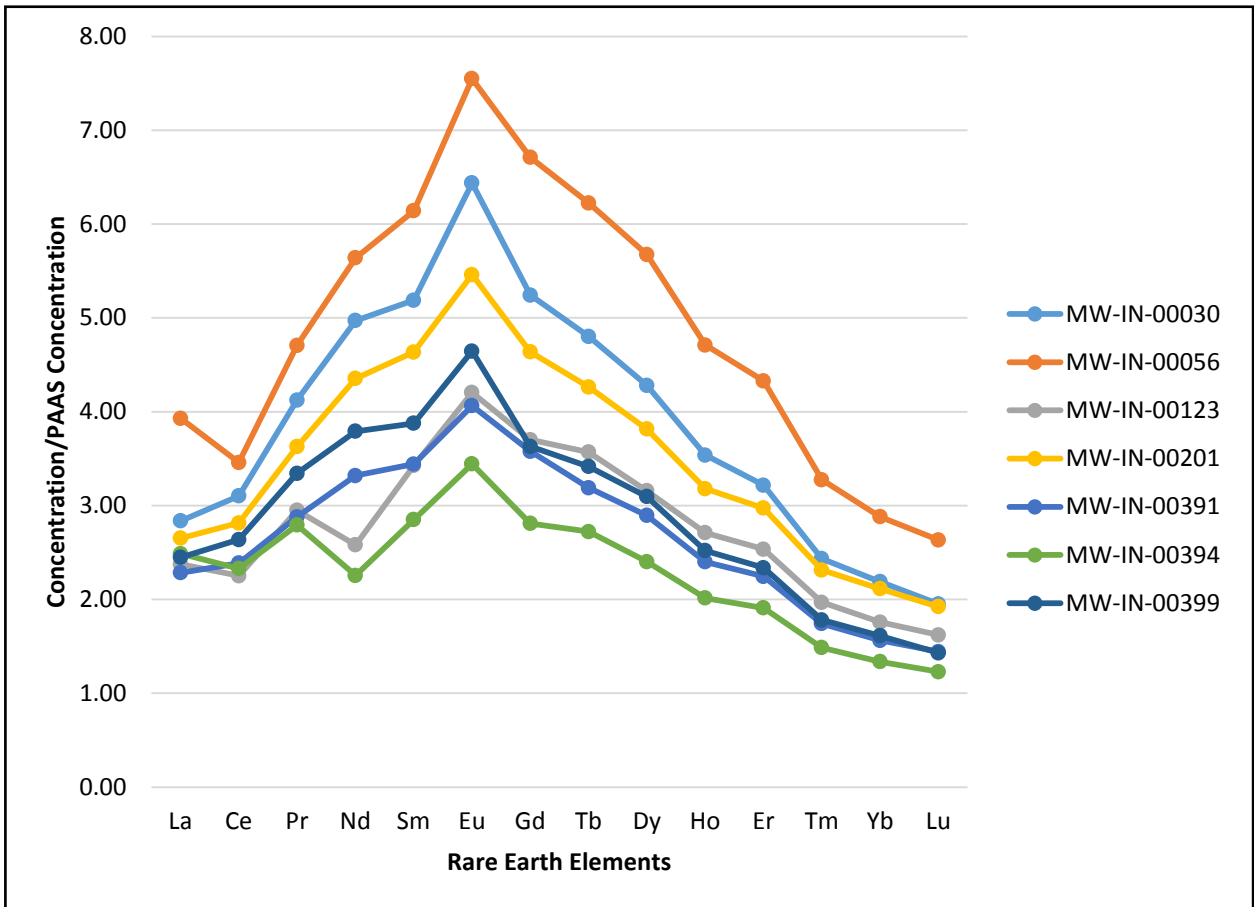


Figure 35 - Inorganic fraction of the Chattanooga shale corrected for dilutions and plotted relatively against rare earth elements.

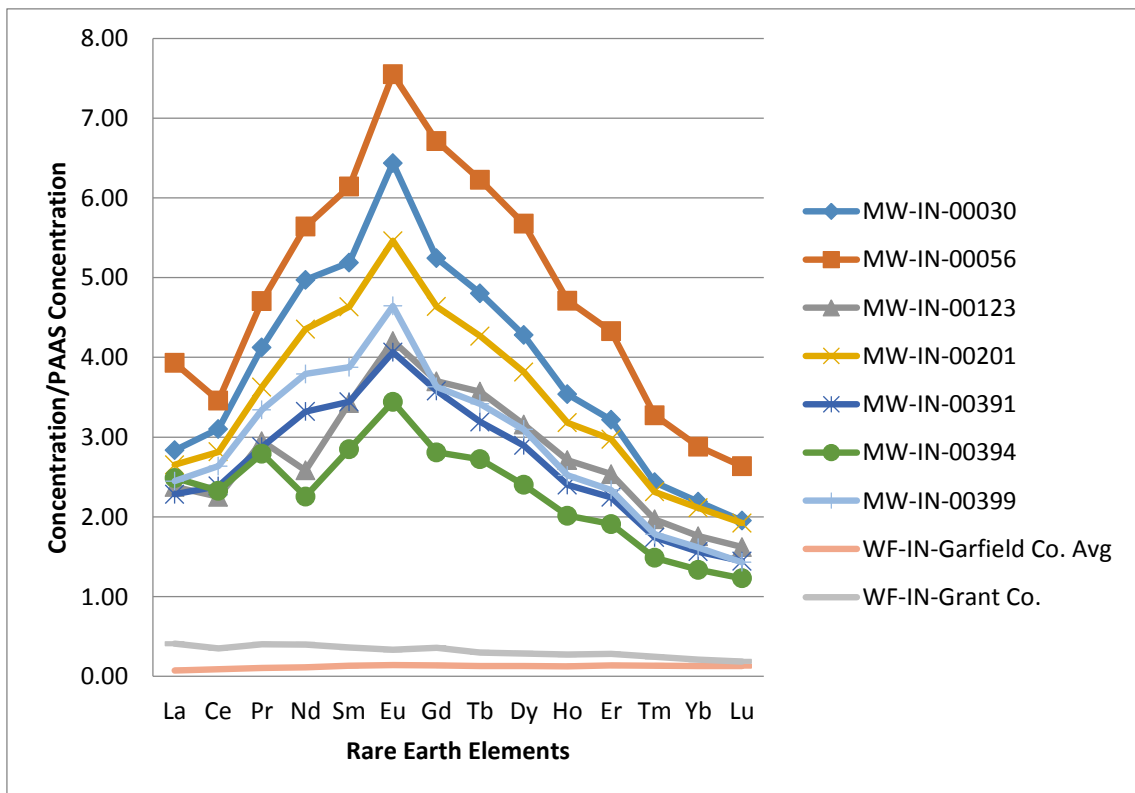


Figure 36 - ICP-MS: Inorganic fraction of the Chattanooga Shale plotted with the Woodford shale inorganic fraction. The bottom two trend lines represent the Woodford.

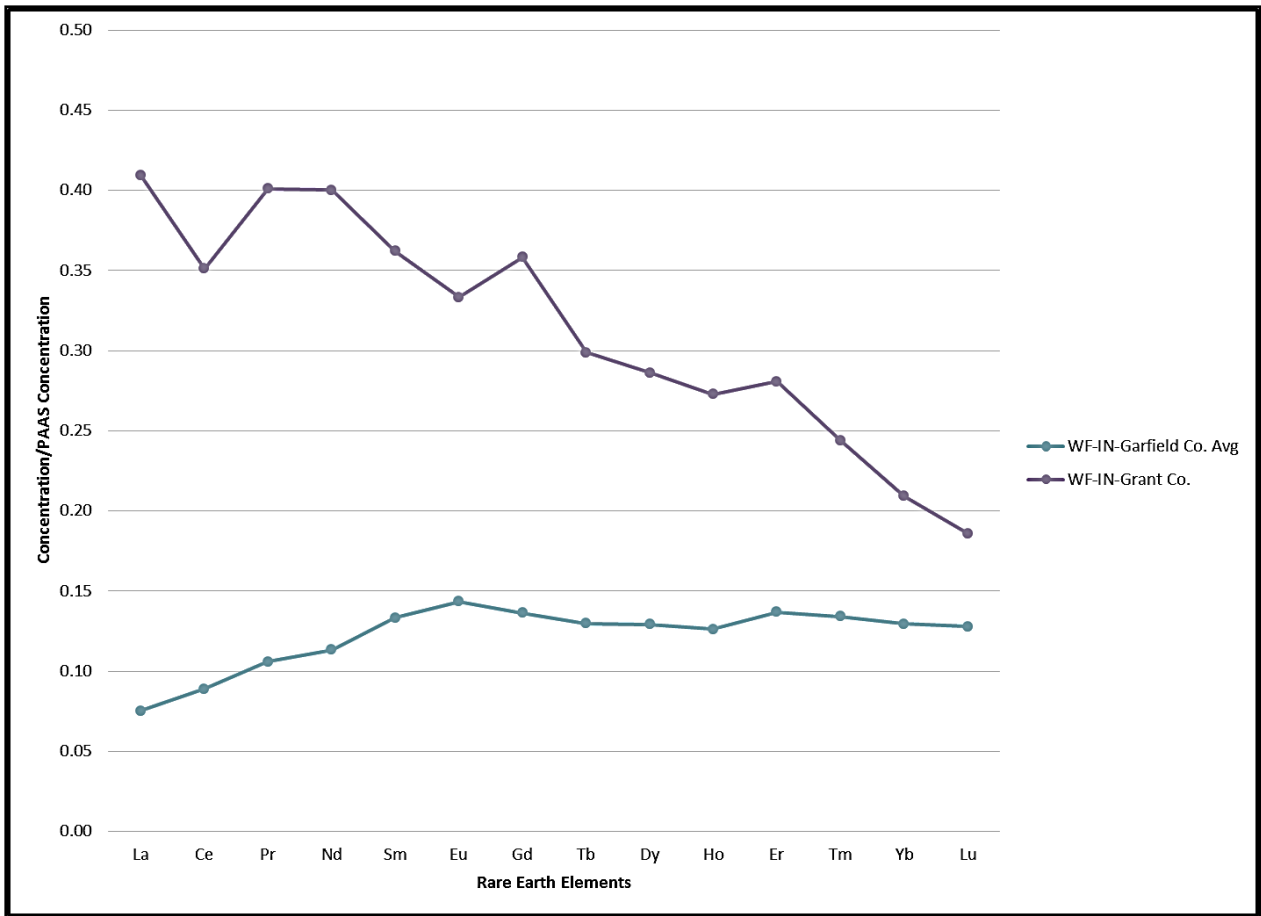


Figure 37 - ICP-MS: Inorganic fraction Woodford shale.

Chapter 6 – Conclusions

No published oil-source rock correlations have been conducted in the Spivey-Grabs-Basil oil field using traditional biomarker fingerprinting, or other methodology that could be found. The combined results from previous studies and this one of the organic potential of Kansas shales show no reason why Kansas rocks would be incapable of generating oil and gas. The most organic rich shale's in Kansas have TOC values even higher in some instances than those found in the Woodford shale in Oklahoma, which is a known source rock.

The biomarker comparisons are conclusive that most, if not all of the oil in the Spivey-Grabs-Basil is genetically the same, or very similar to the Chattanooga shale. While additional analysis should be done in surrounding areas, as well as biomarker comparison with the Woodford shale in Oklahoma, the likelihood of having a potential source rock and a producible oil in the same field that are genetically the same and *not* generatively related is doubtful. However, for a definitive scientific argument to the improbability of such a situation occurring, more studies must be conducted.

The rare earth element analysis of the organic fraction of the source rock appears to agree with the correlation of Chattanooga as a source rock to the Mississippian oils in the Spivey-Grabs field. Inverse relationships of cerium anomalies, europium anomalies, and overall REE enrichments and depletions can all be explained by fractionation between the generated petroleum, and the modified organic matter remaining in the source rock. The larger value of anomalies in the crude oil to the organic matter is a function of its much smaller overall volume.

6.1 – Recommended Future Research

In order to further substantiate the results found in this study, four separate investigations are recommended.

1. Comparisons between the biomarkers in the Chattanooga shale and the Woodford shale should be examined, preferably in north-central Oklahoma near the Kansas border, as well as further south to seek variation within the shale composition.
2. Additional oil-source rock correlations in the state of Kansas, especially within those units which have higher TOC values, ought to be considered. If units with core can be found, results could be more exact, less costly to analyze, and more accurate.
3. Oil to oil correlations across Kansas, especially in fields with compartmentalization might be considered. An investigation into biomarkers and biomarker maturity might prove both surprising, as they did in Evans (2011) and also might lead to the conclusion of a much more complicated burial history for Kansas and other midcontinent plays.
4. The potential of the Chattanooga shale as an unconventional resource should be explored.

References

- Blakely, R. (2015, January). *Dr. Ron Blakey, Professor Emeritus NAU Geology*. Retrieved March 2015, from NAU Geology: <https://www2.nau.edu/rcb7/index.html>
- Chaudhuri, S. (2014). Interpersonal communication.
- Cotton, F. A. (1972). *Advanced Inorganic Chemistry*. New York - London: Interscience Publishers, John Wiley and Sons.
- Demartin, F., Pilati, T., Diella, V., Donzelli, S., & Gramaccioli, C. M. (1991). Alpine monasite: further data. *Canadian Mineralogists*, Vol. 29, 61-67.
- Evans, D. (2011). The compartmentalization and biomarker analysis of the Spivey-Grabs-Basil Field, south-central Kansas. *Thesis Dissertation*, Kansas State University.
- Frensley, R. D. (1965). *Spivey Grabs Field*. US Department of Energy.
- Frensley, R. W. (1965). Spivey-Grabs Field. *Kansas Oil and Gas Fields, Vol. 4 Kansas Geological Survey, 1006*, pp.221-228.
- Gerhard, L. C. (2004). A New Look at an Old Petroleum Province. *Current Research in Earth Sciences, Bulletin 250 (Part 1)*, 1-27.
- Goebel, E. D. (1971). Future petroleum provinces of the Mid-Continent. *Southeast Kansas - Northeast Oklahoma - Southwest Missouri, in Adler*, pp. 1088-1097.
- Grandjean, P., & Albarede, F. (1989). Ion probe measurement of rare earth elements in biogenic phosphates. *Geochimica at Cosmochimica Acta, Vol. 53*, 3179-3183.
- Gratzer, R., Bechtel, A., Sachsenhofer, R. F., Linzer, H., Reischenbacher, D., & Schultz, H. (2011). Oil-oil and oil-source rock correlations in the Alpine Foreland Basin of Austria: Insights from biomarkers and stable carbon isotope studies. *Marine and Petroleum Geology* 28, 1171-1186.
- Gromet, L. P., & Silver, L. T. (1983). Rare earth element distributions among minerals in a granodiorite and their petrogenic implications. *Geochimica at Cosmochimica Acta, Vol. 47*, 925-939.
- Hill, T. J. (2009). *Potential source rocks in the western Kansas petroleum province*. Manhattan, KS: Kansas State University.
- Hunt, J. M. (1995). *Petroleum Geochemistry and Geology: 2nd Edition*. New York: W. H. Freeman and Company.
- Hunt, J. M., Philp, P. R., & Kvenvolden, K. A. (2002). Early developments in petroleum geochemistry. *Organic Geochemistry* 33, 1025-1052.

- Jewett, J. M., O'Connor, H. G., & Zeller, D. E. (2005, August). *Kansas Geological Survey--Stratigraphic Succession in Kansas (1968)*. Retrieved 11 15, 2014, from Kansas Geological Survey: http://www.kgs.ku.edu/Publications/Bulletins/189/07_penn.html
- Korkmaz, S., Kara-Gulbay, R., & Istan, Y. H. (2013). Organic geochemistry of the Lower Cretaceous black shales and oil seep in the Sinop Basin, Northern Turkey: An oil-source rock correlation study. *Marine and Petroleum Geology* 43, 272-283.
- Kwasny, B. (2015). *An investigation of the crude oil in the Spivey-Grabs field of south-central Kansas: an insight into oil type and origin*. Manhattan: Kansas State University.
- Lambert, M. W. (1994). Revised Upper Devonian and Lower Mississippian Stratigraphic Nomenclature in Kansas. *Kansas Geological Survey Bulletin*, 75-78.
- Mazzulo, S. J., Wilhite, B. W., & Woolsey, I. W. (2009). Petroleum reservoirs within a spiculite-dominated depositional sequence: Cowley Formation (Mississippian: Lower Carboniferous), south-central Kansas. *AAPG Bulletin*, Vol. 93, No. 12, 1649-1689.
- McCarthy, K., Neimann, M., & Palmowski, D. P. (2011). Basic Petroleum Geochemistry for Source Rock Evaluation. *Oilfield Review*, v. 23, No. 2, 32-43.
- McIntire, M. C. (2014). Rare earth elements (REE) in crude oil in the Lansing-Kansas City formations in central Kansas: potential indications about their sources, locally derived or long-distance derived. *Thesis Dissertation: Kansas State University*.
- Merriam, D. F. (1963). The geologic history of Kansas. *Kansas Geological Survey Bulletin*, pp. 162, 317.
- Moldowan, J., Peters, K. E., & Walters, C. C. (2005). *The Biomarker Guide: Second Edition: Biomarkers and Isotopes in Petroleum Exploration and Earth History: 2nd edition*, v. 2. United Kingdom: Cambridge University Press.
- Nagasawa, H. (1970). Rare earth concentrations in zircons and apatites and their host dacites and granites. *Earth and Planetary Science Letters*, Vol. 9, 359-364.
- Peters, K. E., Walters, C. C., & Moldowan, J. M. (2006). *The Biomarker Guide: p. 72-118*. New York: Cambridge University Press.
- Philp, R. P. (2004). Formation and Geochemistry of Oil and Gas. In F. T. Mackenzie, *Treaties on Geochemistry, Volume 7: Sediments, Diagenesis, and Sedimentary Rocks* (pp. 223-256). Oxford: Elsevier.
- Ramirez-Caro, D. (2013). Rare earth elements (REE) as geochemical clues to reconstruct hydrocarbon generation history. *Thesis Dissertation: Kansas State University*.
- Romero, A. a. (2012). Organic geochemistry of the Woodford Shale, southeastern Oklahoma: How variable can shales be? *AAPG Bulletin*, v. 96, no. 3, 493-517.

- Seifert, W. K., & Moldowan, J. M. (1986). Use of biomarkers in petroleum exploration. In R. B. Johns, *Methods in Geochemistry and Geophysics: v. 24* (pp. 261-290). Amsterdam: Elsevier.
- Waples, D. W. (1990). Application of sterane and triterpane biomarkers in petroleum exploration. *Bulletin of Canadian Petroleum Geology*, 357-380.
- Watney, W. L., Kruger, L., Davis, J. C., Harff, J., Olea, R. A., & Bohling, G. C. (1999). Validation of sediment accumulation regions in Kansas: USA. In J. Harff, W. Lemke, & K. Stattegger, *Proceedings of symposium, computerized modeling of sedimentary systems* (pp. 341-360). Berlin: Springer.

Appendix A - GeoMark Methodology

PYROLYSIS

1. Sample Requirements for a Typical Geochemical Program

For geochemical analysis a teaspoon (ca. 10 g.) of sample material is needed when TOC, Rock-Eval, vitrinite reflectance and residual hydrocarbon fluid fingerprinting is to be completed. If possible, a tablespoon is preferred. However, it is possible to complete a detailed program with even less sample, although there is dependency on the sample characteristics (e.g., organic richness, abundance of vitrinite, amount of staining).

2. Total Organic Carbon (TOC) – LECO C230 instrument

Leco TOC analysis requires decarbonation of the rock sample by treatment with hydrochloric acid (HCl). This is done by treating the samples with Concentrated HCL for at least two hours. The samples are then rinsed with water and flushed through a filtration apparatus to remove the acid. The filter is then removed, placed into a LECO crucible and dried in a low temperature oven (110 C) for a minimum of 4 hours. Samples may also be weighed after this process in order to obtain a % Carbonate value based on weight loss.

The LECO C230 instrument is calibrated with standards having known carbon contents. This is completed by combustion of these standards by heating to 1200°C in the presence of oxygen. Both carbon monoxide and carbon dioxide are generated and the carbon monoxide is converted to carbon dioxide by a catalyst. The carbon dioxide is measured by an IR cell. Combustion of unknowns is then completed and the response of unknowns per mass unit is compared to that of the calibration standard, thereby the TOC is determined.

Standards are analyzed as unknowns every 10 samples to check the variation and calibration of the analysis. Random and selected reruns are done to verify the data. The acceptable standard deviation for TOC is 3% variation from established value.

3. Rock Eval

Approximately 100 milligrams of washed, ground (60 mesh) whole rock sample is analyzed in the Rock-Eval II instrument. Organic rich samples are analyzed at reduced weights whenever the S2 value exceeds 40.0 mg/g or TOC exceeds 7-8%. Samples must be re-analyzed at lower weights when these values are obtained at 100 mg.

RE-II Operating Conditions

- S1: 300°C for 3 minutes
- S2: 300°C to 550°C at 25°C/min;
hold at 550°C for 1 minute
- S3: trapped between 300 to 390°

RE-VI Operating Conditions

- S1: 300°C for 3 minutes
- S2: 300°C to 600°C at 25°C/min;
hold at 600°C for 1 minute
- S3: measured between 300 to 400°

HAWK Operating Conditions

- S1: 300°C for 3 minutes
- S2: 300°C to 650°C at 25°C/min;
hold at 650°C for 0 minute
- S3: measured between 300 to 400°

Measurements from Rock-Eval are:

- S1: free oil content (mg HC/g rock)
- S2: remaining generation potential (mg HC/g rock)
- Tmax: temperature at maximum evolution of S2 hydrocarbons (°C)
- S3: organic carbon dioxide yield (mg CO₂/ g rock)

Several useful ratios are also utilized from Rock-Eval and TOC data. These are:

- Hydrogen Index (HI): $S2/TOC \times 100$ (in mg HC/g TOC)
- Oxygen Index (OI): $S3/TOC \times 100$ (in mg CO₂/g TOC)
- Normalized Oil Content: $S1/TOC \times 100$ (in mg HC/g TOC)
- S2/S3:
- Production Index (PI): $S1 / (S1+S2)$

Instrument calibration is achieved using a rock standard. Its values were determined from a calibration curve to pure hydrocarbons of varying concentrations. This standard is analyzed every 10 samples as an unknown to check the instrument calibration. If the analysis of the standard ran as an unknown does not meet specifications, those preceding data are rejected, the instrument recalibrated, and the samples analyzed again. However, normal variations in the standard are used to adjust any variation in the calibration response. The standard deviation is considered acceptable under the following guidelines:

- Tmax: $\pm 2^\circ\text{C}$
- S1: 10% variation from established value
- S2: 10% variation from established value
- S3: 20% variation from established value

Analytical data are checked selectively and randomly. Selected and random checks are completed on approximately 10% of the samples. A standard is analyzed as an unknown every 10 samples.

4. Turnaround Time:

The standard turnaround time for sample orders over the past 12 months is approximately 2 to 3 weeks, depending on number of samples in the order.

GCMS EXTRACTION

1. Dionex ASE 350 Quantitative Extraction

10 grams of powdered sample is weighed into a stainless steel cell then sealed with stainless steel caps. The cells are then loaded onto the Dionex ASE 350 instrument where each cell is individually filled with Dichloromethane and pressurized up to 1400 psi for 5 minutes; the solvent is then flushed into a collection vial. This process is repeated 2 additional times before the extraction is complete. The extract is then air dried at room temperature and weighed after all solvent has evaporated in order to obtain the total extract retained.

GEOMARK RESEARCH

CRUDE OIL EXPERIMENTAL METHODS

Whole Crude Gas Chromatography. Crude oils are injected (split mode 70/1) on a 30m x 0.32mm J&W DB-5 column (0.2 μ m film thickness) and temperature programmed from -60° C to 350° C at 12°/min using an Agilent 7890A gas chromatograph. Helium is used as the carrier gas.

Liquid Chromatographic Separation. Subsequent to determining the <C15 fraction (light ends) by evaporation in a stream of nitrogen for 30 min, and asphaltene precipitation using excess n-hexane (overnight at room temperature), the C15+ deasphalted fractions are separated into saturate hydrocarbon, aromatic hydrocarbon, and NSO (nitrogen-sulfur-oxygen compounds or resin) fractions using gravity-flow column chromatography employing a 100-200 mesh silica

gel support activated at 400° C prior to use. Hexane is used to elute the saturate hydrocarbons, methylene chloride to elute the aromatic hydrocarbons, and methylene chloride/methanol (50:50) to elute the NSO fraction. Following solvent evaporation, the recovered fractions are quantified gravimetrically. The C15+ saturate hydrocarbon fraction is subjected to molecular sieve filtration (Union Carbide S-115 powder) after the technique described by West *et al.* (1990) in order to concentrate the branched/cyclic biomarker fraction.

Stable Isotope Analyses. Stable carbon isotopic compositions ($^{13}\text{C}/^{12}\text{C}$) of the C15+ saturate and aromatic hydrocarbon fractions are determined using the combustion technique of Sofer (1980) and a Finnigan Delta E isotope ratio mass spectrometer. Results are reported relative to the PDB standard.

Gas Chromatography/Mass Spectroscopy (GC/MS). GC/MS analyses of C15+ branched/cyclic and aromatic hydrocarbon fractions (in order to determine sterane and terpane biomarker distributions and quantities) are performed using an Agilent 7890A GC (split injection) interfaced to a 5975C mass spectrometer. He is kept at a constant flow rate throughout the analysis. The J&W DB5 column (50 m x 0.2 mm; 0.11 μm film thickness) is temperature programmed from 150° C to 325° C at 2°/min (branched/cyclic) and 100° C to 325° C at 3°/min for aromatics. The mass spectrometer is run in the selected ion mode (SIM), monitoring ions m/z 177, 191, 205, 217, 218, 221, 231 and 259 amu (branched/cyclic) and m/z 133, 156, 170, 178, 184, 192, 198, 231, 239, 245, and 253 (aromatics). In order to determine absolute concentrations of individual biomarkers, a deuterated internal standard (d4-C29 20R sterane; Chiron Laboratories, Norway) is added to the C15+ branched/cyclic hydrocarbon fraction. A deuterated anthracene standard is added to the aromatic hydrocarbon fraction. Response factors (RF) were determined by comparing the mass spectral response at m/z 221 for the deuterated standard to hopane (m/z 191) and sterane (m/z 217) authentic standards. These response factors were found to be approximately 1.4 for terpanes and 1.0 for steranes. Concentrations of individual biomarkers in the branched/cyclic fraction were determined using the equation shown below:

$$\text{Conc. (ppm)} = [(\text{ht. biomarker})(\text{ng standard})]/[(\text{ht. standard})(\text{RF})(\text{mg b/cy fraction})]$$

Appendix B - Additional Figures

| Maturity | Maturation | | | Generation | | |
|------------|--------------------|-----------------------|---------|--------------|---------------------|-------------------------------|
| | R _o (%) | T _{max} (°C) | TAI | Bitumen/TOC* | Bitumen (mg/g rock) | Production index (S1/(S1+S2)) |
| Immature | 0.20–0.60 | <435 | 1.5–2.6 | <0.05 | <50 | <0.10 |
| Mature | | | | | | |
| Early | 0.60–0.65 | 435–445 | 2.6–2.7 | 0.05–0.10 | 50–100 | 0.10–0.15 |
| Peak | 0.65–0.90 | 445–450 | 2.6–2.7 | 0.15–0.25 | 150–250 | 0.25–0.40 |
| Late | 0.90–1.35 | 450–470 | 2.9–3.3 | – | – | >0.40 |
| Postmature | >1.35 | >470 | >3.3 | – | – | – |

Figure 38 - TOC Evaluation. Modified from Peters (2006).

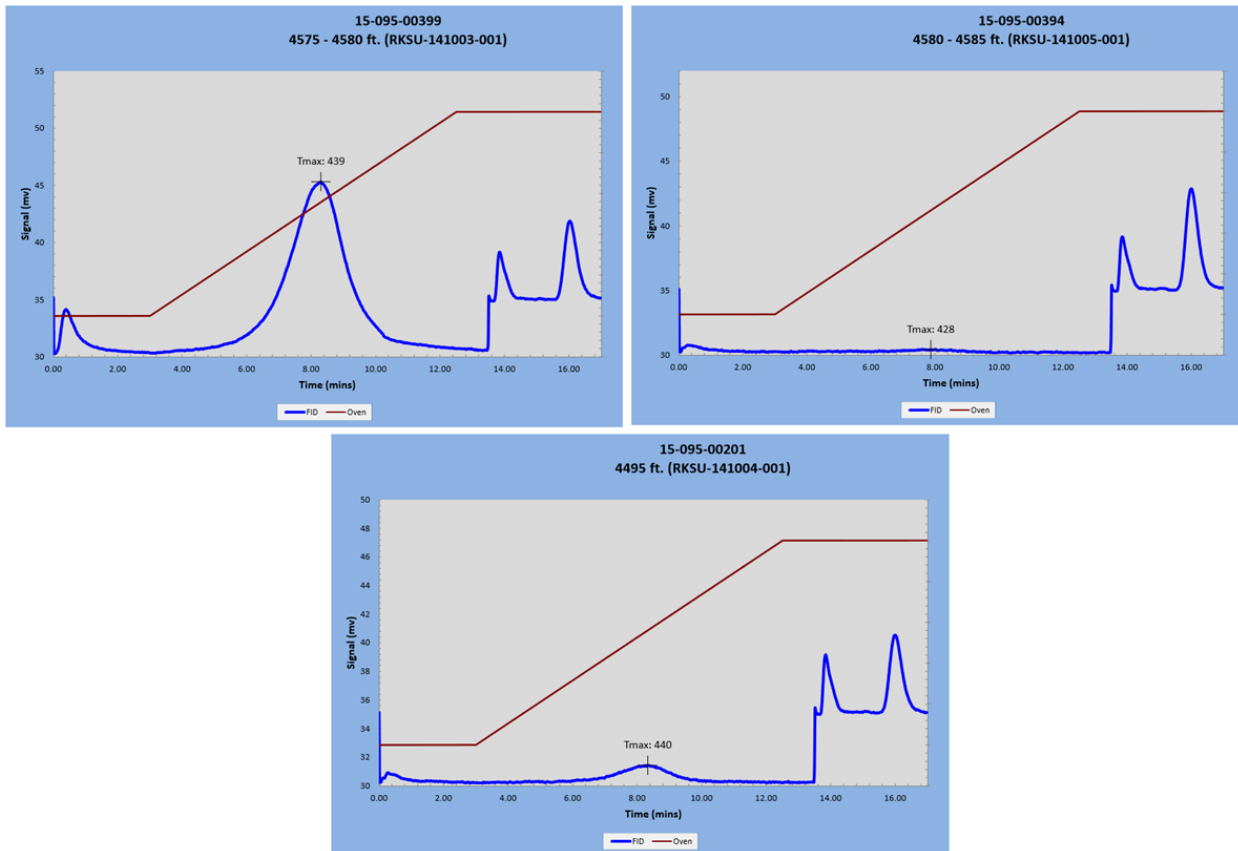


Figure 39 – Additional pyrograms provided by GeoMark laboratories.

| API Number | Upper Depth (ft) | Lower Depth (ft) | Median Depth (ft) | Sample Type | Leco TOC (wt%) | Rock-Eval-2 S1 (mg HCl/g) | Rock-Eval-2 S2 (mg HCl/g) | Rock-Eval-2 S3 (mg CO2/g) | Rock-Eval-2 Tmax (°C) | Calculated %Ro (RE TMAX) | Hydrogen Index (\$2x100/TOC) | Oxygen Index (\$3x100/TOC) | S2/S3 Conc. (mg HCl/mg CO2) | S1/TOC Norm. Oil Content | Production Index (\$1/(\$1+S2)) |
|--------------|------------------|------------------|-------------------|-------------|----------------|---------------------------|---------------------------|---------------------------|-----------------------|--------------------------|------------------------------|----------------------------|-----------------------------|--------------------------|---------------------------------|
| 15-033-21470 | 4.595.00 | 4.599.00 | 4.597.00 | Cuttings | 10.40 | 2.54 | 11.45 | 3.24 | 422 | 0.44 | 110 | 31 | 4 | 24 | 0.18 |
| 15-033-21470 | 4.745.00 | 4.755.00 | 4.750 | Cuttings | 12.85 | 3.50 | 77.79 | 1.14 | 423 | 0.45 | 605 | 9 | 63 | 28 | 0.04 |
| 15-033-21470 | 4.786.00 | 4.792.00 | 4.789 | Cuttings | 10.37 | 3.98 | 58.74 | 0.96 | 425 | 0.49 | 566 | 9 | 61 | 38 | 0.06 |
| 15-033-21470 | 5.012.00 | 5.016.00 | 5.014 | Cuttings | 6.3 | 2.44 | 24.06 | 1.01 | 425 | 0.49 | 362 | 16 | 24 | 39 | 0.09 |
| 15-033-21470 | 5.046.00 | 5.050.00 | 5.048 | Cuttings | 6.93 | 2.58 | 33.64 | 0.79 | 428 | 0.54 | 485 | 11 | 43 | 37 | 0.07 |
| 15-119-21194 | 5.060.00 | 5.064.00 | 5.062 | Cuttings | 6.99 | 2.41 | 36.85 | 0.88 | 427 | 0.53 | 527 | 13 | 42 | 34 | 0.06 |
| 15-119-21194 | 5.309.00 | 5.313.00 | 5.311 | Cuttings | 2.42 | 0.50 | 5.67 | 0.65 | 432 | 0.62 | 373 | 27 | 9 | 21 | 0.08 |
| 15-119-21194 | 5.346.00 | 5.350.00 | 5.348 | Cuttings | 4.16 | 1.05 | 15.52 | 0.67 | 432 | 0.62 | 373 | 16 | 23 | 25 | 0.06 |
| 15-119-21194 | 5.414.00 | 5.418.00 | 5.416 | Cuttings | 4.27 | 0.95 | 17.71 | 0.61 | 431 | 0.60 | 415 | 14 | 29 | 22 | 0.05 |
| 15-119-21194 | 5.668.00 | 5.671.00 | 5.669.5 | Cuttings | 2.81 | 0.40 | 5.09 | 0.56 | 440 | 0.76 | 181 | 20 | 9 | 14 | 0.07 |
| 15-051-25233 | 3.216.00 | 3.220.00 | 3.218 | Cuttings | 10.6 | 4.75 | 36.68 | 2.10 | 419 | 0.38 | 347 | 20 | 17 | 45 | 0.11 |
| 15-135-24314 | 3.885.00 | 3.890.00 | 3.887.5 | Cuttings | 2.34 | 0.48 | 6.38 | 0.93 | 429 | 0.56 | 273 | 40 | 7 | 21 | 0.07 |
| 15-135-24253 | 3.925.00 | 3.930.00 | 3.927.5 | Cuttings | 1.93 | 0.33 | 2.61 | 0.79 | 428 | 0.54 | 130 | 41 | 3 | 17 | 0.12 |
| 15-135-24253 | 4.020.00 | 4.024.00 | 4.022 | Cuttings | 3.2 | 0.75 | 7.18 | 1.19 | 425 | 0.49 | 224 | 37 | 6 | 23 | 0.09 |
| 15-135-24186 | 4.212.00 | 4.218.00 | 4.215 | Cuttings | 10.8 | 4.45 | 52.79 | 1.32 | 424 | 0.47 | 491 | 12 | 40 | 41 | 0.08 |
| 15-135-24314 | 4.232.00 | 4.237.00 | 4.234.5 | Cuttings | 4.92 | 0.96 | 16.49 | 1.17 | 429 | 0.56 | 376 | 24 | 16 | 20 | 0.05 |
| 15-135-22895 | 4.235.00 | 4.240.00 | 4.237.5 | Cuttings | 1.26 | 0.28 | 1.53 | 1.29 | 434 | 0.65 | 121 | 102 | 1 | 22 | 0.15 |
| 15-051-25316 | 3.440.00 | 3.450.00 | 3.445 | Cuttings | 13.3 | 5.26 | 55.49 | 1.79 | 413 | 0.27 | 416 | 13 | 31 | 39 | 0.09 |
| 15-135-24254 | 4.226.00 | 4.232.00 | 4.229 | Cuttings | 1.8 | 0.26 | 2.55 | 0.82 | 429 | 0.56 | 142 | 45 | 3 | 14 | 0.09 |
| 15-135-24253 | 4.275.00 | 4.280.00 | 4.277.5 | Cuttings | 4.44 | 0.90 | 9.79 | 0.95 | 434 | 0.65 | 220 | 22 | 10 | 20 | 0.08 |
| 15-051-25825 | 3.546.00 | 3.549.00 | 3.547.5 | Cuttings | 2.27 | 0.52 | 3.71 | 0.98 | 431 | 0.60 | 163 | 43 | 4 | 23 | 0.12 |
| 15-051-25316 | 3.660.00 | 3.672.00 | 3.666 | Cuttings | 5.21 | 1.71 | 18.49 | 0.72 | 427 | 0.53 | 355 | 14 | 26 | 33 | 0.08 |
| 15-051-25825 | 3.576.00 | 3.580.00 | 3.578 | Cuttings | 2.81 | 0.65 | 10.14 | 0.83 | 427 | 0.53 | 361 | 30 | 12 | 23 | 0.06 |
| 15-051-25316 | 3.725.00 | 3.725.00 | 3.725 | Cuttings | 5.88 | 2.04 | 22.84 | 1.17 | 430 | 0.58 | 388 | 20 | 20 | 35 | 0.08 |

Table 7– Summary of data obtained by TOC and Rock-Eval taken and reformatted from Tyler Hill, 2011. Lab testing conducted by Weatherford Laboratories.

Table 8 -
 Top: Sample cutting information
 Bottom: GeoMark LECO TOC and pyrolysis results

| API Number | Upper Depth (ft) | Lower Depth (ft) | Median Depth (ft) | Sample Type |
|--------------|------------------|------------------|-------------------|-------------|
| 15-095-00030 | 4,645.00 | 4,650.00 | 4,647.50 | Cuttings |
| 15-077-00123 | 4,705.00 | 4,710.00 | 4,707.50 | Cuttings |
| 15-095-00201 | 4,495.00 | | 4,495.00 | Cuttings |
| 15-095-00394 | 4,580.00 | 4,585.00 | 4,582.50 | Cuttings |
| 15-095-00399 | 4,575.00 | 4,580.00 | 4,577.50 | Cuttings |

| API Number | Percent Carbonate (wt%) | LECO TOC (wt%) | Rock-Eval-2 S1 (mg HC/g) | Rock-Eval-2 S2 (mg HC/g) | Rock-Eval-2 S3 (mg CO2/g) | Rock-Eval-2 Tmax (°C) | Calculated % Ro (RE TMAX) | Hydrogen Index (S2x100/TOC) | Oxygen Index (S3x100/TOC) | S2/S3 Conc. (mg HC/mg CO2) | S1/TOC Norm. Oil Content | Production Index (S1/(S1+S2)) |
|--------------|-------------------------|----------------|--------------------------|--------------------------|---------------------------|-----------------------|---------------------------|-----------------------------|---------------------------|----------------------------|--------------------------|-------------------------------|
| 15-095-00030 | 11.57 | 0.72 | 0.32 | 0.98 | 0.39 | 430 | 0.58 | 136 | 54 | 3 | 44 | 0.25 |
| 15-077-00123 | 4.64 | 3.55 | 1.33 | 14.32 | 0.39 | 436 | 0.69 | 403 | 11 | 37 | 37 | 0.08 |
| 15-095-00201 | 22.75 | 0.88 | 0.22 | 1.25 | 0.34 | 440 | 0.76 | 142 | 39 | 4 | 25 | 0.15 |
| 15-095-00394 | 15.73 | 0.80 | 0.20 | 0.42 | 0.52 | 428 | 0.54 | 53 | 65 | 1 | 25 | 0.32 |
| 15-095-00399 | 10.22 | 3.95 | 1.22 | 15.69 | 0.47 | 439 | 0.74 | 397 | 12 | 33 | 31 | 0.07 |

Appendix C - Information on Biomarkers and Rare Earth Elements

Biomarkers

Biomarkers are molecular fossils, sharing a level with former living organisms such as eukaryotes and prokaryotes (Hunt, 2011). These organic remnants are highly complex compounds composed primarily of carbon and hydrogen and found in soils, rocks, and crude oils. According to Moldowan et al. (2005), little to no alteration of these molecules should be expected even after millions of years.

There are three main types of biomarker groups: steranes (m/z 217), terpanes (m/z 191) and *n*-alkanes

Steranes

Eukaryotic organisms are the leading sources for steranes, which are derived from sterols (Volkman, 1988). They generally have between 27 and 30 carbon atoms total in their base structure (Figure 36). Regular and stereochemically altered steranes will generally have altered placements at key points that will reflect maturity based on their spatial alignment towards or away from the structural axis (Seifert and Moldowan, 1986).

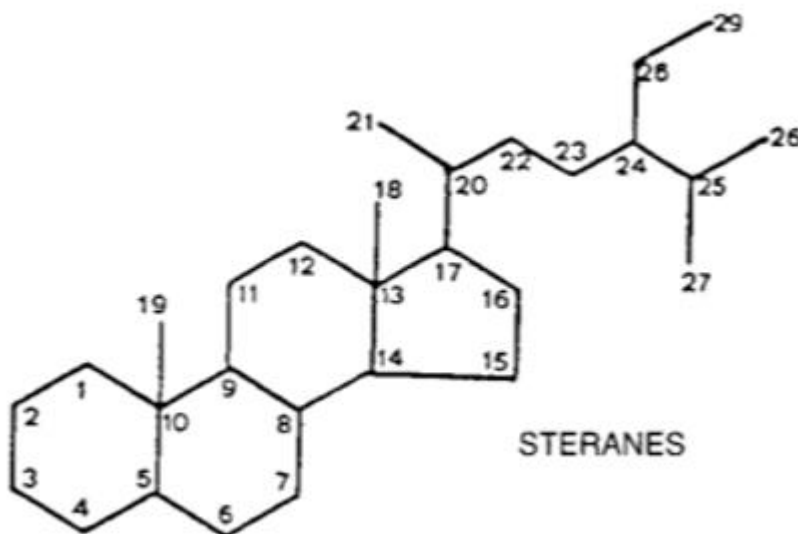


Figure 40 – Sterane compound structure. (Waples et al., 1990)

Terpanes

Another organic compound is classified as a ‘terpane’ and can be used as a biomarker to identify sources and other environmental influences on petroleum (Evans, 2011). Much like steranes, only with more variation in their ring structures, terpanes are probably a product of terpenoid structure bacteria (Waples, 1990) and are structurally altered during catagenesis and diagenesis. Overall, it is resistant to change which makes it a decent biomarker.

There are several substructural markers in the terpane group, including pentacyclic (the most common) and tricyclic terpane’s which are very complicated (Evans, 2011).

n-Alkanes and Isoprenoids

Since there are so many different hydrocarbon variations in oils, a group of organic carbons called the normal *n*-alkanes—which dominated plant waxes—and isoprenoids are used to glean additional information (Philp, 2004).

Alkanes are the basic hydrocarbon structures commonly found in oils consisting of carbon (with 4 valence gaps) and hydrogen (with one electron) and so an extraordinary number of chains can be created in increasing density with added length of up to 40 carbon atoms,

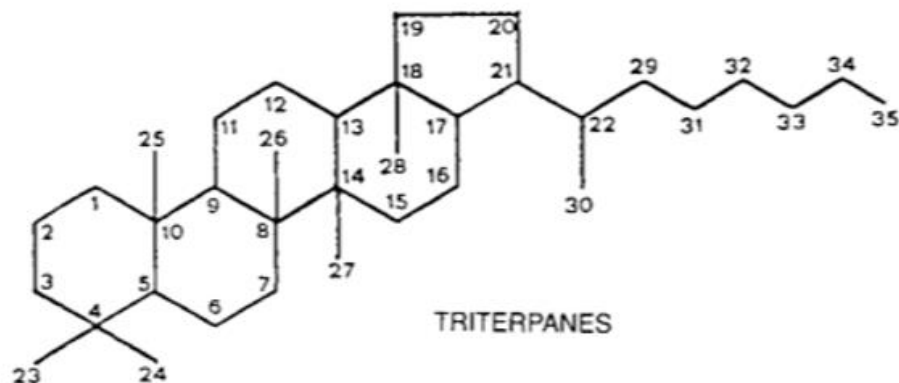


Figure 41 – Terpane compound structure (Waples et al., 1990)

though structural integrity is weakened by length. A hydrocarbon chain with 40 carbon atoms

would be written as C₄₀. The most useful of these chains are between C₁₁ and C₂₅, with C₁₈ and C₁₉ holding the most meaning to petroleum scientists. Increasing maturity is shown as the odd/even predominance is offset by increasing even and decreasing odd *n*-alkanes, “[h]owever, the carbon number range can still be used to differentiate between higher plant versus marine input,” which is how Evans (2011) distinguished a Type II (marine/algal) input (Philp, 2004).

Isoprenoids are C₅ bases and are formed from biosynthesis by polymerization (Peters et al., 2005). Two common isoprenoids used in biomarker analysis are pristane and phytane.

Gas Chromatography/Mass Spectrometry

Moldowan, et al. (2005) describes a GCMS as a machine running six tasks:

1. Compound separation,
2. Movement of separated compounds into an ionizer,
3. Ionization,
4. Mass analysis,
5. Ion detection via electron multiplier, and,
6. Acquisition, processing and display of found data by computer.

The machine gives values for biomarker amounts by first mixing an inert gas (such as helium) with the test material before heating. As the sample heats, biomarkers are separated out due to varying characteristics at different times and amounts which are recorded. After the gas chromatography is completed, mass spectrometry is performed. Using electrons, molecules are alternately charged. Depending on charge assignment, the molecules will be pushed past electrodes where weight is assessed. Biomarkers each have a specific weight and are numerically recorded.

Rare Earth Elements

| | | | | | | | | | | | | | | | | | |
|--|--|--|--|---|---|---|---|---|---|---------------------------------------|--|--|---|---|--|---|-------------------------------------|
| 1 H Hydrogen 1.00794 | | | | | | | | | | | | | | | | | 2 He Helium 4.003 |
| 3 Li Lithium 6.941 | 4 Be Beryllium 9.012182 | | | | | | | | | | | 5 B Boron 10.811 | 6 C Carbon 12.0107 | 7 N Nitrogen 14.00674 | 8 O Oxygen 15.9994 | 9 F Fluorine 18.9984032 | 10 Ne Neon 20.1797 |
| 11 Na Sodium 22.989770 | 12 Mg Magnesium 24.3050 | | | | | | | | | | | 13 Al Aluminum 26.981538 | 14 Si Silicon 28.0855 | 15 P Phosphorus 30.973761 | 16 S Sulfur 32.066 | 17 Cl Chlorine 35.4527 | 18 Ar Argon 39.948 |
| 19 K Potassium 39.0983 | 20 Ca Calcium 40.078 | 21 Sc Scandium 44.955910 | 22 Ti Titanium 47.867 | 23 V Vanadium 50.9415 | 24 Cr Chromium 51.9961 | 25 Mn Manganese 54.938049 | 26 Fe Iron 55.845 | 27 Co Cobalt 58.933200 | 28 Ni Nickel 58.6934 | 29 Cu Copper 63.546 | 30 Zn Zinc 65.39 | 31 Ga Gallium 69.723 | 32 Ge Germanium 72.61 | 33 As Arsenic 74.92160 | 34 Se Selenium 78.96 | 35 Br Bromine 79.904 | 36 Kr Krypton 83.80 |
| 37 Rb Rubidium 85.4678 | 38 Sr Strontium 87.62 | 39 Y Yttrium 88.90585 | 40 Zr Zirconium 91.224 | 41 Nb Niobium 92.90638 | 42 Mo Molybdenum 95.94 | 43 Tc Technetium (98) | 44 Ru Ruthenium 101.07 | 45 Rh Rhodium 102.90550 | 46 Pd Palladium 106.42 | 47 Ag Silver 107.8682 | 48 Cd Cadmium 112.411 | 49 In Indium 114.818 | 50 Sn Tin 118.710 | 51 Sb Antimony 121.760 | 52 Te Tellurium 127.60 | 53 I Iodine 126.90447 | 54 Xe Xenon 131.29 |
| 55 Cs Cesium 132.90545 | 56 Ba Barium 137.327 | 57 La Lanthanum 138.9055 | 72 Hf Hafnium 178.49 | 73 Ta Tantalum 180.9479 | 74 W Tungsten 183.84 | 75 Re Rhenium 186.207 | 76 Os Osmium 190.23 | 77 Ir Iridium 192.217 | 78 Pt Platinum 195.078 | 79 Au Gold 196.96655 | 80 Hg Mercury 200.59 | 81 Tl Thallium 204.3833 | 82 Pb Lead 207.2 | 83 Bi Bismuth 208.98038 | 84 Po Polonium (209) | 85 At Astatine (210) | 86 Rn Radon (222) |
| 87 Fr Francium (223) | 88 Ra Radium (226) | 89 Ac Actinium (227) | 104 Rf Rutherfordium (261) | 105 Db Dubnium (262) | 106 Sg Seaborgium (263) | 107 Bh Bohrium (262) | 108 Hs Hassium (265) | 109 Mt Meitnerium (266) | 110 (269) | 111 (272) | 112 (277) | 113 | 114 | | | | |
| 58 Ce Cerium 140.116 | 59 Pr Praseodymium 140.90765 | 60 Nd Neodymium 144.24 | 61 Pm Promethium (145) | 62 Sm Samarium 150.36 | 63 Eu Europium 151.964 | 64 Gd Gadolinium 157.25 | 65 Tb Terbium 158.92534 | 66 Dy Dysprosium 162.50 | 67 Ho Holmium 164.93032 | 68 Er Erbium 167.26 | 69 Tm Thulium 168.93421 | 70 Yb Ytterbium 173.04 | 71 Lu Lutetium 174.967 | | | | |
| 90 Th Thorium 232.0381 | 91 Pa Protactinium 231.03588 | 92 U Uranium 238.0289 | 93 Np Neptunium (237) | 94 Pu Plutonium (244) | 95 Am Americium (243) | 96 Cm Curium (247) | 97 Bk Berkelium (247) | 98 Cf Californium (251) | 99 Es Einsteinium (252) | 100 Fm Fermium (257) | 101 Md Mendelevium (258) | 102 No Nobelium (259) | 103 Lr Lawrencium (262) | | | | |

Figure 42 – Periodic table of elements with the lanthanide group, or rare earth elements highlighted in dark pink.

The lanthanides, or rare earth elements, are considered transition elements. They are so named for their relative similarity to lanthanum (La) with increasing complexity within their outer electron orbitals. Yttrium and scandium are often considered members of the REE's due to their appearance alongside them in nature (due to their noble gas core and ionic charge) (Cotton, 1972).

The “lanthanide contraction” is a term used to imply the decrease in size of the lanthanum group with increasing atomic number. This occurs due to “the imperfect shielding of one electron by another in the same subshell” (Cotton and Wilkinson, 1972). Using the atomic number, REE's are classed into three separate groups for analysis: 1. Light REE's (AN: 56-63),

2. Middle REE's (AN: 62-67), and 3. Heavy REE's (AN: 64-71). The previous groups are generally referred to as LREE, MREE, and HREE, respectively.

REE's are useful in the analysis of source rock and crude oil, as their presence in both are a result of plant-life undergoing death, burial, and catagenesis (Chaudhuri, 2014).

ICP-MS/ICP-AES

Inductively coupled plasma mass spectrometry (ICP-MS) and inductively coupled plasma atomic emission spectroscopy (ICP-AES) was run through the Laboratory of Hydrology and Geochemistry at the University of Strasbourg in France. The technique allowed for analysis of the organic fraction of the Chattanooga shale, and the silicate and carbonate fractions separately. The separation process required the use of strong, highly purified acids—namely 12N HCl to separate out the carbonate fraction. As this acid is strong enough to release silicate bonds as well, the carbonate-silicate (or inorganic shale constituents) results are combined.

Additional Discussion of Daniel Ramirez-Caro's Results

His organic fraction of solid rock data shows enrichment in heavy lanthanides (Figure 39), and a few positive cerium and europium anomalies. While cerium negative anomalies might be explained by oxidation onto the surface of manganese oxide in depositional seas, with two outliers being explained by terrestrial input, the author states that is conjecture, with a 10% error. Only one of this samples displayed a europium positive anomaly which could also be explained by crystallographic effect.

According to Ramirez-Caro it is wholly possible the heavy REE enrichment in the rock (Figure 39) could have been caused by diagenesis. Enrichment in middle REE's can be easily related to secondary mineralization of phosphates in the Woodford, especially apatite, given known enrichment of phosphates in middle REE's, as well as the presence of apatite nodules in the Woodford shale.

In Ramirez-Caro's silicate-carbonate fraction of solid rock, he relates his data to patterns inherited from sea water.

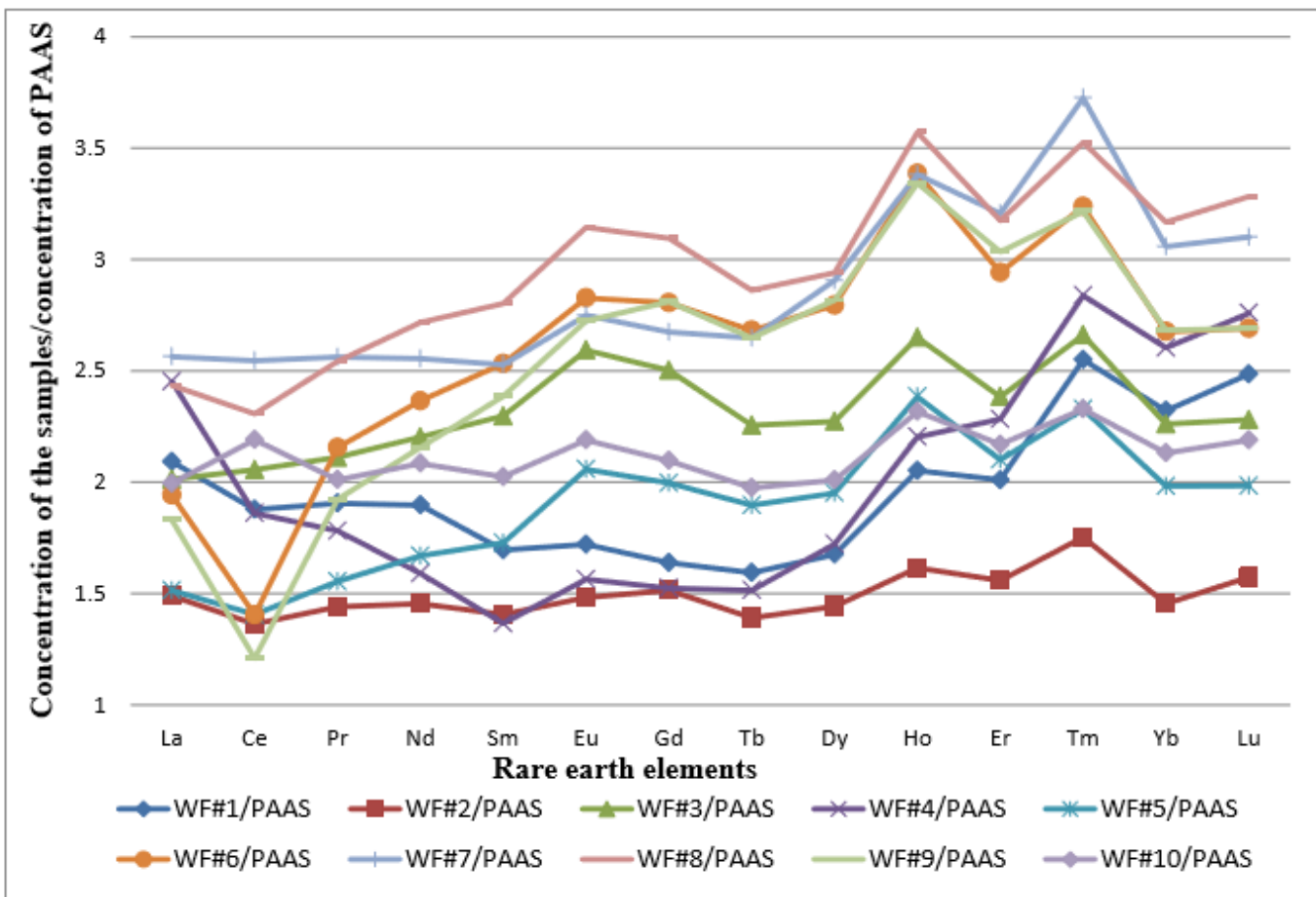


Figure 43 – REE distribution pattern normalized to PAAS for the organic portion of the Woodford shale, taken from Ramirez-Caro, 2013.